

AD _____

Award Number: DAMD17-03-1-0501

TITLE: Brain's DNA Repair Response to Neurotoxicants

PRINCIPAL INVESTIGATOR: Juan Sanchez-Ramos, Ph.D., M.D.

CONTRACTING ORGANIZATION: University of Florida
Tampa, FL 33620

REPORT DATE: July 2005

TYPE OF REPORT: Annual

PREPARED FOR: U.S. Army Medical Research and Materiel Command
Fort Detrick, Maryland 21702-5012

DISTRIBUTION STATEMENT: Approved for Public Release;
Distribution Unlimited

The views, opinions and/or findings contained in this report are those of the author(s) and should not be construed as an official Department of the Army position, policy or decision unless so designated by other documentation.

REPORT DOCUMENTATION PAGE

Form Approved
OMB No. 0704-0188

Public reporting burden for this collection of information is estimated to average 1 hour per response, including the time for reviewing instructions, searching existing data sources, gathering and maintaining the data needed, and completing and reviewing this collection of information. Send comments regarding this burden estimate or any other aspect of this collection of information, including suggestions for reducing this burden to Department of Defense, Washington Headquarters Services, Directorate for Information Operations and Reports (0704-0188), 1215 Jefferson Davis Highway, Suite 1204, Arlington, VA 22202-4302. Respondents should be aware that notwithstanding any other provision of law, no person shall be subject to any penalty for failing to comply with a collection of information if it does not display a currently valid OMB control number. **PLEASE DO NOT RETURN YOUR FORM TO THE ABOVE ADDRESS.**

1. REPORT DATE (DD-MM-YYYY) 01-07-2005		2. REPORT TYPE Annual		3. DATES COVERED (From - To) 1 Jul 2004 – 30 Jun 2005	
4. TITLE AND SUBTITLE Brain's DNA Repair Response to Neurotoxicants				5a. CONTRACT NUMBER	
				5b. GRANT NUMBER DAMD17-03-1-0501	
				5c. PROGRAM ELEMENT NUMBER	
6. AUTHOR(S) Juan Sanchez-Ramos, Ph.D., M.D. E-mail: jsramos@hsc.usf.edu				5d. PROJECT NUMBER	
				5e. TASK NUMBER	
				5f. WORK UNIT NUMBER	
7. PERFORMING ORGANIZATION NAME(S) AND ADDRESS(ES) University of Florida Tampa, FL 33620				8. PERFORMING ORGANIZATION REPORT NUMBER	
9. SPONSORING / MONITORING AGENCY NAME(S) AND ADDRESS(ES) U.S. Army Medical Research and Materiel Command Fort Detrick, Maryland 21702-5012				10. SPONSOR/MONITOR'S ACRONYM(S)	
				11. SPONSOR/MONITOR'S REPORT NUMBER(S)	
12. DISTRIBUTION / AVAILABILITY STATEMENT Approved for Public Release; Distribution Unlimited					
13. SUPPLEMENTARY NOTES Original contains color plates: All DTIC reproductions will be in black and white.					
14. ABSTRACT Parkinson's Disease (PD) is associated with death of dopaminergic (DA) neurons in the substantia nigra (SN) of the brain. Military personnel abroad are at a greater risk of exposure to pesticides and toxins which may selectively damage DA neurons in the SN and increase the probability of development of Parkinson's disease (PD) later in life. The toxins of interest are mitochondrial poisons that create a bioenergetic crisis and generate toxic oxyradicals which damage macromolecules, including DNA. We hypothesize that regulation of the DNA repair response within certain neurons of the SN (the pars compacta) may be a critical determinant for their vulnerability to these neurotoxicants. We have measured regional differences in the brain's capacity to increase repair of oxidized DNA (indicated by oxyguanosine glycosylase (OGG1) activity) to three distinct chemical classes of neurotoxins (MPTP, two mycotoxins, and an organochlorine pesticide). At the end of the second year of the project, we have found that the temporal and spatial profile of OGG1 activity across brain regions elicited by each class of neurotoxicant is distinct and unique. Although all three toxicants cause DA depletion in striatum, only MPTP caused loss of DA neurons in midbrain. However, it is possible that superimposition of age-related loss of DA neurons over the moderate DS depletion caused by OTA may result in early onset parkinsonism.					
15. SUBJECT TERMS No subject terms provided.					
16. SECURITY CLASSIFICATION OF:			17. LIMITATION OF ABSTRACT	18. NUMBER OF PAGES	19a. NAME OF RESPONSIBLE PERSON USAMRMC
a. REPORT U	b. ABSTRACT U	c. THIS PAGE U			19b. TELEPHONE NUMBER (include area code)
			UU	122	

Table of Contents

Cover.....	page 1
SF 298.....	page 2
Body.....	page 4
Key Research Accomplishments.....	page 17
Reportable Outcomes.....	page 19
Conclusions.....	page 20
References.....	page 21
Appendices.....	page 22

BODY

TASK 1. MEASUREMENT OF REGIONAL DIFFERENCES IN OXIDATIVE DNA DAMAGE AND DNA REPAIR RESPONSES ELICITED BY MYCOTOXINS (OCHRATOXIN-A, RUBRATOXIN), ORGANOCHLORINE PESTICIDES (DIELDRIN) AND BY THE CLASSICAL DA NEUROTOXIN, MPTP. (MONTHS 1-18):

We completed the specific objectives listed in the proposal under TASK 1 in the first year as documented in the first annual progress report. Key research accomplishments for Task 1 are listed here:

- 1) The effects of two mycotoxins (ochratoxin-A and rubratoxin-B), and an organochlorine pesticide (dieldrin), on the capacity of brain to repair oxidative damage to DNA was studied and compared to a well-known neurotoxicant (MPTP) that selectively injures the nigro-striatal DA system.
- 2) The acute effects of ochratoxin, MPTP and Dieldrin on DA and its metabolites in the nigro-striatal DA system was measured.
- 3) The regulation of the DNA repair enzyme (OGG1) across brain regions was studied for each of the toxicants.
- 4) A spatial (neuroanatomical) and temporal mapping of the brains DNA repair and anti-oxidative response to the neurotoxicants was produced.

Even though each of the three classes of neurotoxicants studied here is known to interfere with mitochondrial function, the OGG1 activity profile across brain regions has revealed interesting differences in the vulnerability of specific regions of brain to each class of toxicant. Ochratoxin-A produced an initial depression of OGG1 activity in six brain regions, but with time there was an increase in OGG1 in all regions except for a) hippocampus, b) caudate/putamen and c) cerebral cortex. These are the brain regions that are most affected following an episode of hypoxia/ischemia (eg hippocampus, cerebral cortex and globus pallidus). From this profile of OGG1 reactivity, it may be inferred that OTA toxicity mimics the effects of global hypoxia on brain. By contrast, an acute challenge with MPTP resulted in an increase of OGG1 activity in all brain regions within the first 6 hrs. The augmented OGG1 activity was maintained up through 48hr. This response was completely unexpected because MPTP is considered to be a selective nigro-striatal dopamergic neurotoxin and such a wide-spread activation of anti-oxidant and OGG1 activity had never been reported. However, by 72 hrs, there was a significant decrease of repair capacity, most notably in the nigro-striatal DA system. Even though the locus coeruleus was affected by MPTP, as evidenced by a decrease in TH immunoreactivity similar to that observed in s. nigra and striatum, the OGG1 activity in that neuronal population remained at a high level through 72 hours and was consistent with its resistance to MPTP neurotoxicity. In the s. nigra, the big drop in SOD and OGG1 activity at 72 hours was associated with a significant increase in the number of apoptotic cells in that nucleus. Dieldrin's profile of OGG1 activation was distinct from those of MPTP and OTA. Dieldrin triggered a generalized OGG1

response that remained elevated through 72 hrs. There was no drop-off of activity in the striatum or other brain regions.

TASK 2. To measure the effects of chronic low dose administration of a mycotoxin and a pesticide (dieldrin) on brain region oxidative DNA damage and DNA repair (*Months 13-24*):

The following procedures were to be performed:

- a) Administer chronic low dose (via Alzet minipumps) of ochratoxin-A and dieldrin to separate groups of mice.
- b) Measure parameters of oxidative stress and oxidative DNA damage in each of six brain regions
- c) Determine the DNA repair response (activities of Ogg1) in each brain region; measurement of mRNA of other DNA repair genes in those brain regions.
- d) Determine the quantitative relationships between levels of oxidative DNA damage and the expression of the DNA repair enzymes
- e) Measure striatal dopamine and homovanillic acid (HVA); count number of tyrosine hydroxylase immunoreactive cells in midbrain

We have performed most of these tasks with several exceptions and modifications. The “comet assay” was substituted for oxo8dG as the index of oxidative DNA damage in each brain region. The comet assay allowed for efficient processing of individual brain samples for multiple assays, without the need to pool tissue samples. See attached reprint for details of the method (Sava et al., 2006). We have also performed a study of regional brain pharmacokinetics of OTA. This was not listed in the original proposal, but was completed at the beginning of year 2, prior to initiation of the studies listed above in TASK 2. This additional task was undertaken to determine whether the variation in the DNA repair response to OTA across brain regions was related to the distribution and concentrations of OTA in brain regions and not to intrinsic differences in capacity to up-regulate DNA repair in distinct brain regions. In addition we have measured expression of a set of DNA repair genes using real time PCR in hippocampal cells but not yet in other tissues for reasons to be detailed below.

ADDED TASK: PHARMACOKINETICS OF OCHRATOXIN-A (OTA) IN MOUSE BRAIN

A single dose of OTA (3.5 mg/kg) was administered i.p. to mice. The dose chosen was the ED₅₀ for striatal dopamine depletion in experiments performed in the first year of the project (Sava et al., 2006) (Reprint in appendix). After 3, 6, 12, 24 and 72 hrs, groups of 6 mice were euthanatized, brains dissected and assayed for levels of OTA. The method utilized HPLC with fluorescence detection. Brain tissue samples of about 100 mg were sonicated in 2 volumes of absolute ethyl alcohol containing 50 ng/ml of ochratoxin-A (Sigma Chemical, MA) as internal standard. Supernatants obtained after centrifugation (14,000 x g, 5 min, 4°C)

were passed through filters (Acrodisc LC 13 mm syringe filter with 0.45 μ m PVDF membrane) and 20 μ L of supernatant samples were injected onto a reverse phase Microsorb-MV 300-5 C18 column (Varian, inc., CA). The mobile phase consisted of 57% of water, 42% of acetonitrile and 1% of acetic acid. Flow rate was 0.9 mL/min. Peaks were detected with Series 200 fluorescent detector and data were collected and processed with TotalChrom software (PerkinElmer Instruments, MA). At three hrs, the highest concentrations of OTA were measured in the cerebellum (CB), followed by pons (P), cerebral cortex (CX), and medulla (M). Pharmacokinetic parameters were calculated and are summarized in Table 1. The rank order of concentrations of OTA based on area under the curve (AUC) is as follows: CB > P > CX > M > MB > CP > HP > Thal/Ht. Comparing the half-life of elimination ($T_{1/2}$) for each region shows that the pons and midbrain eliminated OTA very slowly ($T_{1/2}$ = 224 and 75 hr, respectively) in contrast to the rapid elimination of the toxin from cerebellum ($T_{1/2}$ = 20 hr).

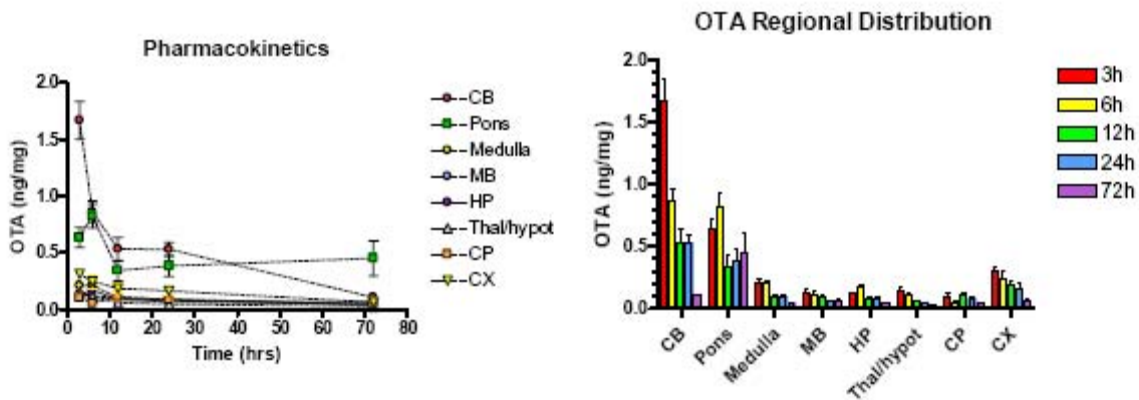


Figure 1 Left panel summarizes the changes over time in regional brain concentrations of OTA following an acute dose of 3.5 mg/kg (i.p.). The right panel depicts the same data organized according to region. Two-way ANOVA shows that brain region accounted for 49.5% of total variance ($p < 0.0001$) and time accounted for 11.5% of total variance ($p < 0.001$). Interaction between brain region and time accounted for 25.8% of variance ($p < 0.0001$). One-way ANOVA of data at 72 hrs showed that the OTA concentrations in all brain regions were significantly different ($p < 0.0001$). Dunnett's multiple comparison test showed that OTA levels in the pons were significantly higher than every other brain region at 72 hrs ($p < 0.05$).

Relationship between brain regional concentration of OTA and parameters of oxidative stress

The time course of acute effects of OTA were investigated in the context of DNA damage, DNA repair and global oxidative stress across mouse brain regions. Oxidative DNA damage, as measured with the "comet assay", was significantly increased in the six brain regions at all time points up to 72 hrs, with peak effects noted at 24 hrs in midbrain (MB), CP (caudate/putamen) and HP (hippocampus). Oxidative DNA repair activity (oxyguanosine glycosylase or OGG1) was inhibited in all regions at 6 hrs, but recovered to control levels in cerebellum (CB) by 72 hrs, and showed a trend to recovery in other regions of brain. Other indices of oxidative stress were also elevated. Lipid peroxidation increased over time throughout the brain.

Table 1: Pharmacokinetic data for OTA across brain regions

	k_{el} (1/h)	$T_{1/2}$ (h)	AUC (ng ^h /uL)	CL (uL/mg ^h)
CB	0.034	20.175	32.107	0.125
Pons	0.003	224.698	31.026	0.129
Medulla	0.020	33.859	6.175	0.648
MB	0.009	75.107	5.578	0.717
HP	0.016	42.582	5.266	0.760
Thal/Ht	0.022	31.104	3.426	1.167
CP	0.015	47.222	5.202	0.769
CX	0.021	32.578	10.087	0.397

The **elimination rate constant (kel)** was calculated from the slope of semi-logarithmical plot of OTA concentration versus time using the least square regression analysis.

The **half-life of OTA** elimination ($T_{1/2}$) was calculated from the equation:

$$T_{1/2} = \ln 2 / k_{el}$$

The **area under curve (AUC)** was calculated by integration of OTA concentration from time zero to infinity according to the formula:

$$AUC_{0-\infty} = AUC_{0-t} + C_f / k_{el}$$

where C_f represents the final measured OTA concentration made at time t .

The **clearance (CL)** of OTA was determined using the following formula:

$$CL = D / AUC_{0-\infty}$$

where D represents OTA dose, namely, 4 ng/mg = 4 mg/kg.

Superoxide dismutase (SOD) activity increased in all regions of brain, but the heightened antioxidant responses were not maintained beyond 24 hrs (Sava et al., 2006). Surprisingly, the distribution of oxidative stress and the DNA repair response across brain regions did not correlate with the concentrations of the toxin (AUC) in each region (See **Figure 2**). Therefore the regional vulnerability to the toxin does not bear a linear relationship to the concentration of the toxin in each region. This observation is still consistent with the hypothesis that vulnerability to injury induced by this toxin is determined by regional differences in capacity to scavenge oxyradicals and/or to repair oxidative DNA damage caused by the toxin.

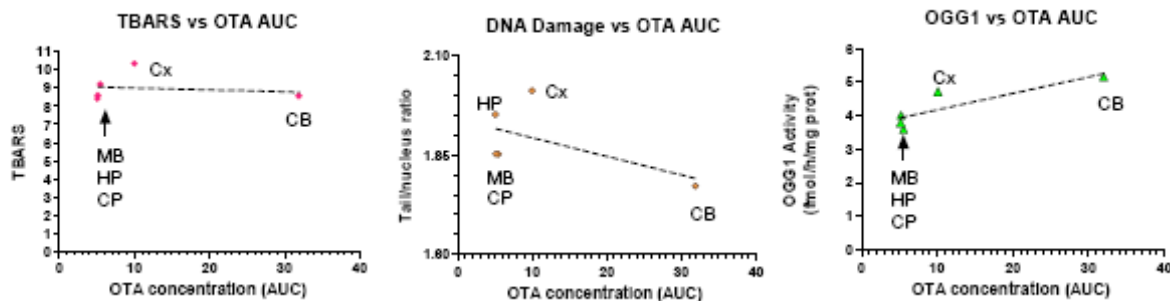


Figure 2. Parameters of oxidative stress plotted as a function of OTA concentration. The pharmacokinetic parameter that reflects the average concentration of OTA over time in each brain region (“area under the curve” or AUC) is plotted on the X-axis. The upper panel plots the relationship between TBARS (index of lipid peroxidation) in each brain region as a function of AUC for OTA. The middle and lower panels show the plots of DNA damage vs AUC and DNA repair activity (OGG1) vs AUC, respectively. The dashed regression line does not differ significantly from zero in all three panels, indicating that there is no linear relationship between the selected parameter of oxidative stress and the AUC in specific brain regions.

TASK 2 EFFECTS OF CHRONIC OTA ON MEASURES OF OXIDATIVE STRESS AND DNA REPAIR

Effects of chronic OTA on glutathione levels: Glutathione is an important component of the intrinsic anti-oxidative system. Alterations of glutathione (especially the relationship between glutathione in the reduced and oxidized state) provide a sensitive indicator of oxidative stress. To study the effects of lower dose exposure to OTA over longer intervals on glutathione levels, 4 groups of animals (n=7 per group) were

given chronic infusions over a period of 2 weeks with implanted osmotic minipumps. Each group received different cumulative doses of OTA; vehicle alone, 4 mg/kg, 8 mg/kg, or 16 mg/kg over a 2 week infusion period. Animals were then euthanized and parameters of oxidative stress were measured in 8 regions of brain. Chronic OTA infusion resulted in a significant dose-dependent decrease in total glutathione levels in all brain

Effects of Chronic OTA Infusion on Glutathione in Brain Regions

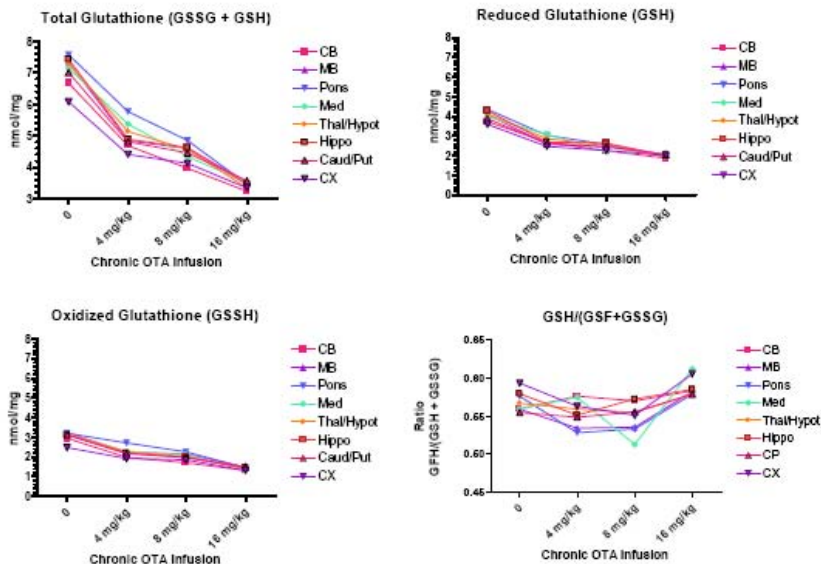


Figure 3 Effects of two weeks of OTA infusion on regional glutathione levels. Total glutathione, reduced (GSH), oxidized (GSSG) and the ratio of reduced to total (GSH/GSH+GSSG) are shown in the 4 panels. Two-way ANOVA of total glutathione levels showed that concentration, but not brain region, contributed significantly ($p < 0.0001$) to total variance. However, 2-way ANOVA of the ratio of reduced to total glutathione (lower right panel) showed that neither dose of OTA nor brain region contributed significantly to total variance.

regions (**Fig 3**). Despite the depletion of total glutathione, the proportion of reduced glutathione relative to total glutathione remained relatively constant in each region with a trend towards

an increase following chronic infusion with the highest dose of OTA. This reflects the capacity of the cells to maintain redox homeostasis in the face of oxidative stress. The ED50 for each brain region (dose that resulted in reduction of glutathione by 50% in that region) is shown in **Table 2**. There was very little difference between regions in the ED50s for total, reduced and oxidized glutathione, suggesting that the capacity to maintain redox status is roughly equal across all brain regions. Hence differences in a brain region's capacity to maintain anti-oxidative redox status through the glutathione system does not appear to play an important role in determining vulnerability to OTA.

Table 2 ED₅₀ for effect of chronic infusion of OTA on Glutathione Levels

Total Glutathione (GSH + GSSG)		Reduced Glutathione (GSH)		Oxidized Glutathione (GSSG)	
	ED ₅₀		ED ₅₀		ED ₅₀
CB	7.49	CB	2.71	CB	1.43
MB	8.81	MB	3.31	MB	1.79
PONS	8.63	PONS	3.38	PONS	1.64
MD	8.36	MD	3.11	MD	1.55
T/H	8.30	T/H	3.12	T/H	1.65
HIPPO	8.75	HIPPO	3.43	HIPPO	1.68
CP	8.50	CP	3.13	CP	1.78
CX	7.09	CX	2.82	CX	1.08

**Chronic OTA
(Effects on SOD)**

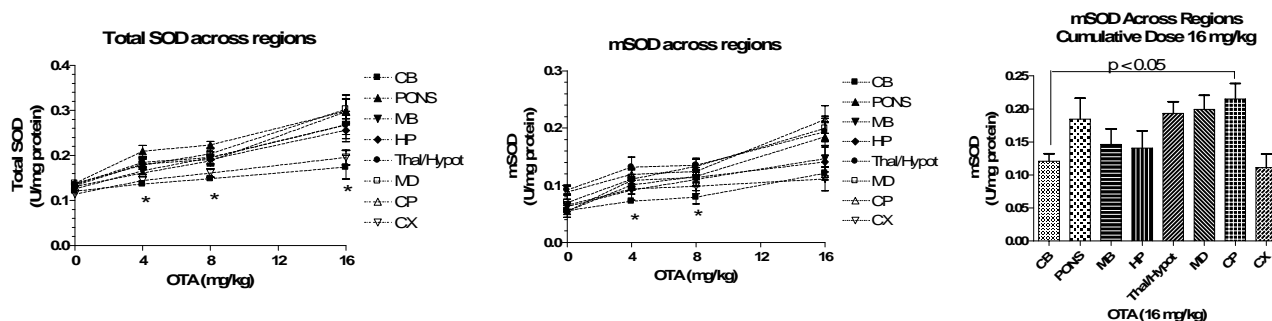


Fig 4 Effects of 2 wk infusion of OTA on SOD activities across brain regions. **Panel on the left** illustrates changes in total SOD as a function of cumulative dose of OTA. Two-way ANOVA reveals that cumulative dose accounts for 50.4% of total variance ($p < 0.001$) and brain region accounts for 12.6% of total variance ($p < 0.001$). * Post hoc t-tests with Bonferroni corrections for multiple comparisons indicate that total SOD activities in CB at 16 mg/kg are significantly less than all regions except for cortex ($p < 0.01$). Total SOD of the CB is also significantly less than PONS at 4, 8 and 16 mg/kg ($p < 0.01$). **Middle panel** illustrates effects of chronic OTA on mSOD across brain regions. Two-way ANOVA shows that both brain region and cumulative dose contribute significantly to total variance of mSOD ($p < 0.0001$ for concentration; $p < 0.0001$ for brain region). T-tests with Bonferroni corrections are indicated by the asterisks which show activities of mSOD in CB are significantly lower than mSOD in PONS, Thal/Hypot, MB, CP at 16 mg/kg ($p < 0.01$); CB mSOD is also significantly lower than mSOD in MB and Thal/hypothal at 4 and 8 mg/kg. **Right panel** focuses on the effects of a cumulative dose of 16 mg/kg on mSOD plotted against brain regions. One-way ANOVA indicates that the means of mSOD activities in the distinct brain regions were significantly different ($p < 0.01$). Post-analysis with Dunnett's multiple comparison test indicates mSOD in CB was significantly different than in CP ($p < 0.05$)

Effects of chronic OTA infusion on SOD activity: The effects of chronic OTA infusion on the activity of total SOD (as well as mitochondrial and cytoplasmic component of the total SOD) was measured in each brain region. SOD activity was increased in all regions in a dose-dependent manner (**Fig 4**). Mitochondrial SOD increased to the greatest degree in the pons (3.5 times the baseline levels), medulla (2.88 x baseline) and caudate/putamen (2.68 x baseline) See **Table 3**.

Table 3. Increase in mitochondrial SOD activity across brain regions after 2 wks infusion of OTA (with cumulative dose of 16 mg/kg).

	A) mean mSOD activity Vehicle (U/mg)	B) mean mSOD activity 16 mg/kg OTA (U/mg)	C) fold increase Ratio B/A
Pons	0.054	0.184	3.47
Medulla	0.069	0.199	2.88
Caudate/putamen	0.088	0.215	2.68
Hippocampus	0.054	0.141	2.61
Midbrain	0.062	0.146	2.35
Cerebellum	0.055	0.121	2.2
Thalamus/hypothal	0.091	0.193	2.14
Cerebral Cortex	0.064	0.111	1.73

These results clearly demonstrate that OTA elicits a global anti-oxidative response in all regions of brain, but the greatest change from baseline was seen in the mitochondrial SOD (mSOD) activity of the pons. Interestingly, the pons was the region with the greatest delay in elimination of the toxin (T_{1/2}) and a high cumulative exposure (AUC) following acute doses of OTA (See **Table 1**). This result suggests that there is a relationship between cumulative exposure and the degree of upregulation of mitochondrial SOD in the pons, indicated (**Figure 5**) but this relationship does not hold for other brain regions.

Effects of Chronic OTA infusion on DNA Repair (OGG1 activity): Groups of 7 mice implanted with Alzet minipumps received 4, 8 and 16 mg/kg of OTA over 2 weeks. After euthanasia, brains were dissected and processed for measurement of OGG1 activities. Chronic OTA infusion resulted in a dose-dependent increase in OGG1 activities in all brain regions (**Fig 6**). No region of brain showed an inhibition or decrease in marked creases in OGG1 activity, not all regions were equally sensitive to the toxin. Using the dose-response curve functions generated from each brain region to estimate an ED₅₀ (the dose of OTA that

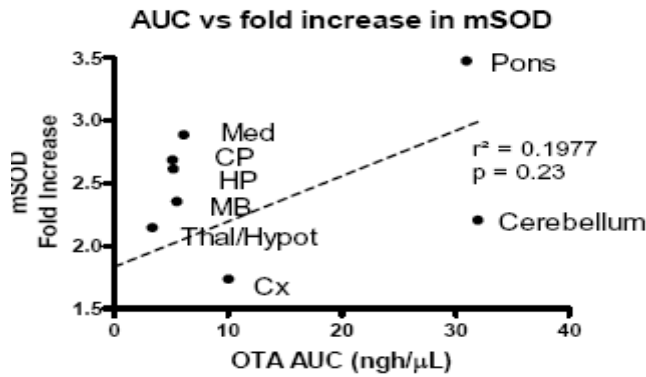


Fig 5. Fold change in mSOD activity after 2 wks of 16 mg/kg cumulative exposure to OTA plotted against AUC for each brain region. The regression line between mSOD and AUC is not significantly different from zero.

resulted in half the maximal rate of OGG1 activity), it was clear that the caudate/putamen (CP) was most sensitive to the toxin; a cumulative dose of 0.65 mg/kg produced half maximal OGG1 activity. The cerebellum was the least sensitive, with respect to dose of OGG1 required to attain half-maximal OGG1 activity ($ED_{50}=2.65$ mg/kg).

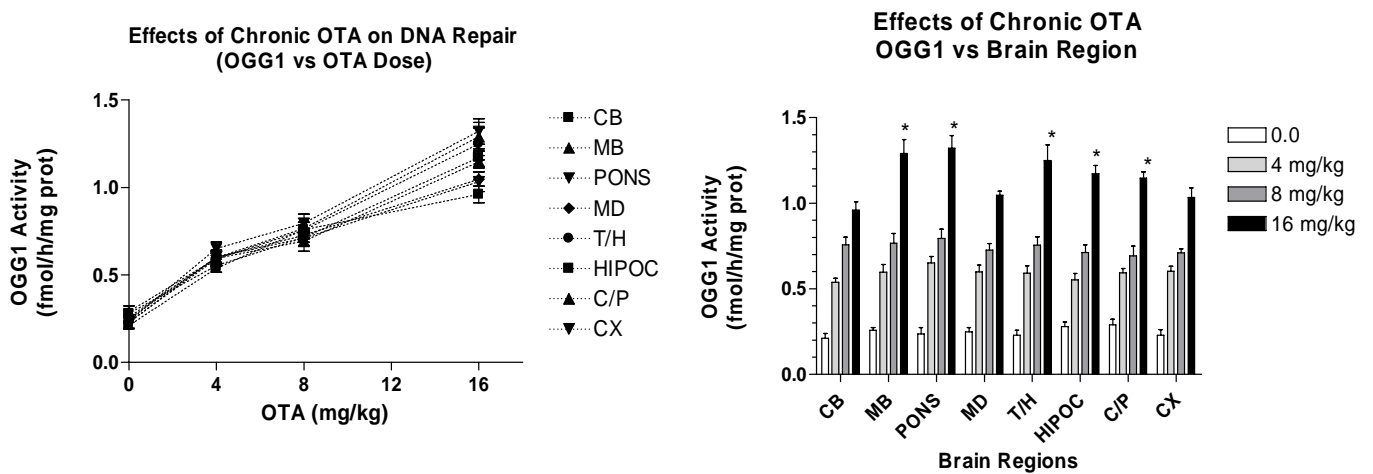
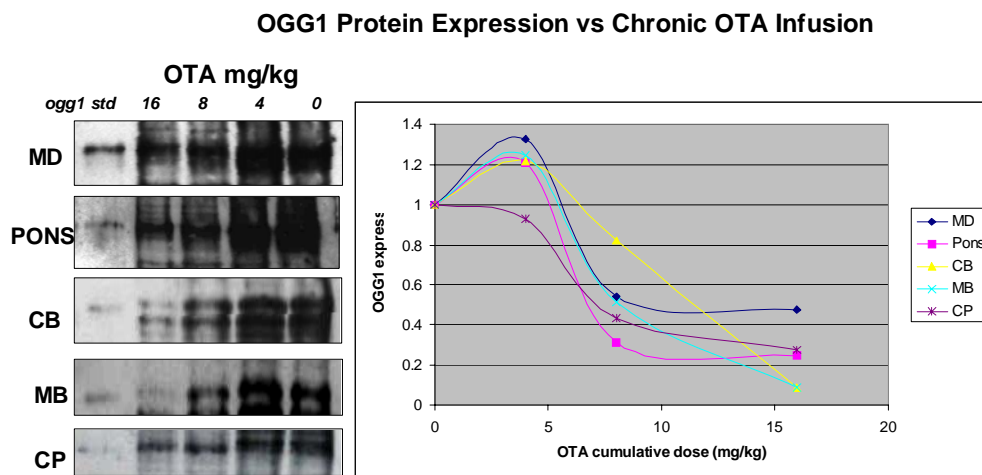


Fig 6 Effects of chronic infusion of OTA via osmotic minipump on OGG1 activities across brain regions. **Left panel:** OGG1 activity plotted against cumulative OTA dose delivered over 2 weeks. All brain regions exhibited a dose-dependent increase in OGG1. Each point is the mean \pm SEM ($n=7$) of OGG1 activity. **Right panel:** Same data of OGG1 activity re-plotted against brain region on the X-axis. Shading of the bars depicts cumulative dose administered over 2 weeks as indicated in the legend. Two-way ANOVA revealed that concentration of OTA and brain regions accounted for 86 % ($p < 0.0001$) and 1.4% ($p=0.0005$), respectively, of the total variance. Interaction between concentration and brain region accounted for 2.18% of total variance ($p=0.0079$). T-tests with the Bonferroni correction for multiple comparisons showed statistically significant differences ($p < 0.05$) at 16 mg/kg between CB and MB, CB and Pons, CB and Thal/hypothal; CB and Hippo; CB and CP (indicated by asterisks).

Effects of Chronic OTA Infusion on OGG1 Protein Expression: In addition to studying effects on OGG1 enzymatic activity, expression of OGG1 protein was measured in brain regions following treatment with

OTA infusion for 2 weeks. Western blots were prepared from tissue extracts from five brain regions (**Fig 7**). Densitometry was performed on the blots and normalized to the standard (control OGG1 protein). The data was plotted as a function of cumulative OTA dose. All brain regions, except CP, exhibited an increase of OGG1 protein following a dose of 4 mg/kg. At higher doses, all regions of brain exhibited decreased OGG1 protein expression.



Densitometry performed with KODAK 1D Image Analysis Software, version 3,6

Fig 7 Western blots of protein extracts from five brain regions of mice treated with chronic infusions of OTA. Left panel shows actual blots from four different animals (each treated with OTA with cumulative doses indicated at the top of the panel: 0, 4, 8 and 16 mg/kg). Blots from 5 regions are illustrated. Panel on right shows OGG1 protein (quantified by densitometry and normalized to time zero) as a function of cumulative OTA dose over two weeks.

The dose-dependent decrease in expression of OGG1 protein in the face of increased OGG1 enzymatic activity at cumulative doses of 8 mg/kg or greater was similar to the results obtained earlier with another mycotoxin, rubratoxin (RB) (Sava et al., 2004). In that study, there was an increase in enzymatic activity, without increase in protein levels. Calculation of kinetic constants showed that RB treatment caused an increase in catalytic efficacy of OGG1. The response to RB-induced oxidative DNA damage was to enhance OGG1 catalytic activity (V_{max}/K_m) by a factor of 1.74. RB also increased affinity of OGG1 for the substrate that was demonstrated by decrease in magnitudes of the Michaelis-Menten constant, K_m . (Sava et al., 2004).

Effects of Chronic OTA infusion on striatal dopamine and metabolites, tyrosine hydroxylase

immuno-reactivity and apoptotic profiles in SN: Four groups of 6 mice each were implanted with Alzet minipumps loaded to deliver cumulative doses of vehicle, 4, 8, and 16 mg/kg over two weeks. The caudate/putamen (CP) from the mice dissected and processed for determination of DA and its principal metabolites, HVA and DOPAC. Chronic infusion of OTA resulted in a dose-dependent decrease in DA and

and an increase in HVA and DOPAC. Peak increase in DA turnover occurred at 8 mg/kg, the cumulative dose which also resulted in statistically significant depletion of DA (See **Fig 8**)

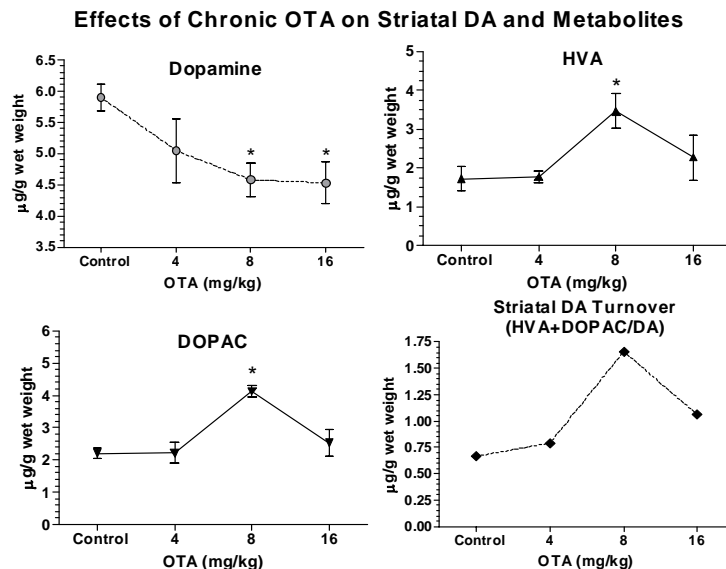


Figure 8 Effects of 2 wk infusion of OTA via osmotic minipump on levels of DA and its metabolites in striatum (caudate/putamen; CP). **Upper left panel:** Levels of DA in caudate/putamen of ICR mice exposed to different cumulative doses (4, 8 and 16 mg/kg). (n=6 for each dose); **Upper right panel:** striatal HVA levels plotted against cumulative OTA dose; **Lower left panel:** striatal DOPAC levels plotted against OTA dose; **Lower right panel;** striatal DA turnover (ratio of [HVA] + [DOPAC] / [DA]) plotted against OTA dose. Two-tailed t-tests, comparing levels of DA or metabolites against control levels, were performed in each panel. Asterisk indicates significant difference relative to the control values ($p < 0.05$).

The maximum depletion of striatal DA was 23% of controls and that was attained with chronic infusion of 8 and 16 mg/kg over two weeks. This degree of DA depletion was much less than the 50% reduction from baseline that resulted from acute administration of 3.6 mg/kg at 72 hrs after injection. Gradual infusion of the toxin was apparently slow enough to permit the development of tolerance to the DA depleting effects. As with the acute effects of OTA, there was no obvious alteration of behavior or locomotor activity induced by slow infusion of the toxin (Sava et al., 2006).

Effects on TH immunocytochemistry: Infusion of OTA (8 mg/kg over 2 weeks) resulted in decreased intensity of TH+ staining in striatum, s. nigra and locus ceruleus that was similar to that observed following acute administration of 4 mg/kg (see (Sava et al., 2006). Similar to the acute effects of OTA, there were no apoptotic profiles noted when TUNEL staining was applied to s. nigra sections (data not shown).

In summary, slow infusion of OTA over two weeks resulted in a 23% reduction of striatal DA, an increase in DA turnover a mild decrease in TH immunostaining in striatum and s. nigra without evidence for cell death (apoptosis).

TASK 2 CONTINUED (EFFECTS OF DIELDRIN)

Effects of Slow Infusion of Dieldrin over Two Weeks on Oxidative DNA Repair: Six groups of mice (n=8 per group) were implanted with Alzet minipumps loaded with dieldrin and calibrated to deliver 3, 6, 12, 24 and 48 mg/kg over a period of 2 weeks. After euthanasia and rapid dissection of brain into seven regions, OGG1 activities were determined. Dieldrin infusion elicited a dose-dependent increase of OGG1 activities in all brain regions, with maximum effects reaching a plateau between 24 and 48 mg/kg (**Fig 9**).

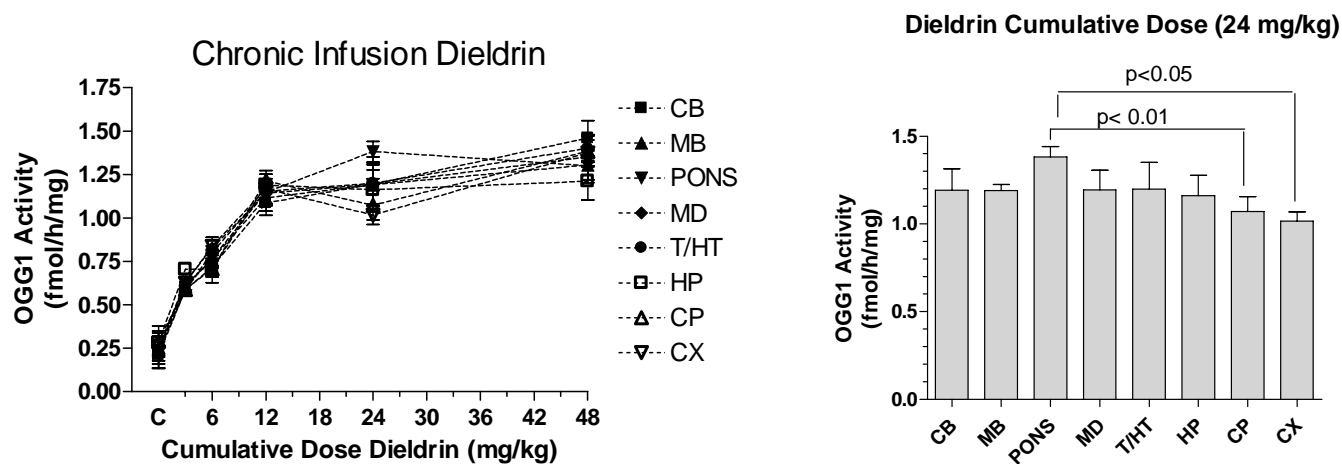


Figure 9 Effects of 2wk infusion of dieldrin on DNA repair (OGG1 activity) Left panel depicts OGG1 activity as a function of the cumulative dose of dieldrin. The increase in OGG1 activity was significantly dependent on the cumulative dose delivered but did not vary significantly as a function of brain region. Two-way ANOVA revealed that cumulative concentration of Dieldrin accounted for 79% of total variance ($p < 0.0001$) and brain regions accounted for 1.84% of total variance ($p = 0.61$). Post-hoc t-tests with Bonferroni corrections for multiple comparisons showed OGG1 activities in the pons were significantly higher than in the CP and CX following a cumulative dose of 24 mg/kg (right panel). CB=cerebellum; MB= midbrain; PONS=pons; MD=medulla; T/HT=thalamus/hypothalamus; HP=hippocampus; CP= caudate/putamen; CX= cerebral cortex.

The effect of dieldrin on OGG1 activity varied significantly as a function of dose (2-way ANOVA; $p < 0.001$) and was independent of brain region ($p = 0.61$). Post-hoc t-tests (corrected for multiple comparisons) showed that OGG1 activity in PONS was significantly higher than in CP ($p < 0.01$) and CX ($p < 0.05$).

Effects of dieldrin infusion on lipid peroxidation: Slow infusion of dieldrin resulted in a dose-dependent increase in oxidative stress across all brain regions as indicated by measurement of lipid peroxidation (**Fig 10**). The maximum effect was produced following infusion of 48 mg/kg over 2 weeks. The increase in lipid peroxidation was significantly dependent on dose and did not vary significantly with brain region. However, post-hoc t-tests revealed that lipid peroxidation was significantly higher in CB than in MB following a dose of 12 mg/kg ($p < 0.05$). Similarly, lipid peroxidation was greater in CB than in the PONS following 24 mg/kg.

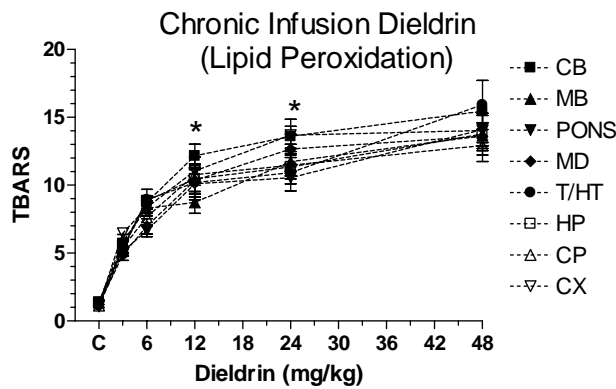


Fig 10. Effects of 2 wk infusion of dieldrin (with minipump) on lipid peroxidation (TBARS units). The increase in TBARS was significantly dependent on the cumulative dose delivered but did not vary significantly as a function of brain region. Two-way ANOVA revealed that cumulative concentration of dieldrin accounted for 76% of total variance ($p < 0.0001$) and brain regions accounted for 0.94% of total variance ($p = 0.36$). * Post-hoc t-tests with Bonferroni corrections for multiple comparisons showed TBARS in the CB were significantly higher than in the MB ($p < 0.05$) following a cumulative dose of 12 mg/kg; TBARS in CB were also significantly higher than in the PONS ($p < 0.05$) following 24 mg/kg.

Effects of Slow Infusion of Dieldrin on SOD: Further evidence of oxidative stress was evidenced by a dose-dependent increase in total SOD activity following slow infusion of dieldrin (**Fig 11**). Mitochondrial SOD also increased following dieldrin infusion and the cumulative dose accounted for most of the variance. When the effects of 24 mg/kg were plotted against brain region, it was clear that mSOD in MB and Thal/Hypot were significantly lower than CB (Fig 11, panel on the right).

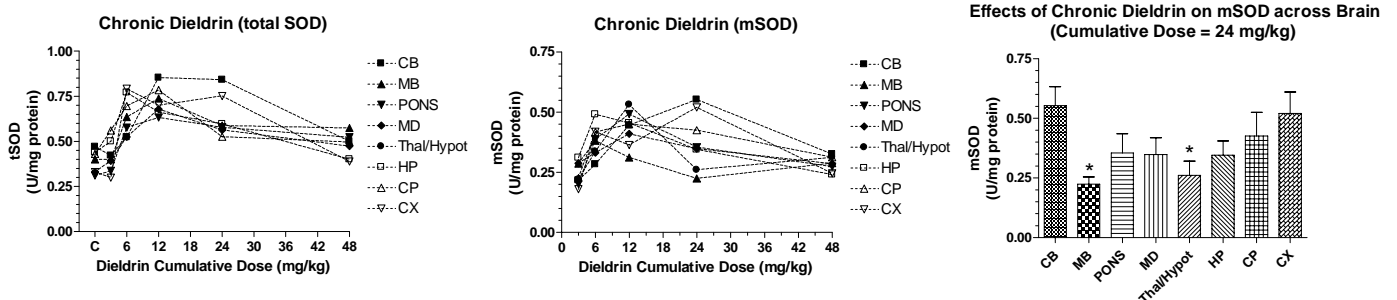


Fig 11. Effects of 2 wk infusion of dieldrin on SOD (total SOD and mitochondrial SOD). **Panel on the left** illustrates changes in total SOD as a function of cumulative dose of dieldrin. Two-way ANOVA reveals that cumulative dose accounts for 23.9% of total variance ($p < 0.001$) and brain region accounts for 2.2% of total variance ($p < 0.13$). * Post hoc t-tests with Bonferroni corrections for multiple comparisons indicate that total SOD activities in CB at 24 mg/kg are significantly greater than MD and CP ($p < 0.05$). **Middle panel** illustrates effects of chronic OTA on mSOD across brain regions. Two-way ANOVA shows that cumulative dose contributes 11.46% of total variance of mSOD ($p < 0.0001$) and brain regions contributes 1.14% of total variance ($p = 0.7$). **Right panel** focuses on the effects of a cumulative dose of 24 mg/kg on mSOD plotted against brain regions. One-way ANOVA indicates that the means of mSOD activities in the distinct brain regions were significantly different ($p = 0.03$). Dunnett's multiple comparison test indicates mSOD in CB was significantly higher than in MB and Thal/Hypot ($p < 0.05$).

Quantitative Expression of DNA Repair Genes Using Real-Time PCR: We have not yet assessed DNA repair gene expression in the SNc and VTA of mouse midbrain. In preparation for this final TASK of the project in Year 3, we have developed a quantitative gene expression assay with the help of professional staff at Applied Biosystems. A panel of nine critical DNA repair genes was designed for a mini-array to run on a real time PCR system (**Table 4**). The method of analyzing data was by relative quantification, describing the changes in expression of the target genes normalized to an endogenous control (18S ribosomal RNA) relative to the sample at time zero (Livak and Schmittgen, 2001). Cell cultures of neural progenitor cells from adult mouse hippocampus were prepared using well described methods (Mignone et al., 2004). Cells were maintained in proliferation media which contains growth factors that keep cells dividing. OTA (1 µg/mL) was added to the culture medium 2 days after plating (time 0 in **Fig 12**). Triplicate samples of cells were harvested at 24 and 72 hours. Total RNA was extracted, cDNA synthesized and processed according to the protocol provided by Applied Biosystems for quantitative RT-PCR. The endogenous control was 18s ribosomal RNA and a second endogenous control was TATA box binding protein as a control for low expression transcripts. RNA samples were applied to mini-plate containing the targets for 9 DNA repair genes. Mean RQ values were determined for each gene and plotted against time (**Fig 12**). Two of the transcripts (*Rad23*) and (*Adprt1* or PARP) were significantly elevated at 24 hrs but decreased well below control levels at 72 hrs. The other 7 genes were decreased at both 24 and 72 hrs, and this included the *ogg1* transcript. Interestingly, we had observed that OGG1 enzymatic activity of these hippocampal neural progenitor cells was increased by 30% at 24 hrs despite the down-regulation of the transcript at that time. There are several explanations for this divergent finding. OTA may directly impede transcription of the *ogg1* gene while at the same time augment catalytic activity of the enzyme. This is possible because OTA may induce conformational changes in the enzyme that alter kinetics of the reaction and result in augmented activity. This latter phenomenon was been noted before when incubating pure OGG1 protein with OTA or rubratoxin (Sava et al., 2004). Also of interest is the marked up-regulation of *RAD23*, a key nucleotide excision repair gene. During blood cell development the removal of DNA adducts, the resealing of repair gaps, and resistance to DNA-reactive drugs has previously been reported to be increased in stem or mature compared to progenitor cells of the same individual (Bracker et al., 2005). On the other hand, the vast majority of differentially expressed repair genes was consistently up-regulated in the progenitor fraction during hematopoiesis (Bracker et al., 2005). A positive correlation of repair function and transcript levels was found for a small number of genes such as *RAD23* or *ATM*, which may serve as key regulators for DNA damage processing via specific pathways. These data indicate that the organism might aim to protect the small number of valuable slow-dividing stem cells by extensive DNA repair,

whereas fast proliferating progenitor cells, once damaged, are rather eliminated by apoptosis.

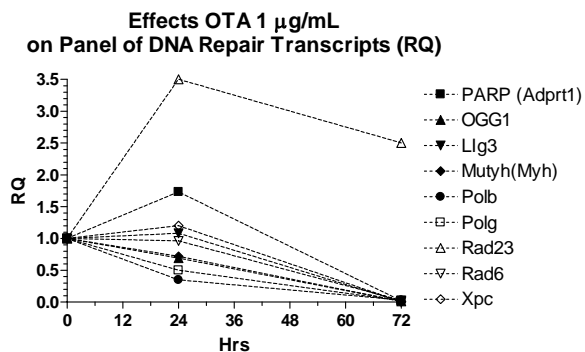


Fig 12. OTA (1 µg/mL) was added to the culture medium 2 days after plating adult hippocampal NSC (time = 0 hr). Cells were harvested at 0, 24 and 72 hours. Total RNA was extracted, converted to cDNA and processed according to the protocol provided by Applied Biosystems for real time PCR (TaqMan Assay). Samples were applied to the custom-designed mini-array containing 9 DNA repair gene targets and 18S ribosomal RNA as endogenous control. Mean RQ values (relative quantification against time 0) were determined for each gene and plotted against time.

Table 4 Selected DNA Repair Genes

<i>POLB</i> ; <i>POLG</i>	DNA repair polymerases
<i>OGG1</i> ; <i>MYH</i> **	Base excision repair (BER)
<i>LIG3</i>	Ligase (a BER factor)
<i>ADPRT</i>	Poly (ADP-ribose) polymerase (PARP)
<i>XPC</i> <i>RAD23</i>	Nucleotide excision repair
<i>RAD6A</i>	Rad6 pathway

** MYH (or MUTYH) repairs the 8-hydroxy-2'-deoxyguanosine (oxo8dG) lesions that are opposite to adenine and also repairs 2-hydroxy-2'-deoxyadenosine opposite guanine.

KEY RESEARCH ACCOMPLISHMENTS AT END OF YEAR 2 (with update to January 2006)

1. **Distribution of OTA in brain:** Pharmacokinetic parameters for ochratoxin-A (OTA) in each brain region were determined based on OTA concentrations measured at 3, 6, 12, 24 and 72 hrs after administration of the toxin. There were no correlations between parameters of oxidative stress (lipid peroxidation, oxidative DNA damage, OGG1 activity) and pharmacokinetic parameters such as elimination half life, area under the curve (reflecting cumulative concentration over time) and clearance. **Therefore the regional brain concentrations of OTA were not critical determinants of the degree of oxidative stress (and oxidative DNA damage and repair) elicited by the toxin in specific brain regions.**

2. **Effects of OTA on striatal DA and metabolites and tyrosine hydroxylase immunoreactivity;** The mycotoxin OTA produced a dose- and time-dependent depletion of striatal dopamine (DA), a decrease in striatal DA turnover and qualitatively diminished striatal tyrosine hydroxylase immunoreactivity without the appearance of apoptotic profiles in s. nigra or striatum. These data are consistent with the finding that striatum (caudate/putamen) was the most sensitive of all brain regions to OTA in terms of the ability to increase OGG1 activity (the striatum had lowest ED50 for stimulation of OGG1 activity). In addition, these alterations in DA levels were not due to degeneration of neurons in the SN.

3. Studies on the **chronic OTA infusion** on oxidative stress, oxidative DNA damage and repair were completed:

a) **Effects on glutathione:** Chronic OTA infusion resulted in a cumulative dose-dependent decrease in total glutathione levels in all brain regions. Despite the depletion of total glutathione, the proportion of reduced glutathione relative to total glutathione remained relatively constant in each region with a trend towards an increase following chronic infusion with the highest dose of OTA. This reflects the capacity of the cells to maintain redox homeostasis in the face of chronic oxidative stress. Hence differences in a brain region's capacity to maintain anti-oxidative redox status through the glutathione system does not appear to play an important role in determining vulnerability to OTA.

b) **Effects on SOD (as well as mitochondrial and cytoplasmic component of the total SOD):** Chronic OTA infusion elicited increases of SOD (both cytoplasmic and mitochondrial) activity in all regions of brain, but the greatest change from baseline was seen in the mitochondrial SOD (mSOD) activity of the pons. The pons was the region with the slowest elimination constant ($T_{1/2}$) and very high cumulative exposure (AUC) following acute doses of OTA. This result suggests that there is a relationship between cumulative exposure and the degree of upregulation of mitochondrial SOD in the pons, but this relationship does not hold for other regions of brain.

c) **Effects on OGG1 activity:** Chronic OTA infusion resulted in a dose-dependent increase in OGG1 activities in all brain regions. No region of brain showed an inhibition or decrease in OGG1 activity at any dose, unlike the early responses to acute doses of OTA, when all regions showed initial and transient inhibition of OGG1 activity. Even though all brain regions were capable of marked increases in OGG1 activity, not all regions were equally sensitive to the toxin. Using the dose-response curve functions generated from each brain region to estimate an ED₅₀ (the dose of OTA that resulted in half the maximal rate of OGG1 activity), it was clear that the caudate/putamen (CP) was most sensitive to the toxin.

d) **Effects on OGG1 protein expression:** All brain regions, except CP, exhibited an increase of OGG1 protein following a cumulative dose of 4 mg/kg over two weeks. At higher doses, all regions of brain exhibited decreased OGG1 protein expression. The dose-dependent decrease in expression of OGG1 protein in the face of increased OGG1 enzymatic activity at cumulative doses of 8 mg/kg or greater was similar to the results obtained earlier with another mycotoxin, rubratoxin (RB) (Sava et al., 2004). In that study, there was an increase in enzymatic activity, without increase in protein levels. Calculation of kinetic constants showed that RB treatment caused an increase in catalytic efficacy of OGG1. The response to RB-induced oxidative DNA damage was to enhance OGG1 catalytic activity (V_{max}/K_m) by a factor of 1.74. RB also increased affinity of OGG1 for the substrate that was demonstrated by decrease in magnitudes of the Michaelis-Menten constant, K_m . (Sava et al., 2004). This may be the mechanism for the increased OGG1 enzymatic activity despite a decrease in total protein expressed.

4. Effects of Chronic Administration of Dieldrin: Dieldrin infusion elicited a dose-dependent increase of OGG1 activities in all brain regions, with maximum effects reaching a plateau between 24 and 48 mg/kg. Slow infusion of dieldrin also resulted in a dose-dependent increase in oxidative stress across all brain regions as indicated by measurement of lipid peroxidation and increases in total SOD and mSOD. The maximum effect on lipid peroxidation was produced following infusion of 48 mg/kg over 2 weeks. Lipid peroxidation was significantly dependent on dose and did not vary significantly with brain region. Mitochondrial SOD also increased following dieldrin infusion and the cumulative dose accounted for most of the variance. When the effects of 24 mg/kg were plotted against brain region, it was clear that mSOD in MB and Thal/Hypot were significantly lower than CB. Experiment that remains to be performed in Task 2 include: effects of chronic dieldrin on striatal DA and metabolites.

REPORTABLE OUTCOMES

1. Acute neurotoxic effects of the fungal metabolite Ochratoxin-A (see attached reprint). This report is the

first to describe depletion of striatal dopamine following single doses of OTA. In addition, the regional vulnerability to OTA was explored in the context of regional differences in oxidative DNA repair, and other parameters of oxidative stress.

2. Neuroanatomical mapping of DNA repair and antioxidative responses in mouse brain: effects of a single dose of MPTP (manuscript re-submitted). Results obtained demonstrate that OGG1 is activated across many brain regions in response to MPTP. This response was completely unexpected because MPTP is considered to be a selective nigro-striatal dopaminergic neurotoxin and such a widespread activation of antioxidant and OGG1 activity had never been reported. However, by 72 h, there was a decrease of repair capacity, most notably in the nigro-striatal DA system. In SN, the drop in SOD and OGG1 activity at 72 h was associated with a significant increase in the number of apoptotic cells in that nucleus. To summarize, the temporal and spatial profile of MPTP-triggered DNA repair and antioxidant activity at 72 h was consistent with the well-known localized toxicity for the nigro-striatal DA system.

3. Can Low Level, Non-lethal Exposure to Ochratoxin-A Cause Parkinsonism?

(Sava et al, J. Neurosci. in press, see attached manuscript). An invited lecture on this topic was presented at the World Federation of Neurology, held in Sydney, Australia in November, 2005. This is the first report in which pharmacokinetic parameters of OTA distribution in mouse brain were determined. Interestingly, those regions of brain with the highest cumulative exposure are *not* those most sensitive to the toxin. The continuous subcutaneous administration of OTA at low doses over a period of two weeks caused small, but significant depletion of striatal DA. OTA also caused pronounced global oxidative stress, evoking a strong anti-oxidative and DNA repair response across the entire brain. Even though the depletion of striatal DA did

not cause overt parkinsonism in these mice, it is important to consider that the superimposition of normal age-related decline in striatal DA may possibly result in signs of parkinsonism such as slowness of movement and rigidity in the mice. Without completing understanding why DA terminals in striatum are especially vulnerable to OTA, it is likely that a toxic insult to the nigro-striatal system will increase the risk of developing Parkinson's Disease at an earlier age than normal. This hypothesis can be tested by studying the long term consequences of episodes of OTA exposure in mice during the aging process. In the real world, it will be important to monitor the neurological status of Gulf War veterans as they age.

4. Effects of chronic OTA infusion on parameters of oxidative stress in brain regions (manuscript in preparation). This report will be a thorough documentation of the effects of chronic infusion of low doses of OTA, and will be contrasted with the effects of acute OTA administration in explaining striatal vulnerability to the toxin.

5. Effects of acute and chronic Dieldrin administration on parameters of oxidative stress, DNA damage and repair in brain regions (manuscript in preparation). Although dieldrin has been shown to be toxic for DA neurons *in vitro*, administration of dieldrin *in vivo* has not resulted in damage specific to DA neurons of midbrain. The manuscript will address this discrepancy, pointing out that the earlier work on dieldrin cytotoxicity utilized dissociated fetal midbrain cultures (Sanchez-Ramos et al., 1998).

CONCLUSIONS

Three toxicants (ochratoxin-A, Dieldrin, MPTP) from distinct chemical families were chosen for study on the basis of their reported capacity to interfere with mitochondrial function. The patterns of oxidative stress across brain regions elicited by each of these agents was distinct and unique. All three toxicants clearly induced oxidative stress, produced oxidative DNA damage and stimulated oxidative DNA repair (OGG1) across all brain regions when given acutely, or in the case of OTA and dieldrin, when infused slowly over two weeks. Despite clear evidence of DA depletion, increase in DA turnover and decrease in striatal and nigral TH immunoreactivity, Though OTA is a mitochondrial toxin, it should be emphasized that OTA has been reported to have additional mechanisms of action including inhibition of protein synthesis and interference with DNA synthesis (and formation of DNA adducts) (Dirheimer and Creppy, 1991; Pfohl-Leszkowicz et al., 1993; Grosse et al., 1995).

So far, our starting hypothesis has not been supported by the evidence accumulated to date. We had postulated that DA neurons were especially vulnerable to mitochondrial toxins because of diminished DNA repair capacity intrinsic to those neuronal populations. We have not demonstrated a lesion specific to DA neurons with either dieldrin or OTA given acutely or by slow infusion over two weeks. Only MPTP clearly caused a lesion selective for nigral DA neurons. And yet MPTP, which is considered a highly specific DA

neurotoxin, also caused a widespread oxidative stress and elicited increases of oxidative DNA repair (OGG1) in all brain regions. Therefore, the focus on capacity to repair DNA as the explanation for selective vulnerability (pathocllisis) to mitochondrial toxins may be a failed hypothesis. We have not given up on the hypothesis yet, because all our studies to date have been performed on relatively gross tissue samples that contain a mixture on many neuronal phenotypes, glia, endothelial cells, and fibers in passage. To truly test our hypothesis will require assessment of the DNA repair response of selected panel of DNA repair genes (real time PCR) in subsets of DA neurons (from s. nigra and ventral tegmental area) harvested from midbrain by laser capture microdissection and using our new gene expression miniarray (As proposed in TASK 3).

However, it is possible that OTA may be toxic for a subset of neural cells distinct from those we had predicted to be vulnerable. It has become apparent that the toxicity of OTA for the brain may be selective for cells that are in a proliferative state. For the sake of efficiency in developing the gene expression panel, we utilized proliferating hippocampal neural progenitors in cell culture wells. Serendipitously, it was noted that OTA caused a marked decrease in viability of these hippocampal cells compared to differentiated hippocampal neurons. This was an unexpected observation because proliferating cells generally are more efficient in their DNA repair systems (Stedeford et al., 2001). Since adult hippocampus retains a reserve of neural stem/progenitor cells that replace lost neurons when needed throughout life, it is possible that OTA exposure may impact on this ability of this structure to maintain its functional integrity over time. Indeed it is known that mycotoxin exposure can result in deficits in cognitive functions subserved by the hippocampus.

As a result of these insights, we hypothesize that OTA will cause deficits in cognition because of its impact on the proliferative population of neural stem/progenitor cells that reside in hippocampus. OTA, when fed to adult rats in the diet or when administered to adult mice, accumulates in brain and causes oxidative DNA damage (Belmadani et al., 1998; Sava et al., 2006). Humans exposed to “toxic molds” have been reported to suffer significant and measurable cognitive deficits involving several domains, including memory, learning, attention, processing speed, and executive functions (Etzel, 2002; Gordon and Cantor, 2004; Gordon et al., 2004). In light of the critical role played by hippocampus in cognitive function, and the importance of neurogenesis in this structure throughout life, the impact of mycotoxins (eg. OTA) on hippocampal functional integrity is highly relevant from both molecular pathogenetic and clinical perspectives.

Citations

- Belmadani A, Tramu G, Betbeder AM, Creppy EE (1998) Subchronic effects of ochratoxin A on young adult rat brain and partial prevention by aspartame, a sweetener. *Hum Exp Toxicol* 17:380-386.
- Bracker TU, Giebel B, Spanholtz J, Sorg UR, Klein-Hitpass L, Moritz T, Thomale J (2005) Stringent regulation of DNA repair during human hematopoietic differentiation: a gene expression and functional analysis. *Stem Cells*.
- Dirheimer G, Creppy EE (1991) Mechanism of action of ochratoxin A. *IARC Sci Publ*:171-186.
- Etzel RA (2002) Mycotoxins. *Jama* 287:425-427.
- Gordon WA, Cantor JB (2004) The diagnosis of cognitive impairment associated with exposure to mold. *Adv Appl Microbiol* 55:361-374.
- Gordon WA, Cantor JB, Johanning E, Charatz HJ, Ashman TA, Breeze JL, Haddad L, Abramowitz S (2004) Cognitive impairment associated with toxigenic fungal exposure: a replication and extension of previous findings. *Appl Neuropsychol* 11:65-74.
- Grosse Y, Baudrimont I, Castegnaro M, Betbeder AM, Creppy EE, Dirheimer G, Pfohl-Leszkowicz A (1995) Formation of ochratoxin A metabolites and DNA-adducts in monkey kidney cells. *Chem Biol Interact* 95:175-187.
- Livak KJ, Schmittgen TD (2001) Analysis of relative gene expression data using real-time quantitative PCR and the 2(-Delta Delta C(T)) Method. *Methods* 25:402-408.
- Mignone JL, Kukekov V, Chiang AS, Steindler D, Enikolopov G (2004) Neural stem and progenitor cells in nestin-GFP transgenic mice. *J Comp Neurol* 469:311-324.
- Pfohl-Leszkowicz A, Grosse Y, Kane A, Creppy EE, Dirheimer G (1993) Differential DNA adduct formation and disappearance in three mouse tissues after treatment with the mycotoxin ochratoxin A. *Mutat Res* 289:265-273.
- Sanchez-Ramos J, Facca A, Basit A, Song S (1998) Toxicity of dieldrin for dopaminergic neurons in mesencephalic cultures. *Exp Neurol* 150:263-271.
- Sava V, Reunova O, Velasquez A, Harbison R, Sanchez-Ramos J (2006) Acute neurotoxic effects of the fungal metabolite ochratoxin-A. *Neurotoxicology* 27:82-92.
- Sava V, Mosquera D, Song S, Stedeford T, Calero K, Cardozo-Pelaez F, Harbison R, Sanchez-Ramos J (2004) Rubratoxin B elicits antioxidative and DNA repair responses in mouse brain. *Gene Expr* 11:211-219.
- Stedeford T, Cardozo-Pelaez F, Nemeth N, Song S, Harbison RD, Sanchez-Ramos J (2001) Comparison of base-excision repair capacity in proliferating and differentiated PC 12 cells following acute challenge with dieldrin. *Free Radic Biol Med* 31:1272-1278.

APPENDIX

PUBLICATIONS

- P 24 Sava V, Reunova O, Velasquez A, Harbison R, Sanchez-Ramos J (2006) Acute neurotoxic effects of the fungal metabolite ochratoxin-A. *Neurotoxicology* 27:82-92.
- P 35 Sava V, Reunova O, Velasquez A, Sanchez-Ramos J (2006, re-submitted for review) Neuroanatomical Mapping Of DNA Repair And Antioxidative Responses In Mouse Brain: Effects Of A Single Dose Of MPTP
- P 68 Sava V, Mosquera D, Song S, Stedeford T, Calero K, Cardozo-Pelaez F, Harbison R, Sanchez-Ramos J (2004) Rubratoxin B elicits antioxidative and DNA repair responses in mouse brain. *Gene Expr* 11:211-219.
- P 95 Sava V, Reunova O, Velasquez A, Sanchez-Ramos J (2006) Can Low Level, Non-lethal Exposure to Ochratoxin-A Cause Parkinsonism? *J. Neurosci* (in press)

ABSTRACTS

- P 120 Acute Ochratoxin-A Neurotoxicity: Kinetics of distribution of the toxin, indices of oxidative stress and DNA repair activities in mouse brain
- P 121 Mycotoxins: Can Low Level, Non-lethal Exposure Result in Parkinsonism?
- P122 Regulation of DNA Repair in the MPTP Mouse Model of Parkinson's Disease

Acute neurotoxic effects of the fungal metabolite ochratoxin-A

V. Sava^{a,c}, O. Reunova^{a,c}, A. Velasquez^{a,c}, R. Harbison^b, J. Sánchez-Ramos^{a,c,*}

^a *University of South Florida, Department of Neurology (MDC 55), 12901 Bruce B. Downs Blvd., Tampa, FL 33612, USA*

^b *College of Public Health, University of South Florida, Tampa, FL, USA*

^c *Research Service, James Haley VA, Tampa, FL, USA*

Received 31 January 2005; accepted 12 July 2005

Available online 2 September 2005

Abstract

Ochratoxin-A (OTA) is a fungal metabolite with potential toxic effects on the central nervous system that have not yet been fully characterized. OTA has complex mechanisms of action that include evocation of oxidative stress, bioenergetic compromise, inhibition of protein synthesis, production of DNA single-strand breaks and formation of OTA–DNA adducts. The time course of acute effects of OTA were investigated in the context of DNA damage, DNA repair and global oxidative stress across six brain regions. Oxidative DNA damage, as measured with the “comet assay”, was significantly increased in the six brain regions at all time points up to 72 h, with peak effects noted at 24 h in midbrain (MB), CP (caudate/putamen) and HP (hippocampus). Oxidative DNA repair activity (oxyguanosine glycosylase or OGG1) was inhibited in all regions at 6 h, but recovered to control levels in cerebellum (CB) by 72 h, and showed a trend to recovery in other regions of brain. Other indices of oxidative stress were also elevated. Lipid peroxidation and superoxide dismutase (SOD) increased over time throughout the brain. In light of the known vulnerability of the nigro-striatal dopaminergic neurons to oxidative stress, levels of striatal dopamine (DA) and its metabolites were also measured. Administration of OTA (0–6 mg/kg i.p.) to mice resulted in a dose-dependent decrease in striatal DA content and turnover with an ED₅₀ of 3.2 mg/kg. A single dose of 3.5 mg/kg decreased the intensity of tyrosine hydroxylase immunoreactivity (TH+) in fibers of striatum, TH+ cells in substantia nigra (SN) and TH+ cells of the locus ceruleus. TUNEL staining did not reveal apoptotic profiles in MB, CP or in other brain regions and did not alter DARPP32 immunoreactivity in striatum. In conclusion, OTA caused acute depletion of striatal DA on a background of globally increased oxidative stress and transient inhibition of oxidative DNA repair.

© 2005 Elsevier Inc. All rights reserved.

Keywords: Ochratoxin-A; Oxyguanosine glycosylase; Superoxide dismutase; Dopamine; Tyrosine hydroxylase; Apoptosis; Substantia nigra; Striatum

1. Introduction

Ochratoxin-A (OTA) is a metabolite produced by *Aspergillus ochraceus* and *Penicillium verrucosum* that accumulates in the food chain because of its long half-life (Galtier, 1991; Kuiper-Goodman and Scott, 1989). In view of its ubiquity, the possible contribution of OTA to the development of human and animal diseases has been investigated (see review Marquardt and Frohlich, 1992). OTA has been shown to induce a tubulointerstitial nephropathy in animals (Krogh et al., 1974) and enzymuria (Kane et al., 1986a,b) similar to Balkan endemic nephropathy found in humans (Krogh, 1992; Krogh et al., 1974; Petkova-Bocharova et al., 1988). In addition to nephrotoxicity, OTA disrupts blood coagulation (Galtier et al., 1979; Gupta et al., 1979) and glucose metabolism (Pitout, 1968). It is

immunosuppressive (Creppy et al., 1983b; Haubeck et al., 1981; Lea et al., 1989; Stormer and Lea, 1995), teratogenic (Arora et al., 1983; Fukui et al., 1992; Szczech and Hood, 1981) and genotoxic (Creppy et al., 1985; Pfohl-Leskowicz et al., 1991).

Investigation of the effects of acute and chronic exposure to OTA on the nervous system has been scarce, even though development of nervous tissue appears to be very susceptible to the deleterious effects of OTA (Hayes et al., 1974; Wangikar et al., 2004). OTA has been reported to induce teratogenic effects in neonates (rats and mice) exposed in utero, characterized by microcephaly and modification of the brain levels of free amino acids (Belmadani et al., 1998). OTA was also reported to be neurotoxic to adult male rats fed OTA in the diet. Neurotoxicity, indicated by concentration of lactic dehydrogenase released from the dissected brain tissue, was more pronounced in the ventral mesencephalon, hippocampus, and striatum than in the cerebellum (Belmadani et al., 1998).

* Corresponding author. Tel.: +1 813 974 6022; fax: +1 813 974 7200.

E-mail address: jsramos@hsc.usf.edu (J. Sánchez-Ramos).

The bio-concentration of OTA in these brain regions did not correlate with toxicity (Belmadani et al., 1998).

The mechanism responsible for toxicity to neural tissues is not clear, but studies in peripheral organs and tissues reveal a spectrum of actions. The mechanisms of toxicity implicated include inhibition of protein synthesis, mitochondrial impairment, oxidative stress and DNA damage (Creppy et al., 1985, 1990; Dirheimer and Creppy, 1991; Gautier et al., 2001).

OTA-induced damage to DNA, evidenced by formation of single-strand breaks, has been reported to occur both in vitro and in vivo (Creppy et al., 1985). The DNA damage was shown to be reversible with time suggesting that variation in capacity to repair DNA may account in part for differences in vulnerability to OTA between tissues. OTA was also reported to induce single-strand breaks in a concentration-dependent manner in canine kidney cells and this effect could be potentiated by inhibition of DNA repair (Lebrun and Follmann, 2002). Other studies have demonstrated OTA–DNA adducts in mouse and monkey kidney after OTA treatment (Grosse et al., 1995). In kidney, liver and spleen, several modified nucleotides were clearly detected in DNA, 24 h after administration of OTA, but their levels varied significantly in a tissue and time-dependent manner over a 16-day period. The OTA–DNA adducts were not quantitatively and qualitatively the same in the three organs examined due to differences of metabolism in these organs and differences in the efficiency of DNA repair processes (Pfohl-Leszkwicz et al., 1993).

OTA treatment can increase oxidative stress in peripheral organs. Administration of OTA (1 mg/kg) to rats resulted in a 22% decrease in alpha-tocopherol plasma levels and a five-fold increase in the expression of the oxidative stress responsive protein heme oxygenase-1, specifically in the kidney (Gautier et al., 2001). More direct evidence of oxidative stress was derived from studies, which utilized electron paramagnetic resonance spectroscopy to measure the generation of hydroxyl radicals, in rat hepatocyte mitochondria and microsomes incubated with OTA and metabolites (Hoehler et al., 1997).

OTA toxicity is associated with inhibition of both protein and RNA synthesis (Dirheimer and Creppy, 1991). OTA is known to interfere with the charging of transfer ribonucleic acids (tRNA) with amino acids (Dirheimer and Creppy, 1991). In particular, OTA has been shown to inhibit bacterial, yeast and liver phenylalanyl-tRNA synthetases (Dirheimer and Creppy, 1991). The inhibition is competitive to phenylalanine and is reversed by an excess of this amino acid. OTA has also been shown to inhibit enzymes that use phenylalanine as a substrate such as phenylalanine hydroxylase (Dirheimer and Creppy, 1991).

Mitochondrial dysfunction has been shown to be involved in the development of OTA-induced toxicity in proximal renal tubule cells (Aleo et al., 1991). Respiration was reduced in the absence and presence of a phosphate acceptor using site I (glutamate/malate) and site II (succinate) respiratory substrates 15 and 30 min after exposure to 10^{-3} M OTA, implicating an action of OTA at both electron transport sites (Aleo et al., 1991). However, in isolated rat liver mitochondria, inhibition kinetic studies revealed that OTA is an uncompetitive inhibitor

of both succinate-cytochrome *c* reductase and succinate dehydrogenase while sparing cytochrome oxidase and NADH dehydrogenase activity (Complex I) at concentrations less than 10^{-5} M (Wei et al., 1985).

The objective of the present study was to evaluate the extent of OTA neurotoxicity across mouse brain regions in the context of oxidative stress, oxidative DNA damage and DNA repair. Deficits in DNA repair have long been implicated in a number of neurodegenerative diseases, including Alzheimer's disease and Parkinson's disease. It was our goal to determine whether regional differences in DNA repair capacity predicts vulnerability to the toxin. We hypothesized that OTA-induced oxidative DNA damage would not be homogeneous across all brain regions but would reflect the capacity of distinct regions of brain to respond with antioxidative repair processes. Given the body of evidence that nigro-striatal DA neurons are especially vulnerable to oxidative stress, we also hypothesized that DA levels in striatum would be affected by OTA. Hence, we measured the effects of OTA on striatal dopamine (DA) levels and parameters of oxidative stress in six brain regions cerebellum (CB), cortex (CX), hippocampus (HP), midbrain (MB), caudate/putamen (CP) and pons/medulla (PM). Parameters of oxidative stress measured included lipid peroxidation (thiobarbituric acid-reactive substances or TBARS), SOD activity, oxidative DNA damage and repair. The enzymatic activity of DNA glycosylase served as the index of DNA repair.

2. Materials and methods

2.1. Materials

Ochratoxin-A, SOD and dihydrobenzylamine were purchased from Sigma (St. Louis, MO). Protease inhibitors and DNA glycosylase were from Boehringer Mannheim (Indianapolis, IN, USA). 32 P-ATP was from NEN Life Science Products (Wilmington, DE). Rabbit anti-tyrosine hydroxylase was purchased from Pel-Freez Biologicals (Arkansas, AR). Rabbit primary antibodies to DARPP32 (dopamine and cyclic AMP regulated phosphoprotein) were purchased from Chemicon, CA. ApopTag in situ Apoptosis Detection Kit and goat anti-rabbit secondary antibody were from Chemicon, CA. All other reagents were from Sigma Chemical Co.

2.2. Animals and treatment

The animal protocol used in this study was approved by the University of South Florida IUCAC committee. The protocol was also reviewed and approved by the Division of Comparative Medicine of the University, which is fully accredited by AAALAC International and managed in accordance with the Animal Welfare Regulations, the PHS Policy, the FDA Good Laboratory Practices, and the IACUC's Policies.

Male Swiss ICR mice (22 ± 2 g) were obtained from the Jackson Laboratories (Bar Harbor, ME). They were housed five per cage at the temperature of 21 ± 2 °C with 12 light/dark

cycle and free access to food and water. Mice were divided into experimental (total $n = 70$) and control (total $n = 20$) groups. Animals were injected with either OTA dissolved in 0.1 M NaHCO_3 mg/kg i.p. or vehicle (0.1 M NaHCO_3). After injection with OTA or vehicle, mice were observed for changes in spontaneous behavior three times each day until euthanasia. The response to handling was also noted. In particular, evidence for toxic effects such as claspings of limbs in response to being held by the tail was to be recorded. Groups of mice were euthanatized with CO_2 at 6, 24, and 72 h after injection with OTA or vehicle. The brains were removed and immediately dissected on ice.

2.3. Isolation of brain regions

Brains were separated into six regions under a dissecting stereo-microscope in the following order. The cerebellar peduncles were cut first, and brain stem was removed from the diencephalon. The ventral and dorsal parts of midbrain (MB) were dissected at the level of the caudal end of the cerebral peduncles at the junction with the pons. The pons and medulla (PM) were separated together by cutting the pontomedullary junction. The cerebral hemispheres were opened with a sagittal cut along the longitudinal tissue and hippocampus (HP) was isolated, followed by caudate and putamen (CP). Finally, cerebellum (CB) and cerebral cortex (CX) were harvested and all the samples were kept frozen at -70°C until assayed (see Fig. 1).

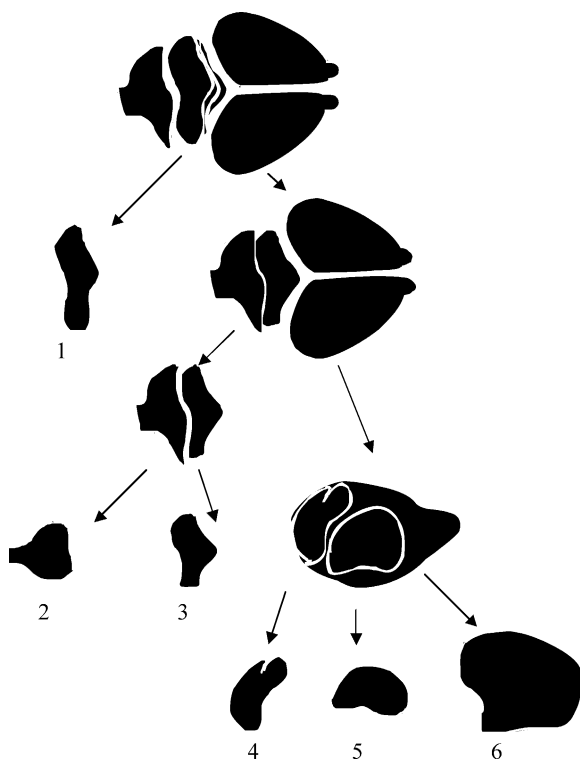


Fig. 1. Each mouse brain was dissected on ice under a stereo-microscope into six regions: (1) cerebellum (CB); (2) pons/medulla (PM); (3) midbrain (MB); (4) hippocampus (HP); (5) caudate/putamen (CP); (6) cerebral cortex (CX).

2.4. Evaluation of OTA neurotoxicity

Mice of either sex were distributed into six groups containing eight animals with an equal number of both sexes in each group. The first group of untreated animals was considered as a control, and the other five groups were treated with OTA given intraperitoneally in doses of 0–6 mg/kg of body weight. Striatal dopamine concentration was measured with HPLC 24 h after OTA administration, and the dose that caused 50% reduction in striatal DA concentrations (ED₅₀) was calculated using the GraphPad Software, Inc. (San Diego, CA). The ED₅₀ was determined for eight animals in each group.

2.5. DNA damage evaluated by the comet assay

The comet assay was based on a modification of a previously published method (Schindewolf et al., 2000). Two layers of agarose were prepared. For the first layer, 85 μL 1% (w/v) high-melting point (HMP) agarose (Sigma) prepared at 95°C in PBS was pipetted onto fully frosted microscope slides, covered with coverslip and allowed to set at 4°C for 10 min. Cells were dissociated with 3% trypsin and RNase following washing in PBS, centrifuged at $700 \times g$ for 15 min and resuspended at 2×10^5 in 85 μL 1% (w/v) low-melting point (LMP) agarose (Sigma). The cell suspension was then pipetted over the set HMP agarose layer, covered with coverslip and allowed to set at 4°C for 10 min. After the coverslips were removed, the slides were immersed in pre-chilled lysis solution [2.5 M NaCl, 100 mM sodium EDTA, 10 mM Tris, pH adjusted to 10 using NaOH pellets, 1% Triton X-100 (v/v) (added immediately before use)] for 60 min at 4°C to remove cellular proteins. Following lysis, slides were placed in a gel electrophoresis unit and incubated in fresh alkaline electrophoresis buffer (300 mM NaOH, 1 mM EDTA, pH 13) for 40 min at room temperature, before being electrophoresed at 25 V (300 mA) for 30 min at 4°C . All the above procedures were conducted in the dark to minimize extraneous sources of DNA damage. Following electrophoresis, the slides were immersed in neutralization buffer (0.4 M Tris-HCl, pH 7.5) and gently washed three times for 5 min at 4°C to remove alkalis and detergents. SYBR Green (50 μL ; Trevigen, Gaithersburg, MD) was added to each slide to stain the DNA, then covered with a coverslip and kept in the dark before viewing. Slides were examined at $250\times$ magnification on a Zeiss inverted fluorescence microscope (Zeiss, Germany) at 460 nm. One hundred randomly selected nonoverlapping cells were visually assigned a score based on perceived comet tail length migration and relative proportion of DNA in the comet tail. The extent of DNA damage was calculated as follows:

$$\text{DNA damage} = \text{tail length} / \text{diameter of comet head}.$$

2.6. Assessment OGG1 activity

The procedure for extraction of DNA glycosylase was similar to that described previously (Cardozo-Pelaez et al., 2000). Punched tissues were sonicated in homogenization

buffer containing 20 mM Tris, pH 8.0, 1 mM EDTA, 1 mM dithiothriol (DTT), 0.5 mM spermine, 0.5 mM spermidine, 50% glycerol and protease inhibitors and homogenates were rocked for 30 min after addition of 1/10 volume of 2.5 M KCl. Samples were spun at 14,000 rpm for 30 min and supernatants were collected.

The OGG1 activities in supernatants were determined using duplex oligonucleotide containing 8-oxodG as incision substrate. For preparation of the incision assay, 20 pmol of synthetic probe containing 8-oxodG (Trevigen, Gaithersburg, MD) was labeled with ^{32}P at the 5' end using polynucleotide T4 kinase (Boehringer Mannheim, Germany). Unincorporated free ^{32}P -ATP was separated on G25 spin column (Prime; Inc., Boulder, CO). Complementary oligonucleotides were annealed in 10 mM Tris, pH 7.8, 100 mM KCl, 1 mM EDTA by heating the samples 5 min at 80 °C and gradually cooling at room temperature.

Incision reactions were carried out in a mixture (20 μL) containing 40 mM HEPES (pH 7.6), 5 mM EDTA, 1 mM DTT, 75 mM KCl, purified bovine serum albumin, 100 fmol of ^{32}P -labeled duplex oligonucleotide, and extracted guanosine glycosylase (30 μg of protein). The reaction mixture was incubated at 37 °C for 2 h and products of the reaction were analyzed on denaturing 20% polyacrylamide gel. Pure OGG1 served as positive control and untreated duplex oligonucleotide was used for negative control. The gel was visualized with a Biorad-363 Phosphoimager System. The incision activity of OGG1 was calculated as the amount of radioactivity in the band representing specific cleavage of the labeled oligonucleotide over the total radioactivity. Data were normalized to equal concentration of protein, the concentration of which was measured using the bicinchoninic acid assay (Smith et al., 1985).

2.7. SOD assay

Determination of superoxide dismutase activity in mouse brain was based on inhibition of nitrite formation in reaction of oxidation of hydroxylammonium with superoxide anion radical (Elstner and Heupel, 1976). Nitrite formation was generated in a mixture contained 25 μL xanthine (15 mM), 25 μL hydroxylammonium chloride (10 mM), 250 μL phosphate buffer (65 mM, pH 7.8), 90 μL distilled water and 100 μL xanthine oxidase (0.1 U/mL) used as a starter of the reaction. Inhibitory effect of inherent SOD was assayed at 25 °C during 20 min of incubation with 10 μL of brain tissue extracts. Determination of the resulted nitrite was performed upon the reaction (20 min at room temperature) with 0.5 mL sulfanilic acid (3.3 mg/mL) and 0.5 mL α -naphthylamine (1 mg/mL). Optical absorbance at 530 nm was measured on Ultrospec III spectrophotometer (Pharmacia, LKB). The results were expressed as units of SOD activity calculated per milligram of protein. The amount of protein in the samples was determined using the bicinchoninic acid (Smith et al., 1985).

2.8. Lipid peroxidation assay

Formation of lipid peroxide derivatives was evaluated by measuring thiobarbituric acid-reactive substances (TBARS)

according to a previously reported method (Cascio et al., 2000). Briefly, the different regions of brain were individually homogenized in ice-cold 1.15% KCl (w/v); then 0.4 mL of the homogenates were mixed with 1 mL of 0.375% TBA, 15% TCA (w/v), 0.25N HCl and 6.8 mM butylated-hydroxytoluene (BHT), placed in a boiling water bath for 10 min, removed and allowed to cool on ice. Following centrifugation at 3000 rpm for 10 min, the absorbance in the supernatants was measured at 532 nm. The amount of TBARS produced was expressed as nmol TBARS/mg protein using malondialdehyde bis(dimethyl acetal) for calibration.

2.9. Measurement of dopamine and metabolites

HPLC with electrochemical detection was employed to measure levels of dopamine (DA) as previously reported in our laboratory (Cardozo-Pelaez et al., 1999). Tissue samples were sonicated in 50 volumes of 0.1 M perchloric acid containing 50 ng/mL of dihydrobenzylamine (Sigma Chemical, MA) as internal standard. After centrifugation (15,000 $\times g$, 10 min, 4 °C), 20 μL of supernatant was injected onto a C18-reversed phase RP-80 catecholamine column (ESA, Bedford, MA). The mobile phase consisted of 90% of a solution of 50 mM sodium phosphate, 0.2 mM EDTA, and 1.2 mM heptanesulfonic acid (pH 4) and 10% methanol. Flow rate was 1.0 mL/min. Peaks were detected by a Coulchem 5100A detector (ESA). Data were collected and processed with TotalChrom software (Perkin Elmer Instruments).

2.10. Tissue preparation

Mice were euthanatized after 72 h of a single injection with OTA. They were then perfused via the heart and ascending aorta with 25 mL ice-cold phosphate buffered saline (0.1 M PBS), followed by 50 mL freshly prepared 4% paraformaldehyde in PBS (pH 7.4). Brains were rapidly removed and immersion fixed for 24 h in freshly prepared 4% paraformaldehyde. The brains were then incubated for 24 h in 30% sucrose to cyroprotect them. For tyrosine hydroxylase immunohistochemistry, tissue blocks were cut and mounted in a Leitz cryostat and sectioned using the Paxinos mouse brain atlas as a guide (Paxinos and Franklin, 2001). Tissue sections to be used for tyrosine hydroxylase immunochemistry were selected from the striatal block (Bregma +0.14 at level of anterior commissure to Bregma +1.18); and hippocampal and midbrain block (Bregma -2.8 to -3.46) and the cerebellar/pons block (Bregma -5.84 to -6.24). For TUNEL staining, sagittal sections of 25- μm thickness were placed on Superfrost/Plus Microscope Slides (precleaned) and processed with immunohistochemical staining methods as described below.

2.11. Immunohistochemistry

Mouse brains were placed in ice-cold aluminum brain molds and cut into 2 mm coronal blocks. These tissue blocks were mounted in a cryostat and sectioned using a mouse brain atlas as a guide (Paxinos and Franklin, 2001). In several mouse brains,

tissue was blocked into two mid-sagittal parts and tissue sections (25 μm thin) were cut in the parasagittal plane to include the entire extent of striatum, pallidum and midbrain. Tissue sections to be used for tyrosine hydroxylase immunohistochemistry were selected from the striatal block (Bregma +0.14 at level of anterior commissure to Bregma +1.18); and hippocampal and midbrain block (Bregma -2.8 to -3.46) and the cerebellar/pons block (Bregma -5.84 to -6.24). For TUNEL staining sections were sampled from all the blocks encompassing forebrain to cerebellum and brainstem. Thin sections (25 μm) were placed on Superfrost/Plus Microscope Slides (precleaned) and processed by using the staining method described below.

2.11.1. Tyrosine hydroxylase (TH) immunoreactivity

Tissue sections were fixed for 30 min at room temperature in 4% paraformaldehyde prepared on PBS (pH 7.4) and then transferred to PBS containing 5% sucrose. After 15 min of incubation sections were treated with 10% H_2O_2 in 95% MeOH for 30 min at room temperature to destroy endogenous peroxidase. Then sections were blocked at room temperature during 60 min with 10% goat serum (Sigma Chemicals, MI) prepared on PBS containing 0.3% Triton X-100. Rabbit anti-tyrosine hydroxylase (Pel-Freez Biologicals, Arkansas) was the primary antibody (1:1000) and it was prepared in PBS containing 10% goat serum and 0.3% Triton X-100. The sections were incubated with primary antibody overnight at 4 °C and then washed in three changes of PBS for 10 min each. Goat anti-rabbit (Chemicon, CA) secondary antibody was prepared on PBS/Triton X-100 buffer (1:300) and incubated with samples for 60 min at room temperature. Then sections were washed for 10 min in three changes of PBS, treated with avidin–biotin–complex (Vectastain ABC Kit (Peroxidase Standard*), Vector Labs, CA) for 60 min and developed with 3,3'-diaminobenzidine (DAB Substrate Kit, Vector Labs, CA) at room temperature during 2–5 min. Finally the sections were rinsed with distilled water to stop reaction and then dehydrated in ethanol, and cleared in xylene. Controls for nonspecific staining were performed for evaluation in which either primary or secondary antibody was applied alone.

2.11.2. TUNEL assay

TUNEL staining was performed following the methods described in ApopTag Plus Fluorescein In Situ Apoptosis Detection Kit (S7111) and ApopTag Peroxidase In Situ Apoptosis Detection Kit (S7100) (Chemicon, CA). Slide-mounted tissue sections were post-fixed in precooled ethanol:acetic acid (2:1) for 5 min at -20 °C in a Coplin jar and rinsed two times for 5 min with PBS. For ApopTag Peroxidase staining slices were quenched in 3.0% hydrogen peroxidase in PBS for 5 min at room temperature and rinsed twice with PBS for 5 min each time. Equilibration buffer was immediately applied directly to the specimen for 20 s at room temperature. TdT enzyme was pipetted onto the sections following by incubation in a humidified chamber for 1 h at 37 °C. Specimens were placed in a Coplin jar containing working strength stop/wash buffer and incubated for 10 min at room temperature.

After triple rinsing in PBS, the sections were incubated with anti-digoxigenin conjugate (fluorescence) or anti-digoxigenin peroxidase conjugate accordingly in a humidified chamber for 30 min at room temperature. The specimen for fluorescence apoptosis staining were rinsed with PBS (4×2 min) and mounted on a glass cover slip with Vectashield mounting medium containing DAPI or PI (Vector Labs, CA). The specimens for peroxidase staining were rinsed with PBS (4×2 min) and color was provided in peroxidase substrate (DAB Substrate KIT for peroxidase, Vector Labs). Then sections were rinsed in three changes of dH_2O for 1 min each wash and counterstained in methyl green (Vector Labs). The specimens were dehydrated and mounted under a glass coverslip in mounting medium. Samples were then examined with bright field microscopy or in the case of fluorescently tagged antibodies, with a Zeiss Scanning Confocal microscope (Model LSM510).

2.11.3. Rabbit anti-DARPP32

Sections were immunostained for DARPP32, a protein expressed by striatal neurons and which has been used to characterize effects of toxicants on striatal neurons (Haug et al., 1998; Stefanova et al., 2003). Cryosections were rinsed in PBS three times for 10 min each wash. Then the sections were incubated with “blocking” solution (PBS containing 10% goat serum (Sigma, Missouri), 0.3% Triton X-100) at room temperature for 60 min. Primary antibody rabbit anti-DARPP32 (Chemicon, CA) diluted in carrier solution (PBS, goat serum, Triton X-100, primary antibody 1:300) was placed onto the sections and incubated overnight at 4 °C.

Secondary antibody goat anti-rabbit secondary (Alexa Fluor 594 (rodamine) Chemicon, CA) was applied to the slides (PBS, Triton X-100, secondary antibody—1:300) for 60 min at room temperature. Finally, the sections were rinsed with PBS (3×10 min) and mounted on a glass cover slip with Vectashield mounting medium containing DAPI (Vector Labs, CA). Appropriate controls without primary antibodies were also prepared to assess nonspecific immunohistochemical staining. In some sections, propidium iodide (PI) from Molecular Probes (Eugene, OR) was used to counterstain nucleic acid. Laser Scanning confocal microscopy (Zeiss LSM 510) was used to resolve TUNEL-stained tissues counterstained with PI.

2.12. Statistical analysis

The results were reported as mean \pm S.E.M. for at least five individual samples of specific brain regions, assayed in duplicate. Two-way ANOVA was performed to assess the contribution of brain region, time of analysis and their interaction on variance. Post-hoc *t*-tests with Bonferroni corrections were performed to compare values at each time point to control (untreated) values.

For electrophoresis, two different gels were run. The differences between samples were analyzed by the Student's *t*-test, and a $p < 0.05$ was considered as statistically significant. The Pearson correlation coefficients between DNA repair

Table 1

Development of TBARS response in different regions of mouse brain following i.p. administration of 3.5 mg/kg of OTA

Brain regions	TBARS (pmol/mg protein)			
	Control	6 h	24 h	72 h
CB	2.44 ± 0.2	3.99 ± 0.35*	5.54 ± 0.48*	8.54 ± 0.77*
PM	2.41 ± 0.17	4.80 ± 0.43*	6.09 ± 0.55*	9.13 ± 0.89*
HP	2.23 ± 0.21	4.69 ± 0.4*	6.03 ± 0.52*	8.57 ± 0.88*
MB	3.17 ± 0.28	4.22 ± 0.33*	6.09 ± 0.53*	9.16 ± 0.81*
CP	2.65 ± 0.22	3.58 ± 0.32*	5.63 ± 0.49*	8.39 ± 0.79*
CX	3.19 ± 0.27	4.01 ± 0.41*	6.78 ± 0.63*	10.31 ± 0.98*

* The values are significantly ($p < 0.05$) different compared to controls. All results represented by mean ± S.E.M.

(OGG1) and basal DNA damage (comet assay) across brain regions were determined at each time point by correlation analysis using GraphPad Software, Inc. (San Diego, CA).

3. Results

Administration of OTA at doses less than 6 mg/kg i.p. (below the reported LD50 of 39.5 mg/kg i.p. in mice, Moroi et al., 1985) did not elicit obvious alterations in mouse behavior and locomotor activity at any time up to 3 days after treatment. Behavior was not measured instrumentally, but was based on visual inspections over the course of 3 days and response to handling. In particular, there was no abnormal posturing or clamping of limbs when mice were picked up by the tail.

Administration of a single dose of OTA (3.5 mg/kg i.p.) rapidly evoked oxidative stress across all brain regions. TBARS levels, indicators of lipid peroxidation, increased in a monophasic time-dependent manner in all brain regions of animals exposed to OTA as compared to control mice (Table 1). This same dose of OTA caused a rapid upregulation of SOD activities in all regions of brain, with peak values reached after 24 h. However, the elevation of the SOD antioxidative response was maintained only for a short time, returning to control levels or below after 72 h (Table 2).

Oxidative DNA damage, estimated from the comet assay (Fig. 2), was increased early across all brain regions (Fig. 3) and remained elevated at all time points. Peak elevation was

Table 2

Development of SOD response in different regions of mouse brain during intoxication caused by i.p. administration of 3.5 mg/kg of OTA

Brain regions	SOD (U/g protein)			
	Control	6 h	24 h	72 h
CB	0.39 ± 0.04	0.38 ± 0.03	0.71 ± 0.07*	0.35 ± 0.03
PM	0.557 ± 0.05	0.61 ± 0.05	0.8 ± 0.08*	0.37 ± 0.03
HP	0.37 ± 0.03	0.39 ± 0.03	0.81 ± 0.07*	0.33 ± 0.03
MB	0.36 ± 0.03	0.44 ± 0.04	0.79 ± 0.07*	0.34 ± 0.02
CP	0.34 ± 0.02	0.36 ± 0.03	0.73 ± 0.06*	0.32 ± 0.02
CX	0.53 ± 0.04	0.55 ± 0.04	0.91 ± 0.08*	0.36 ± 0.04

* The values are significantly ($p < 0.05$) different compared to controls. All results represented by mean ± S.E.M.

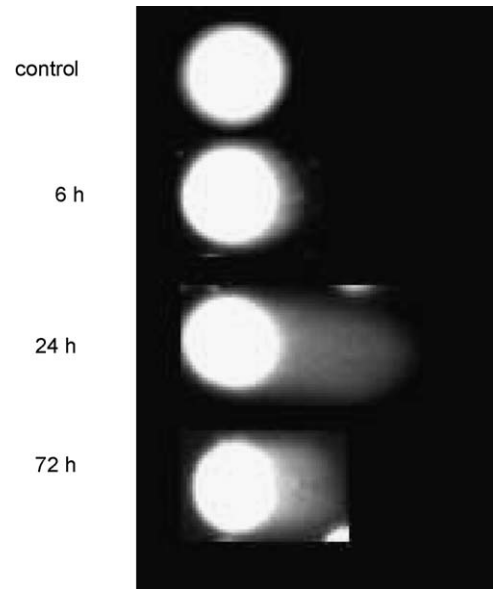


Fig. 2. Representative photomicrographs of "comets" in the substantia nigra obtained at 6, 24 and 72 h after OTA injection (3.5 mg/kg, i.p.).

observed at 24 h where the magnitude of increase ranged from 1.8 to 2.9 times the control levels. The MB, CP and HP showed the highest levels of oxidative DNA damage.

Concomitant with the increased levels of oxidative DNA damage, the DNA repair enzyme OGG1 was significantly decreased across all brain regions at 6 h with a gradual return to near normal levels by 72 h (Fig. 4). The activity of OGG1 across the six brain regions was inversely correlated to basal levels of DNA damage at all time points except for 72 h (the Pearson correlation coefficients were -0.88 at 0 h; -0.89 at 6 h; -0.85 at 24 h; -0.45 at 72 h—see Fig. 5). Oxidative DNA repair activity recovered completely by 72 h in CB but

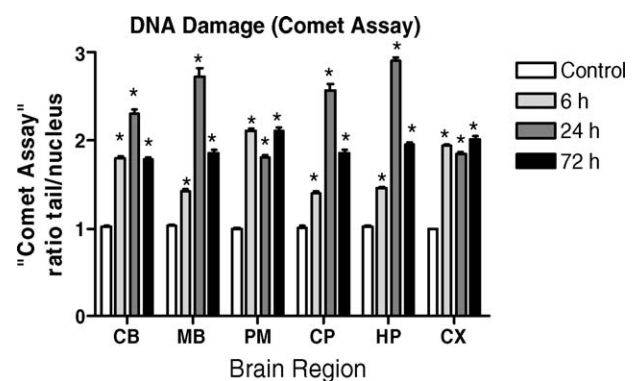


Fig. 3. Time course of effects of OTA on DNA damage across six brain regions mice following administration of OTA (3.5 mg/kg, i.p.). The extent of DNA damage was calculated from relative changes in length of comet tails. The mean ± S.E.M. was determined from the average of 50 cells calculated for three animals in each experimental group (control, 6, 24 and 72 h). Two-way ANOVA revealed that brain region and time each contributed significantly to the variance ($p < 0.0001$); there was no statistically significant interaction between time course and region. Post-hoc comparison of values at each time point compared to controls revealed significant increases at each time point for each region (asterisks indicate $p < 0.05$; t -test with Bonferroni correction for multiple comparisons).

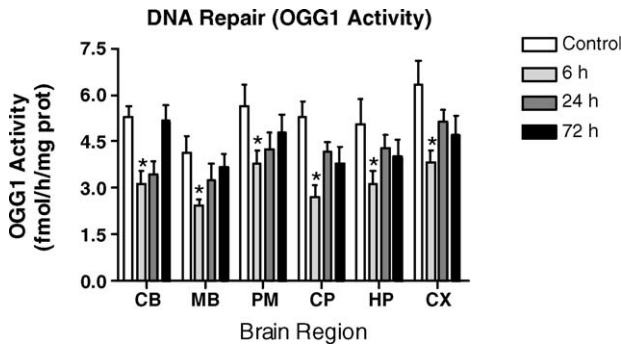


Fig. 4. Time course of OTA effects on OGG1 activity across specific brain regions. Results are expressed as mean \pm S.E.M. ($n = 4-6$ samples per brain region). Two-way ANOVA revealed that brain region and time each contributed significantly to the variance ($p < 0.0001$); there was no statistically significant interaction between time course and region. Post-hoc comparison of values at each time point compared to controls revealed significant decreases at 6 h in each region (asterisks indicate $p < 0.05$; t -test with Bonferroni correction for multiple comparisons).

remained depressed in all other regions despite a trend towards recovery. The CP, CX and HP exhibited the least degree of recovery of OGG1 activity; at 72 h, the CP remained inhibited by 28%, the CX by 26% and the HP by 21% compared to control OGG1 levels.

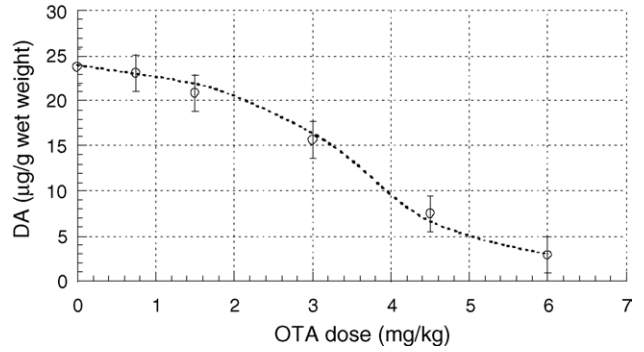


Fig. 6. Dose–response curve obtained following i.p. administration of OTA. DA concentration was measured in CP of ICR mice 24 h after administration of OTA. The results are expressed as mean \pm S.E.M. Data averaged for five animals.

In light of the long-standing premise that the nigro-striatal DA system is vulnerable to oxidative stress (a view that has been recently challenged, Ahlskog, 2005), we measured levels of DA and its metabolites in the striatum. OTA administration resulted in a dose-dependent decrease in striatal (caudate/putamen) DA with an ED₅₀ of 3.2 mg/kg (Fig. 6). A time-course study of the effects of a single dose (3.5 mg/kg i.p.) revealed an early (6 h) 1.38-fold elevation of

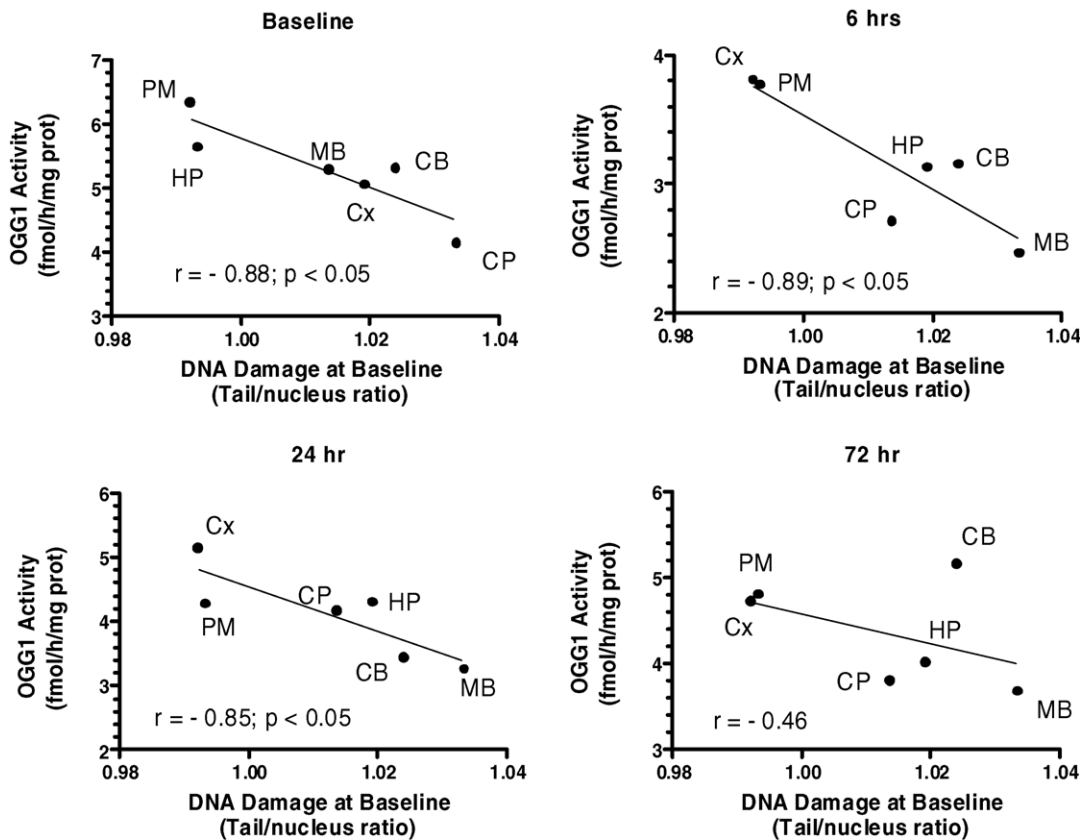


Fig. 5. Relationship between DNA repair (OGG1) and basal levels of oxidative damage in six brain regions. Each panel plots OGG1 activity against the baseline oxidative DNA damage (tail/nucleus ratio of the comet assay) in each brain region at 6, 24 and 72 h after a single dose of OTA (3.5 mg/kg). Pearson correlation coefficients were determined for each time point shown in the four panels. There was a significant inverse correlation between DNA repair activity and baseline level of DNA damage across regions at all time points except 72 h.

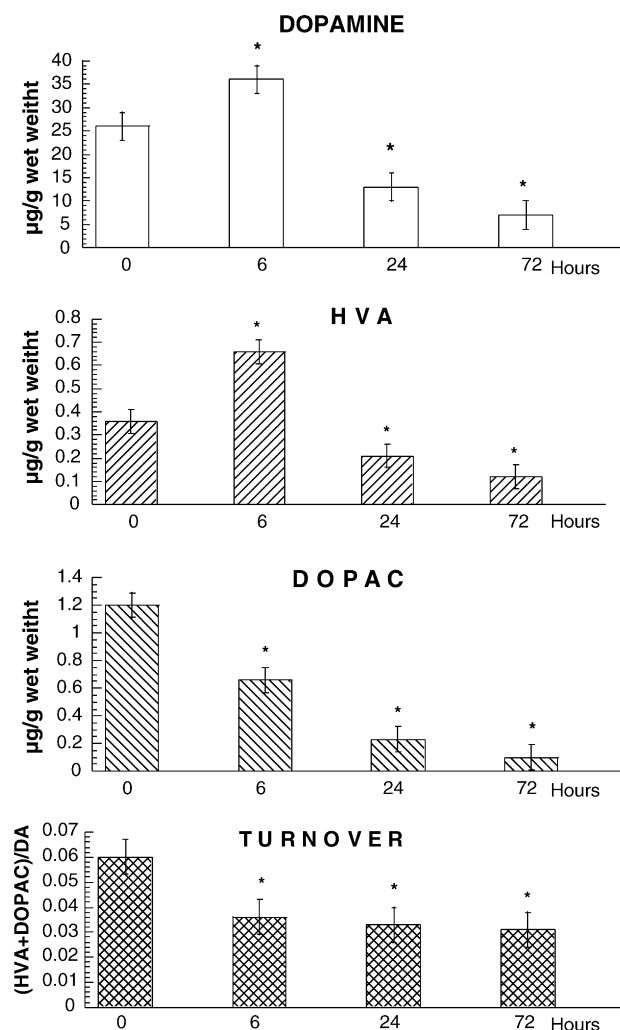


Fig. 7. Effect of OTA administration (3.5 mg/kg, i.p.) on DA metabolism during time course of developed intoxication in brain of ICR mice. Asterisks indicate significance of differences against control ($p < 0.05$). The results are expressed as mean \pm S.E.M. ($n = 6$).

DA as compared to control (Fig. 7). After 24 h, DA concentration dropped to 46% of control levels and declined even further by 72 h. A similar kinetic profile was recorded for HVA, while DOPAC levels did not increase at 6 h but showed a steady decline. The turnover of DA calculated as ratio of (HVA + DOPAC)/DA was significantly reduced at all time points (Fig. 7).

Catecholaminergic cells and terminals in the SN, CP and locus ceruleus were affected by OTA as evidenced by a qualitative decrease in tyrosine hydroxylase (TH) immunoreactivity in those structures (Fig. 8, rows A–C). However, the decreased immunostaining was not a result of OTA-induced cell death because TUNEL staining across these and other brain regions failed to reveal apoptotic nuclei (data not shown). DARPP32 immunostaining of cells of the striatum and midbrain (SNpars reticulata) did not reveal differences between OTA and control brains, indicating that there was no direct cytopathic effect on this population of neurons by 72 h after administration (Fig. 8, rows D and E).

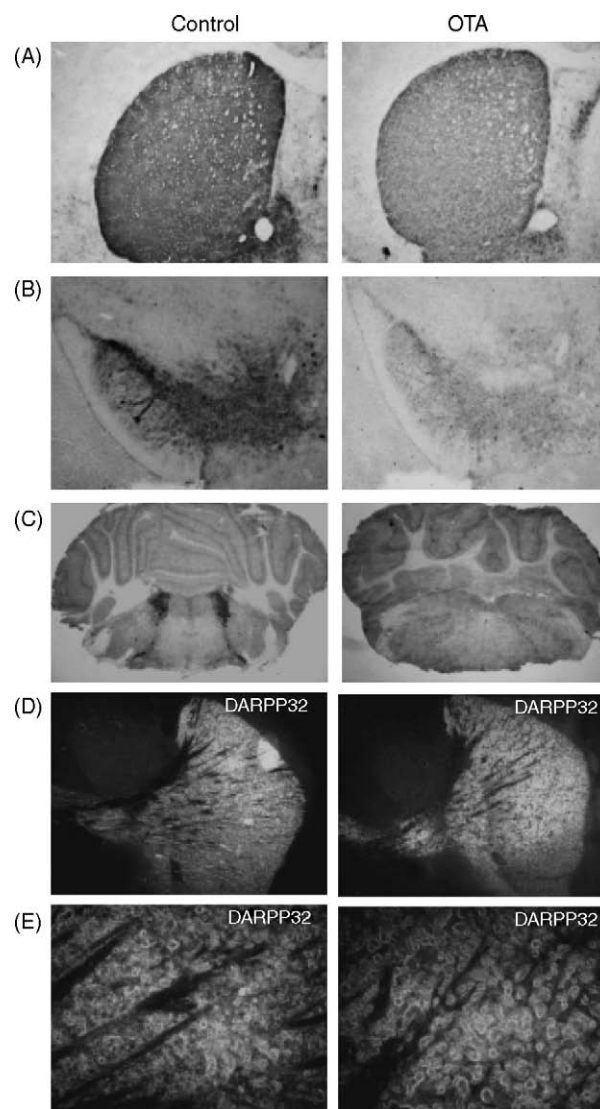


Fig. 8. Representative photomicrographs of TH immunoreactivity in the caudate putamen (row A), substantia nigra (row B) and locus ceruleus (row C) obtained 72 h after OTA injection (3.5 mg/kg, i.p.). Controls are in the left-hand panels. Intensity of TH immunoreactivity is decreased in all three loci in mice treated with OTA. DARPP32 immunohistochemistry is shown in rows D and E. Parasagittal cut through striatum (CP) showing no difference in DARPP32 signal intensity and distribution in OTA-treated compared to control mouse brains (magnification in row D = 40 \times ; in row E = 200 \times).

4. Discussion

Administration of OTA, at a single dose (3.5 mg/kg) that is approximately 10% of the reported LD50, resulted in widespread oxidative stress across six brain regions. This was evidenced by significant increases in lipid peroxidation and oxidative DNA damage across all brain regions. Furthermore, OTA treatment elicited an early and sustained surge in activity of SOD, a major oxyradical scavenger, across all brain regions. Unlike the monophasic SOD activation, the oxidative DNA repair response exhibited a biphasic response, with an initial inhibition of OGG1 activity followed by a trend towards recovery to normal levels after 3 days. This is quite different

than the acute effects of another pro-oxidant agent, diethyl maleate (DEM), which elicited an early (6 h after injection) and significant upregulation of OGG1 in mouse CB, CX, PM, but not in MB, CP or HP, despite equally decreased glutathione levels in all brain regions (Cardozo-Pelaez et al., 2002). In addition, the DNA repair response to rubratoxin-A (RTA), a mycotoxin with poorly understood complex mechanisms of action in brain, was similar but not identical to that of diethyl maleate. Administration of a single dose of RTA resulted in significant upregulation of the DNA repair enzyme OGG1 in CB, CP, and CX, but not in HP, MB and PM at 24 h, in the presence of *decreased or unchanged levels* of lipid peroxidation in all regions (Sava et al., 2004). In the present study, the OGG1 activity was suppressed equally in all brain regions and only the CB recovered to baseline levels by 72 h, while other regions (CP, HP and CX) approached baseline but stayed mildly suppressed. It should be pointed out that the results in the DEM and RTA experiments cannot be directly compared with the present findings because only a single time point was assessed (6 h in the DEM study and 24 h in the RTA study) and no measurements of DA levels in striatum were made in those earlier experiments (Sava et al., 2004).

Based on our previous work with diethyl maleate and rubratoxin-A, we had expected that the DNA repair response to OTA would show that some regions of brain were more capable of OGG1 upregulation than others. Our working hypothesis was based on the concept that variation in DNA repair was a potential factor in determining neuronal vulnerability; deficient DNA repair processes have been associated with Parkinson's disease (PD) as well as with other neurodegenerative diseases such as Alzheimer's disease, amyotrophic lateral sclerosis (ALS) and Huntington's disease (HD) (Lovell et al., 2000; Mazzarello et al., 1992; Robbins et al., 1985). In addition, we have previously shown that the uneven distribution of oxidative DNA damage across brain regions caused by endogenous or exogenous factors was determined, in part, by the intrinsic capacity to repair oxidative DNA damage (Cardozo-Pelaez et al., 1999, 2000). In those earlier studies, and in the present report, we focused on oxyguanosine glycosylase (OGG1), a key enzyme involved in the repair of the oxidized base, 8-hydroxy-2'-deoxoguanosine (8-oxoG). This reaction results in hydrolysis of the *N*-glycosylic bond between the 8-oxoG and deoxyribose, releasing the free base and leaving an apurinic/aprimidinic (AP) site in DNA. Such AP sites are cytotoxic and mutagenic, and must be further processed. Some DNA glycosylases also have an associated AP lyase activity that cleaves the phosphodiester bond 3' to the AP site (Dianov et al., 1998). Un-repaired DNA damage in post-mitotic cells, such as neurons, can result in disruption of transcriptionally active genes, cellular dysfunction and apoptosis (Hanawalt, 1994). Hence it was reasonable to hypothesize that diminished DNA repair capacity in populations of neurons would be associated with increased vulnerability to potentially genotoxic agents. Since the CP and MB showed a relatively diminished OGG1 activity and increased oxidative DNA damage (comet assay), we postulated that the DA terminals of the striatum would suffer damage.

This concept was supported by the report of increased oxidative DNA damage in substantia nigra and striatum in post-mortem brain from PD cases (Sanchez-Ramos et al., 1994), and by the observation that MB and CP were less able to upregulate OGG1 repair activity in response to the pro-oxidant, diethylmaleate (Cardozo-Pelaez et al., 2002). To further test this hypothesis, we measured the effects of OTA on striatal DA levels. Administration of OTA caused a dose-dependent decrease of striatal DA and a decrease in DA turnover. The nearly 50% reduction in striatal DA caused by a single dose (3.5 mg/kg i.p.) did not produce observable changes in daytime mouse behavior or locomotor activity, though it is likely that more sensitive, quantitative measures of behavior may reveal alterations. This dose of OTA also resulted in diminished TH immunoreactivity in the CP and MB as well as in the locus ceruleus (which contains noradrenergic neurons). The effects of OTA on catecholaminergic systems appeared to reflect a potentially reversible action rather than a cytotoxic effect because we found no evidence of cell death by 72 h. There were no apoptotic profiles found in SN and CP or any other region of the brain. In addition, there did not appear to be cytotoxic effects on striatal neurons identified by DARPP32 immunostaining.

It may be that the more rapid return of OGG1 activity to normal by 3 days in CB reflects an uneven distribution of the mycotoxin across brain regions. In the present report, the distribution of the toxin itself across brain regions was not investigated. However, previously published reports indicate that the cerebellum, ventral midbrain, and striatum accumulate the highest levels of OTA after 8 days of intragastric administration of a low dose (289 μ g/kg/day) (Belmadani et al., 1998). Cerebellar concentrations of OTA accounted for 34% of the total brain OTA and one might expect that this structure would exhibit the greatest degree of oxidative stress and decreased capacity to repair oxidative DNA damage. On the contrary, the present findings demonstrate that the cerebellum exhibited complete recovery of OGG1 activity whereas other regions, reported to accumulate much lower levels of OTA, did not recover DNA repair capacity to as great an extent. Similarly, it has been reported that the cerebellum exhibited the least degree of cytotoxicity evidenced by LDH release; the greatest release of LDH was reported to be in ventral midbrain, hippocampus, and striatum which accumulated much less OTA than the cerebellum (Belmadani et al., 1998). Hence the relationship between regional concentration of OTA and regional vulnerability to the toxin is not clear.

A potential explanation for the observations reported here relates to bioenergetic compromise evoked by OTA. This mycotoxin has been reported to inhibit succinate-dependent electron transfer activities of the respiratory chain, but at higher concentrations will also inhibit electron transport at Complex I (Aleo et al., 1991; Wei et al., 1985). The nigro-striatal dopaminergic system is well known to be especially vulnerable to the mitochondrial toxicants, MPTP and rotenone, especially when the latter toxicant is administered chronically at low doses (Betarbet et al., 2000; Hasegawa et al., 1990; Vyas et al., 1986). Other mitochondrial poisons like nitropropionic acid

and malonate interfere with succinate dehydrogenase/Complex II. These Complex II inhibitors result in lesions primarily localized to striatum (Calabresi et al., 2001; Schulz et al., 1996). Bioenergetic compromise may lead to persistent activation of NMDA receptors which results in excitotoxicity mediated by the neurotransmitter glutamate in regions of brain richly innervated by glutamatergic fibers, accounting for the vulnerability of the striatum and pallidum, and possibly the SN (Greenamyre et al., 1999; Turski and Turski, 1993). In addition, Ca^{2+} entering neurons through NMDA receptors has 'privileged' access to mitochondria, where it causes free-radical production and mitochondrial depolarization (Greenamyre et al., 1999). Hence the bioenergetic compromise induced by OTA may be responsible for the generation of free radicals and reactive oxygen species that resulted in global oxidative damage to DNA and lipids, as reported here and damage to proteins through generation of oxygen free radicals and nitric oxide, as reported elsewhere (Bryan et al., 2004; Thomas and Mallis, 2001).

Of course OTA may also be toxic through other mechanisms. Due to its chemical structure (chlorodihydroisocoumarin linked through an amide bond to phenylalanine), OTA inhibits protein synthesis by competition with phenylalanine in the aminoacylation reaction of phenylalanine-tRNA (Bunge et al., 1978; Creppy et al., 1983a) and phenylalanine hydroxylase activity (Creppy et al., 1990). These actions could lead to impairment of the synthesis of DOPA, dopamine and catecholamines or enzymes involved in metabolism of DA. Interestingly, the initial effect of OTA was to release DA resulting in increased striatal DA and HVA levels at 6 h, but with a decreased level of striatal DOPAC. It is known that DOPAC levels in striatum decline when DA nerve terminals are exposed to drugs which release newly synthesized DA, possibly because intraneuronal monoamine oxidase is deprived of its main substrate (Zetterstrom et al., 1988). Longer term studies will be required to determine the extent to which the effects of OTA on striatal DA and its metabolites is permanent or reversible.

To summarize, OTA administered at a dose that is 10% of the LD50, resulted in significant reduction of striatal DA, DA turnover and TH immunoreactivity in catecholaminergic neurons and fibers. This was not associated with apoptosis in SN, CP, HP, CB or with loss of striatal neuron immunostaining for DARPP32. OTA evoked pronounced global oxidative stress, possibly related to its inhibition of mitochondrial function. Regional variation in DNA repair did not appear to explain effects on catecholaminergic neurons. The vulnerability of the nigro-striatal system to OTA remains unclear and many questions remain to drive on-going and future investigations. For example, what are the long-term consequences of chronic administration of more clinically relevant low doses of OTA? Does a rigid-akinetic syndrome develop and is it reversible? Given that data derived from analysis of six macro-dissected brain regions are crude approximations for the cellular and molecular events occurring in specific populations of neurons, it will be important to develop refined sampling methods, including microdissection of specific neuro-anatomical

loci and laser capture microdissection techniques for analysis of specific neuronal phenotypes.

Acknowledgements

This study was supported by USAMRMC #03281031 and a VA Merit Review Grant.

References

- Ahlskog JE. Challenging conventional wisdom: the etiologic role of dopamine oxidative stress in Parkinson's disease. *Mov Disord* 2005;20:271–82.
- Aleo MD, Wyatt RD, Schnellmann RG. Mitochondrial dysfunction is an early event in ochratoxin A but not oosporein toxicity to rat renal proximal tubules. *Toxicol Appl Pharmacol* 1991;107:73–80.
- Arora RG, Frolen H, Fellner-Feldegg H. Inhibition of ochratoxin A teratogenesis by zearalenone and diethylstilboestrol. *Food Chem Toxicol* 1983;21:779–83.
- Belmadani A, Tramu G, Betbeder AM, Steyn PS, Creppy EE. Regional selectivity to ochratoxin A, distribution and cytotoxicity in rat brain. *Arch Toxicol* 1998;72:656–62.
- Betarbet R, Sherer TB, MacKenzie G, Garcia-Osuna M, Panov AV, Greenamyre T. Chronic systemic pesticide exposure reproduces features of Parkinson's disease. *Nat Neurosci* 2000;3:1301–6.
- Bryan NS, Rassaf T, Maloney RE, Rodriguez CM, Saijo F, Rodriguez JR, et al. Cellular targets and mechanisms of nitrosylation: an insight into their nature and kinetics in vivo. *Proc Natl Acad Sci USA* 2004;101:4308–13.
- Bunge I, Dirheimer G, Rosenthaler R. In vivo and in vitro inhibition of protein synthesis in *Bacillus stearothermophilus* by ochratoxin A. *Biochem Biophys Res Commun* 1978;83:398–405.
- Calabresi P, Gubellini P, Picconi B, Centonze D, Pisani A, Bonsi P, et al. Inhibition of mitochondrial complex II induces a long-term potentiation of NMDA-mediated synaptic excitation in the striatum requiring endogenous dopamine. *J Neurosci* 2001;21:5110–20.
- Cardozo-Pelaez F, Brooks PJ, Stedford T, Song S, Sanchez-Ramos J. DNA damage, repair, and antioxidant systems in brain regions: a correlative study. *Free Radic Biol Med* 2000;28:779–85.
- Cardozo-Pelaez F, Song S, Parthasarathy A, Hazzi C, Naidu K, Sanchez-Ramos J. Oxidative DNA damage in the aging mouse brain. *Movement Disord* 1999;14:972–80.
- Cardozo-Pelaez F, Stedford TJ, Brooks PJ, Song S, Sanchez-Ramos JR. Effects of diethylmaleate on DNA damage and repair in the mouse brain. *Free Radic Biol Med* 2002;33:292–8.
- Cascio C, Guarneri R, Russo D, De Leo G, Guarneri M, Piccoli F, et al. Pregnenolone sulfate, a naturally occurring excitotoxin involved in delayed retinal cell death. *J Neurochem* 2000;74:2380–91.
- Creppy EE, Chakor K, Fisher MJ, Dirheimer G. The mycotoxin ochratoxin A is a substrate for phenylalanine hydroxylase in isolated rat hepatocytes and in vivo. *Arch Toxicol* 1990;64:279–84.
- Creppy EE, Kane A, Dirheimer G, Lafarge-Frayssinet C, Mousset S, Frayssinet C. Genotoxicity of ochratoxin A in mice: DNA single-strand break evaluation in spleen, liver and kidney. *Toxicol Lett* 1985;28:29–35.
- Creppy EE, Kern D, Steyn PS, Vleggaar R, Rosenthaler R, Dirheimer G. Comparative study of the effect of ochratoxin A analogues on yeast aminoacyl-tRNA synthetases and on the growth and protein synthesis of hepatoma cells. *Toxicol Lett* 1983a;19:217–24.
- Creppy EE, Stormer FC, Rosenthaler R, Dirheimer G. Effects of two metabolites of ochratoxin A, (4R)-4-hydroxyochratoxin A and ochratoxin alpha, on immune response in mice. *Infect Immun* 1983b;39:1015–8.
- Dianov G, Bischoff C, Piotrowski J, Bohr VA. Repair pathways for processing of 8-oxoguanine in DNA by mammalian cell extracts. *J Biol Chem* 1998;273:33811–6.
- Dirheimer G, Creppy EE. Mechanism of action of ochratoxin A. *IARC Sci Publ* 1991;171–86.

- Elstner EF, Heupel A. Inhibition of nitrite formation from hydroxyl-ammonium chloride: a simple assay for superoxide dismutase. *Anal Biochem* 1976;70:616–20.
- Fukui Y, Hayasaka S, Itoh M, Takeuchi Y. Development of neurons and synapses in ochratoxin A-induced microcephalic mice: a quantitative assessment of somatosensory cortex. *Neurotoxicol Teratol* 1992;14:191–6.
- Galtier P. Pharmacokinetics of ochratoxin A in animals. *IARC Sci Publ* 1991;187–200.
- Galtier P, Boneu B, Charpentreau JL, Bodin G, Alvinerie M, More J. Pathophysiology of haemorrhagic syndrome related to ochratoxin A intoxication in rats. *Food Cosmet Toxicol* 1979;17:49–53.
- Gautier JC, Holzhaeuser D, Markovic J, Gremaud E, Schilter B, Turesky RJ. Oxidative damage and stress response from ochratoxin A exposure in rats. *Free Radic Biol Med* 2001;30:1089–98.
- Greenamyre JT, MacKenzie G, Peng TI, Stephens SE. Mitochondrial dysfunction in Parkinson's disease. *Biochem Soc Symp* 1999;66:85–97.
- Grosse Y, Baudrimont I, Castegnaro M, Betbeder AM, Creppy EE, Dirheimer G, et al. Formation of ochratoxin A metabolites and DNA-adducts in monkey kidney cells. *Chem Biol Interact* 1995;95:175–87.
- Gupta M, Bandopadhyay S, Paul B, Majumder SK. Hematological changes produced in mice by ochratoxin A. *Toxicology* 1979;14:95–8.
- Hanawalt PC. Transcription-coupled repair and human disease: perspective. *Science* 1994;266:1957–8.
- Hasegawa E, Takeshige K, Oishi T, Murai Y, Minakami S. 1-Methyl-4-phenylpyridinium (MPP+) induces NADH-dependent superoxide formation and enhances NADH-dependent lipid peroxidation in bovine heart sub-mitochondrial particles. *Biochem Biophys Res Commun* 1990;170:1049–55.
- Haubeck HD, Lorkowski G, Kolsch E, Rosenthaler R. Immunosuppression by ochratoxin A and its prevention by phenylalanine. *Appl Environ Microbiol* 1981;41:1040–2.
- Haug LS, Ostvold AC, Torgner I, Roberg B, Dvorakova L, St'astny F, et al. Intracerebroventricular administration of quinolinic acid induces a selective decrease of inositol(1,4,5)-trisphosphate receptor in rat brain. *Neurochem Int* 1998;33:109–19.
- Hayes AW, Hood RD, Lee HL. Teratogenic effects of ochratoxin A in mice. *Teratology* 1974;9:93–7.
- Hoehler D, Marquardt RR, McIntosh AR, Hatch GM. Induction of free radicals in hepatocytes, mitochondria and microsomes of rats by ochratoxin A and its analogs. *Biochim Biophys Acta* 1997;1357:225–33.
- Kane A, Creppy EE, Rosenthaler R, Dirheimer G. Biological changes in kidney of rats fed subchronically with low doses of ochratoxin A. *Dev Toxicol Environ Sci* 1986a;14:241–50.
- Kane A, Creppy EE, Rosenthaler R, Dirheimer G. Changes in urinary and renal tubular enzymes caused by subchronic administration of ochratoxin A in rats. *Toxicology* 1986b;42:233–43.
- Krogh P. Role of ochratoxin in disease causation. *Food Chem Toxicol* 1992;30:213–24.
- Krogh P, Axelsen NH, Elling F, Gyrd-Hansen N, Hald B, Hyldgaard-Jensen J, et al. Experimental porcine nephropathy. Changes of renal function and structure induced by ochratoxin A-contaminated feed. *Acta Pathol Microbiol Scand [A]* 1974;1–21.
- Kuiper-Goodman T, Scott PM. Risk assessment of the mycotoxin ochratoxin A. *Biomed Environ Sci* 1989;2:179–248.
- Lea T, Steien K, Stormer FC. Mechanism of ochratoxin A-induced immunosuppression. *Mycopathologia* 1989;107:153–9.
- Lebrun S, Follmann W. Detection of ochratoxin A-induced DNA damage in MDCK cells by alkaline single cell gel electrophoresis (comet assay). *Arch Toxicol* 2002;75:734–41.
- Lovell MA, Xie C, Markesbery WR. Decreased base excision repair and increased helicase activity in Alzheimer's disease brain. *Brain Res* 2000;855:116–23.
- Marquardt RR, Frohlich AA. A review of recent advances in understanding ochratoxicosis. *J Anim Sci* 1992;70:3968–88.
- Mazzarello P, Poloni M, Spadari S, Focher F. DNA repair mechanisms in neurological diseases: facts and hypotheses. *J Neurol Sci* 1992;112:4–14.
- Moroi K, Suzuki S, Kuga T, Yamazaki M, Kanisawa M. Reduction of ochratoxin A toxicity in mice treated with phenylalanine and phenobarbital. *Toxicol Lett* 1985;25:1–5.
- Paxinos G, Franklin KBJ. The mouse brain in stereotaxic coordinates. San Diego, CA: Academic Press; 2001.
- Petkova-Bocharova T, Chernozemsky IN, Castegnaro M. Ochratoxin A in human blood in relation to Balkan endemic nephropathy and urinary system tumours in Bulgaria. *Food Addit Contam* 1988;5:299–301.
- Pfohl-Leschkowicz A, Chakor K, Creppy EE, Dirheimer G. DNA adduct formation in mice treated with ochratoxin A. *IARC Sci Publ* 1991;245–53.
- Pfohl-Leschkowicz A, Grosse Y, Kane A, Creppy EE, Dirheimer G. Differential DNA adduct formation and disappearance in three mouse tissues after treatment with the mycotoxin ochratoxin A. *Mutat Res* 1993;289:265–73.
- Pitout MJ. The effect of ochratoxin A on glycogen storage in the rat liver. *Toxicol Appl Pharmacol* 1968;13:299–306.
- Robbins JH, Otsuka F, Tarone RE, Polinsky RJ, Brumback RA, Nee LE. Parkinson's disease and Alzheimer's disease: hypersensitivity to X-rays in culture cell lines. *J Neurol Neurosurg Psychiatry* 1985;48:916–23.
- Sanchez-Ramos J, Overvik E, Ames BN. A marker of oxylradical-mediated DNA damage (oxo8dG) is increased in nigro-striatum of Parkinson's disease brain. *Neurodegeneration (incorporated into Exp Neurol)* 1994;3:197–204.
- Sava V, Mosquera D, Song S, Stedeford T, Calero K, Cardezo-Pelaez F, et al. Rubratoxin B elicits antioxidative and DNA repair responses in mouse brain. *Gene Expression* 2004;11:211–9.
- Schindewolf C, Lobenwein K, Trinczek K, Gomolka M, Soewarto D, Fella C, et al. Comet assay as a tool to screen for mouse models with inherited radiation sensitivity. *Mamm Genome* 2000;11:552–4.
- Schulz JB, Henshaw DR, MacGarvey U, Beal MF. Involvement of oxidative stress in 3-nitropropionic acid neurotoxicity. *Neurochem Int* 1996;29:167–71.
- Smith PK, Krohn RI, Hermanson GT, Mallia AK, Gartner FH, Provenzano MD, et al. Measurement of protein using bicinchoninic acid. *Anal Biochem* 1985;150:76–85.
- Stefanova N, Puschban Z, Fernagut PO, Brouillet E, Tison F, Reindl M, et al. Neuropathological and behavioral changes induced by various treatment paradigms with MPTP and 3-nitropropionic acid in mice: towards a model of striatonigral degeneration (multiple system atrophy). *Acta Neuropathol (Berl)* 2003;106:157–66.
- Stormer FC, Lea T. Effects of ochratoxin A upon early and late events in human T-cell proliferation. *Toxicology* 1995;95:45–50.
- Szczecz GM, Hood RD. Brain necrosis in mouse fetuses transplacentally exposed to the mycotoxin ochratoxin A. *Toxicol Appl Pharmacol* 1981;57:127–37.
- Thomas JA, Mallis RJ. Aging and oxidation of reactive protein sulfhydryls. *Exp Gerontol* 2001;36:1519–26.
- Turski L, Turski WA. Towards an understanding of the role of glutamate in neurodegenerative disorders: energy metabolism and neuropathology. *Experientia* 1993;49:1064–72.
- Vyas I, Heikkila RE, Nicklas WJ. Studies on the neurotoxicity of MPTP: inhibition of NAD-linked substrate oxidation by its metabolite, MPP+. *J Neurochem* 1986;46:1501–7.
- Wangikar PB, Dwivedi P, Sharma AK, Sinha N. Effect in rats of simultaneous prenatal exposure to ochratoxin A and aflatoxin B(1). II. Histopathological features of teratological anomalies induced in fetuses. *Birth Defects Res B Dev Reprod Toxicol* 2004;71:352–8.
- Wei YH, Lu CY, Lin TN, Wei RD. Effect of ochratoxin A on rat liver mitochondrial respiration and oxidative phosphorylation. *Toxicology* 1985;36:119–30.
- Zetterstrom T, Sharp T, Collin AK, Ungerstedt U. In vivo measurement of extracellular dopamine and DOPAC in rat striatum after various dopamine-releasing drugs; implications for the origin of extracellular DOPAC. *Eur J Pharmacol* 1988;148:327–34.

NEUROANTOMICAL MAPPING OF DNA REPAIR AND ANTIOXIDATIVE RESPONSES IN MOUSE BRAIN: EFFECTS OF A SINGLE DOSE OF MPTP

V. Sava^{1,2}; O. Reunova^{1,2}; A. Velaquez^{1,2}; J. Sanchez-Ramos^{1,2*}

¹ Department of Neurology, University of South Florida, Tampa, FL

²Research Service, James Haley VA, Tampa, FL

* **Corresponding author:** Dr. Juan R. Sanchez-Ramos, The Helen E. Ellis Professor of Neurology, University of South Florida, Department of Neurology (MDC 55), 12901 Bruce B. Downs Blvd., Tampa, FL 33612, USA; Tel: (813) 974-6022; Fax: (813) 974-7200; E-mail: jsramos@hsc.usf.edu

ABSTRACT

The neuroanatomical distribution of base excision repair activity, an important DNA repair mechanism, has not been previously studied in the context of neurotoxicant induced oxidative stress. MPTP is known to be a selective dopamine (DA) neurotoxicant, but its effects on base excision repair and endogenous antioxidant activity are more widespread than expected. The early effects of an acute challenge with N-methyl-4-phenyl-1,2,3,6-tetrahydropyridine (MPTP) on DNA repair and antioxidative responses were investigated in micro-dissected mouse brain. Oxyguanosine glycosylase (OGG1) and superoxide dismutase (SOD) enzymatic activities were measured at 12, 24, 48 and 72 hrs in 44 loci of mouse brain, harvested with a micro-punch cannula under stereomicroscopic guidance. A single dose of MPTP (20 mg/kg) elicited early increases in OGG1 and SOD activities throughout all regions of brain. In some sampled loci, notably the SN and hippocampus, the heightened DNA repair and antioxidant responses were not maintained beyond 48 hrs. Other loci from cerebellum, cerebral cortex and pons maintained high levels of activity up through 72 hrs. Levels of dopamine (DA) were decreased significantly at all time points and remained below control levels in nigro-striatal and mesolimbic systems (ventral tegmental area and nucleus accumbens). Assessment of apoptosis by TUNEL staining revealed a significant increase in number of apoptotic nuclei in the substantia nigra at 72 h and not in other loci. The marked degree of apoptosis that became evident in SN at 72 h was associated with large decreases in SOD and DNA repair activity at that locus. In conclusion, MPTP elicited global effects on DNA repair and antioxidant activity all regions of brain, but the most vulnerable loci were unable to maintain elevated DNA repair and antioxidant responses.

Key words: oxyguanosine glycosylase, superoxide dismutase , dopamine, tyrosine hydroxylase, apoptosis, N-methyl-4-phenyl-1,2,3,6-tetrahydropyridine (MPTP), substantia nigra, striatum

INTRODUCTION

Aging is associated with increasing levels of oxidative DNA damage in all organs except the brain and testes (Fraga *et al.* 1990). The stable measures of oxidative DNA damage in whole brain homogenates masked the variation in DNA damage across neuroanatomically defined brain regions. Analysis of DNA damage in specific brain regions revealed increased levels of DNA adducts formed by reaction of oxygen radicals with DNA. In the mouse, there was an age-dependent accumulation of 8-hydroxy-2'-deoxyguanosine (oxo8dG) in total DNA extracted from brain regions involved in locomotor control. These increased levels of the oxidized base relative to the unoxidized 2'-deoxyguanosine were associated with a decline in spontaneous locomotor activity and balance in the aged mice (Cardozo-Pelaez *et al.* 2000; Cardozo-Pelaez *et al.* 1999). In addition, the increase in oxo8dG levels in striatum correlated with decline in striatal dopamine (DA) in old mice (Cardozo-Pelaez *et al.* 1999). In the human brain, steady-state levels of oxidative DNA damage, indicated by oxo8dG, were increased in the substantia nigra, basal ganglia and cortex of idiopathic Parkinson Disease (PD) cases compared to controls [Sanchez-Ramos, 1994 #241; Alam, 1997 #202]. Most of the age-dependent increases in oxo8dG measured in total DNA extracted from brain was attributed to the oxidative DNA damage that occurs in mitochondria (Mecocci *et al.* 1993).

The enzyme 8-oxoguanine DNA glycosylase 1 (OGG1) participates in a key step of base excision repair, one of many DNA repair mechanisms that maintain the integrity of the genome in proliferating cells and that ensure faithful expression of transcriptionally active genes in post-mitotic cells. OGG1 activity has been shown to be inversely related to the levels of the damaged base (oxo8dG) in macro-dissected brain regions (Cardozo-Pelaez *et al.* 2000). In addition, OGG1 activity is increased in a region-specific manner following treatment with diethylmaleate, a compound that reduces glutathione levels in the cell (Cardozo-Pelaez *et al.* 2002). A single treatment with diethylmaleate elicited a significant increase (~2-fold) in the activity of OGG1 in three gross brain regions with low basal levels of activity (cerebellum, cortex, and pons/medulla). There was no change in the activity of OGG1 in those regions with high basal levels of activity (hippocampus, caudate/putamen, and midbrain). These studies clearly demonstrated that base excision repair can be upregulated in the CNS and that the increased repair activity correlated with a reduction in the levels of DNA damage. It is important to point out that alternative repair systems exist to minimize the effects of an increased load of oxo8dG, evidenced by the viability of homozygous *ogg1(-/-)* null mice (Klungland *et al.* 1999). These OGG1 “knockout” mice accumulate abnormal levels of oxo8dG in their genomes, and despite the increase in potentially miscoding DNA lesions, they exhibited only a moderately, but significantly,

elevated spontaneous mutation rate in nonproliferative tissues, did not develop malignancies, and showed no marked pathological changes (Klungland *et al.* 1999). However, the effects of oxidative stress in carefully microdissected brains of OGG1 knockout mice has not been reported. In fact, the absence of a neuroanatomical map of OGG1 activity in normal mice provided the impetus for the present study.

The primary objective for the present study was to create a neuroanatomical map of the distribution of base excision repair capacity, indicated by OGG1 activities. Since the response to oxidative stress involves an upregulation of endogenous anti-oxidant activity as well as DNA repair, we also mapped the distribution of superoxide dismutase (SOD) activity across the brain. The assay for OGG1 utilized in the study was sensitive enough to be applied to tissue samples weighing no more than 1 mg. The dissection technique permitted analysis of 44 samples from each brain. The method is limited in that only total OGG1 activity (nuclear and mitochondrial) can be assessed. However, the detailed map of the neuroanatomical distribution of total OGG1 activity will provide a useful baseline for studying an important aspect of the brain's DNA repair capacity under various experimental conditions. The secondary objective was to test the hypothesis that a selective neurotoxicant, such as MPTP, would create oxidative stress localized to the nigro-striatal system. Other regions that escape the toxic effects of MPTP would be expected to have little evidence for oxidative stress or highly efficient antioxidant and DNA repair activities. The effects of a mitochondrial toxicant, oxchratoxin-A, with more global effects on brain were also studied and reported in a separate publication (See this issue).

In the present report, we investigated the early time-course and neuroanatomical distribution of the DNA repair and anti-oxidative responses in multiple loci across the brain of mice following a single dose of MPTP. In addition, levels of striatal DA and its metabolites were measured at the same time points to determine the relationship between DNA repair and the toxicity for DA neurons in the nigro-striatal system .

2. Materials and methods

2.1. Materials

MPTP, SOD, goat serum and dihydrobenzylamine were purchased from Sigma (St. Louis, MO). Protease inhibitors and DNA glycosylase were from Boehringer Mannheim (Indianapolis, IN, USA). ³²P-ATP was from NEN Life Science Products (Wilmington, DE). G25 spin columns were from Prime;

Inc. (Boulder, CO). T4 polynucleotide kinase was from Stratagene (Austin, TX). Rabbit Anti-Tyrosine Hydroxylase was purchased from Pei-Freez Biologicals (Arkansas, AR). ApopTag *in situ* Apoptosis Detection Kit, rat anti-DAT primary antibody, and goat anti-rat secondary antibody were from Chemicon International (Temecula, CA). Avidin-biotin-complex Vectastain ABC Kit and DAB-kit was from Vector Labs (Burlingame, CA). All other reagents were from Sigma Chemical Co.

2.2. Animals and treatment

Male C57BL/J6 mice were (22 ± 2 g) obtained from the Jackson Laboratories (Bar Harbor, ME). They were housed at the temperature of 21 ± 2 °C with 12 light/dark cycle and free access to food and water. Mice were divided into control (n=8) and 4 experimental (n=8) groups received either normal saline (control) or MPTP (20 mg/kg, ip) injections. Animals were sacrificed in 12, 24, 48 and 72 h after administration of MPTP. The brains were rapidly removed from the skull and placed in ice-cold saline for transfer to a cryostat chamber for coronal sectioning.

2.3. Tissue micro-dissection

Brain coronal sections of 1 mm thickness were prepared at -10 °C in a cryostat chamber using a Brain Matrices mouse brain mold (Braintree Sci., Inc., MA). The coronal sections were mounted on Superfrost/Plus microscope slides (Fisherbrand, PA) and stored at -70°C until harvesting of specific brain regions. Prior to freezing, dissection landmarks were briefly confirmed.

The harvesting of brain tissue from specific loci of each coronal section was performed under a stereo microscope (WILD Heerbrugg, Switzerland). Punch micro-dissection of the tissue from the coronal sections utilized a Brain Tissue Punch Set (Vibratome, MO). The stage of the microscope was replaced with a variable temperature thermo-electric Cold Plate (Oven Ind., Inc., PA). The tissue sections were placed on the plate at -15 °C, a temperature that permitted precise punching without rendering the slice brittle and liable to fracture. Punches were obtained from both right and left sides of the brain using a cannula of 1 mm diameter designed for this specific purpose (Vibratome, MO). The cannula was equipped with a spring action inner probe that permitted easy ejection of the sample into a 1.5 ml plastic tube. Collected samples were stored in the 1.5 mL plastic tubes at -70 °C until biochemical procedure. Dissection was documented using a DEI-470 (Optronics Eng., CA) video camera connected to computer and images were processed with MGI VideoWave III software. Selection and identification of the sites for micro-dissection was based on the mouse brain atlas(Paxinos

and K.B.J. 2001). In total, 44 different loci were harvested in each mouse brain using micro-punch dissection.

2.4. Assessment of OGG1 activity

The procedure for extraction of DNA glycosylase was similar to that described previously (Cardozo-Pelaez *et al.* 2000). Micro-punches of brain tissue were sonicated in homogenization buffer contained 20 mM Tris, pH 8.0, 1 mM EDTA, 1 mM dithiotrietol (DTT), 0.5 mM spermine, 0.5 mM spermidine, 50% glycerol and protease inhibitors and homogenates were rocked for 30 min after addition of 1/10 vol 2.5 M KCl. Samples were spun at 14,000 rpm for 30 min and supernatants were collected.

The OGG1 activities in supernatants were determined using duplex oligonucleotide containing 8-oxoG as incision substrate. For preparation of the incision assay, twenty pmol of synthetic probe containing 8-oxodG (Trevigen, Gaithersburg, MD) was labeled with P³² at the 5' end using polynucleotide T4 kinase (Boehringer Mannheim, Germany). Unincorporated free ³²P-ATP was separated on G25 spin column (Prime; Inc., Boulder, CO). Complementary oligonucleotides were annealed in 10 mM Tris, pH 7.8, 100 mM KCl, 1 mM EDTA by heating the samples 5 min at 80°C and gradually cooling at room temperature.

Incision reactions was carried out in mixture (20 μ L) containing 40 mM HEPES (pH 7.6), 5 mM EDTA, 1 mM DTT, 75 mM KCl, purified bovine serum albumin, 100 fmol of ³²P-labeled duplex oligonucleotide, and extracted guanosine glycosilase (30 μ g of protein). The reaction mixture was incubated at 37°C for 2 hours and products of the reaction were analyzed on denaturing 20% polyacrylamide gel. Pure OGG1 served as positive control and untreated duplex oligonucleotide was used for negative control. The gel was visualized on Biorad-363 Phosphoimager System. The incision activity of OGG1 was calculated as the amount of radioactivity in the band representing specific cleavage of the labeled oligonucleotide over the total radioactivity. Data were normalized to equal concentrations of protein, the concentration of which was measured using the bicincho ninic acid assay (Smith *et al.* 1985)

2.5. SOD assay

Determination of SOD activity in mouse brain was based on inhibition of nitrite formation in reaction of oxidation of hydroxylammonium with superoxide anion radical (Elstner and Heupel 1976). Nitrite formation was generated in a mixture contained 25 μ L xanthine (15 mM), 25 μ L hydroxylammonium chlorode (10 mM), 250 μ L phosphate buffer (65 mM, pH 7.8), 90 μ L distilled

water and 100 μ L xanthine oxidase (0.1 U/mL) used as a starter of the reaction. Inhibitory effect of inherent SOD was assayed at 25°C during 20 min of incubation with 10 μ L of brain tissue extracts. Determination of the resulted nitrite was performed upon the reaction (20 min at room temperature) with 0.5 mL sulfanilic acid (3.3 mg/mL) and 0.5 mL α -naphthylamine (1 mg/mL). Optical absorbance at 530 nm was measured on Ultrospec III spectrophotometer (Pharmacia, LKB). The results were expressed as units of SOD activity calculated per milligram of protein. The amount of protein in the samples was determined using the bicinchoninic acid (Smith *et al.* 1985)

2.6. Measurement of dopamine

HPLC with electrochemical detection was employed to measure levels of dopamine (DA) as previously reported in our laboratory (Cardozo-Pelaez *et al.* 1999) Punched tissue samples were sonicated in 50 volumes of 0.1 M perchloric acid containing 50 ng/ml of dihydrobenzylamine (Sigma Chemical, MA) as internal standard. After centrifugation (15,000 x g, 10 min, 4°C), 20 ml of supernatant was injected onto a C18-reversed phase RP-80 catecholamine column (ESA, Bedford, MA). The mobile phase consisted of 90% of a solution of 50 mM sodium phosphate, 0.2 mM EDTA, and 1.2 mM heptanesulfonic acid (pH 4) and 10% methanol. Flow rate was 1.0 ml/min. Peaks were detected by a Coulochem 5100A detector (ESA). Data were collected and processed with TotalChrom software (Perkin Elmer Instruments).

2.7. Immunohistochemistry

Brains from several animals at each time point was allocated for immunocytochemical study. Frozen sections of 1 mm thickness were additionally sliced in cryostat for 25 μ m preparations. Every fifth section was selected. Thin sections were placed on Superfrost/Plus Microscope Slides (precleaned) and processed by using different staining methods as described below.

2.7.1. Tyrosine hydroxylase (TH) immunohistochemistry

Slide-mounted tissue sections were fixed for 30 min at room temperature in 4% paraformaldehyde prepared on PBS (pH 7.4) and then transferred to PBS containing 5% sucrose. After 15 min of incubation sections were treated with 10% H₂O₂ in 95% MeOH for 30 min at room temperature to destroy endogenous peroxidase. Then sections were blocked at room temperature during 60 min with 10% Goat Serum (Sigma Chemicals, MI) prepared on PBS containing 0.3% Triton X-100. Rabbit Anti-Tyrosine Hydroxylase (Pel-Freez Biologicals, Arkansas) was served as primary antibody

(1:1000) and it was prepared on PBS containing 10% Goat Serum and 0,3% Triton X-100. The sections were incubated with primary antibody overnight at 4 °C and then washed in 3 changes of PBS for 10 min each. Goat Anti-Rabbit (Chemicon, CA) secondary antibody was prepared on PBS/Triton X-100 buffer (1:300) and incubated with samples for 60 min at room temperature. Then sections were washed for 10 min in 3 changes of PBS, treated with avidin-biotin-complex (Vectastain ABC Kit (Peroxidase Standard*), Vector Labs, CA) for 60 min and developed with 3,3'-diaminobenzidine (DAB Substrate Kit, Vector Labs, CA) at room temperature during 2-5 min. Finally the sections were rinsed with distilled water to stop reaction and then dehydrated in ethanol, and cleared in xelene. Controls for nonspecific staining were performed for evaluation in which either primary or secondary antibody were applied alone.

2.7.2. TUNEL assay

TUNEL staining was performed in accordance to Manual of ApopTag *In Situ* Apoptosis Detection Kit (Chemicon, CA). Briefly, slide-mounted tissue sections were fixed for 10 min. at room temperature with 1% paraformaldehyde prepared on PBS (pH 7.4) and rinsed two times for 5 min of PBS. Slides were post-fixed in precooled ethanol:acetic acid (2:1) for 5 min. at -20 °C in a Coplin jar and rinsed two times for 5 min with PBS. Equilibration buffer was immediately applied directly to the specimens for 20 sec. at room temperature. TdT enzyme was pipetted onto the sections following by incubation in a humidified chamber for 1 h at 37 °C. Specimen were placed in a coplin jar containing working strength stop/wash buffer and incubated for 10 min. at room temperature. After triple rinsing in PBS, the sections were incubated with anti-digoxigenin conjugate in a humidified chamber for 30 min in dark at room temperature. Finally, the specimens were rinsed with PBS (4 x 2 min) and mounted on a glass cover slip with Vectashield mounting medium containing DAPI (Vector Labs, CA).

2.8. Statistical analysis

The results were reported as mean \pm SEM for 3 to 6 sets of brain loci for each time point. Two-tailed t-tests were applied in the analysis of the DA and metabolites data. Two-way ANOVA was utilized to evaluate the contribution of time after MPTP and neuroanatomical distribution to the total variance of OGG1 and SOD data (GraphPad Software, Inc; San Diego, CA). This was followed by t-tests with Bonferroni corrections to compare results against control values at time zero for each neuro-anatomical locus.

RESULTS

Tissue samples with consistent dimensions of 1 mm diameter by 1 mm in thickness were harvested with a tissue punch cannula from 7 serial coronal sections prepared from each mouse brain. Sampling sites were identified with the assistance of a mouse brain atlas and documented for subsequent confirmation with a microscope-mounted digital camera (see **Table 1**). (Paxinos and K.B.J. 2001). Forty-four loci from each brain were collected and analyzed for DNA repair activity (OGG1) and endogenous antioxidant activity (SOD). Nineteen of the 44 loci were sampled bilaterally (from both the right and left side of the same neuroanatomical site) and analyzed individually. Specific loci from midbrain (s. nigra and ventral tegmental area) and striatum (caudate-putamen and n. accumbens) were analyzed for levels of DA and metabolites.

A single dose of MPTP (20 mg/kg i.p.) produced a decrease in DA levels in the nigro-striatal and mesolimbic (VTA-N. acb) systems. The time-course of DA decline is illustrated in **Figure 1**. DA concentration in CP reached its lowest level at 24 hr (26% of control levels). In SN, where the DA neuron cell bodies reside, the DA concentration reached its lowest level (15% of control) at a later time, 48 hr. Similarly, DA concentration reached the lowest level (52% of control) in the N.Acb at 24 hrs while the levels in the VTA, where DA neuron cell bodies reside, were reduced to the lowest level (23% of control) at 72 h. The DA levels in N. Acb appeared to be recovering slightly by 72 h. These results are consistent with other reports suggesting that VTA and its projection field in the N. accumbens are less susceptible to MPTP than the nigro-striatal system (German *et al.* 1996).

Concomitant with the decreasing DA levels in the nigro-striatal system, the endogenous antioxidant SOD activity increased significantly with a peak at 48 h and then a decline below control level at 72 h. In VTA and N. accumbens SOD also increased and peaked at 48 hrs but then declined below control levels at 72 h (**Fig. 2**).

Repair of oxidative DNA damage (OGG1) also increased with time in the nigro-striatal DA system, reaching a peak at 48 h and declining, but not dipping below control levels, at 72 h (**Fig. 3**, upper panel). In particular, OGG1 activity in SN returned to near control levels by 72 h. In caudate-putamen and in the ventral striatum (NAcb), the activity of OGG1 remained higher than control at 72 hr. Collating both profiles of OGG1 and SOD responses in SN and VTA loci showed (**Fig. 4**) a high correlation between them ($r^2 = 0.9987$).

The SN, striatum (both dorsal and ventral) and locus ceruleus revealed a marked decrease in tyrosine hydroxylase (TH) immunoreactivity (image not shown). Unlike the SN, the site encompassing the locus ceruleus was able to maintain repair of oxidized DNA damage above control levels through 72 hours (See Table 2 Loci 1 and 3).

Examination of all other brain regions also revealed significant increases in OGG1 and SOD activity, a finding that was unexpected given that MPTP is considered to be selectively toxic for the dopaminergic nigro-striatal system, especially when given at a low dose. The extent of OGG1 elevation and the time-course varied across regions (See Summary Tables 2, 3 and **Figure 5**). The greatest magnitude of change was seen late (72 hrs) in primary motor cortex which exhibited a 6 fold increase (locus 27, Table 1). The temporal pattern of change in hippocampal loci revealed early OGG1 and SOD activation followed by decline to control levels at 72 similar to that observed in SN (**Fig 6 and 7**). Other regions such as those in cortical loci (**Fig 7 and 8**), exhibited a late rise of OGG1 and SOD whereas loci in ponto-cerebellum had an early and sustained elevation of OGG1 and SOD up through 72 hrs.

Although there was a strong correlation between the temporal profile of OGG1 and SOD activity in SN and VTA, the correlation between OGG1 and SOD in other regions of brain was very low at the early time points ($r^2=0.3234$). With time after MPTP intoxication, the correlation between OGG1 and SOD activities gradually strengthened (**Fig. 8**) suggesting an enhanced capacity to withstand MPTP toxicity in regions of brain other than the nigro-striatal system.

Assessment of apoptosis using TUNEL staining revealed a large increase in apoptotic nuclei in the SN, but not in striatum or hippocampus, at 72 hours (**Fig. 9, 10**). The proportion of TUNEL-positive cells (ratio between green fluorescent cells and DAPI blue stained nucleus) was significantly increased compared to control, only at 72 h. Apoptotic nuclei were rare at 12, 24 or 48 h. Concomitant with the marked degree of apoptosis that became evident in SN at 72 h, there was a large drop-off of anti-oxidative and DNA repair activity in this locus. Apparently the oxidative challenge elicited by MPTP was unable to be controlled by the vigorous increase in SOD and OGG1 activities in the SN.

DISCUSSION

This is the first study dedicated to mapping the distribution of OGG1 and SOD across microdissected neuroanatomical regions of brain. It is also the first study to explore the immediate and early effects of MPTP across the entire brain in the context of repair of a specific DNA repair enzyme and antioxidant processes. Micro-dissected tissue samples spanning the entire brain were studied in order to contrast the repair processes in SN and striatum with repair processes in regions of brain that are resistant or invulnerable to the toxicant. The data presented here show that MPTP creates oxidative stress across all brain regions and elicits DNA repair and anti-oxidative responses of varying degrees and time courses in these brain regions.

As expected, a single dose of MPTP (20 mg/kg i.p.) resulted in a rapid decrease of DA concentration in both the nigro-striatal system and the mesolimbic DA system (VTA – Nac). The depletion of DA occurred earlier in the DA terminal fields of the caudate-putamen and NAc than in the loci which house the cell bodies (SN and VTA). This result has been noted before and suggests that the initial injury occurs in DA terminals with a subsequent dying back phenomenon (Hornykiewicz 1992). In addition to DA loss, TH immunoreactivity was markedly decreased in both the nigro-striatal and mesolimbic DA systems as well as in the locus ceruleus. The loss of TH in the SN was associated with a sharp rise at 72 hours of apoptotic nuclei, suggesting that loss of TH in this locus was due to cell death and not to down-regulation of TH expression.

The OGG1 and SOD responses to MPTP challenge varied as a function of time and neuroanatomical locus. The SN, VTA and hippocampal loci were characterized by an early rise in OGG1 and SOD followed by a significant drop to levels equal to or below control levels by 72 hrs. The significant drop in SN OGG1 and SOD at 72 hrs corresponded to the appearance of apoptotic nuclei in the SN. In contrast to these sites, many cortical loci exhibited small increases in OGG1 and SOD activities in the early response to MPTP peaking late at 72 hr. Another pattern was exemplified by ponto-cerebellar loci (including locus ceruleus), where the increased activity occurred early at 12 hrs and was maintained at a high level up to 72 hrs after MPTP. The magnitude of the increases in SOD activity across all regions of brain was similar to the changes in OGG1 activity, even though there was a weak correlation between OGG1 and SOD activities in the first 24 hrs following MPTP. The correlation between OGG1 and SOD activities actually improved with time. The highest correlation factor between OGG1 and SOD was found in the SN. The generation of superoxide anion and the oxidation of guanosine, signals for activation of SOD and OGG1 respectively, likely occurred in close temporal proximity at this site.

Why are DA neurons of the SN, especially the pars compacta, so vulnerable to oxidative stress induced by MPTP and other mitochondrial toxicants (like rotenone) when compared to the relative invulnerability of other neurons? A combination of factors may make them exquisitely sensitive to bioenergetic compromise. DA neurons have a high metabolic rate dependent exclusively on oxidative phosphorylation and they also contain high concentrations of metals, especially forms of iron that catalyze oxyradical processes (Riederer *et al.* 1989; Sanchez-Ramos *et al.* 1989). The metabolism of the DA molecule by MAO generates oxyradicals (Langston *et al.* 1987) and the DA neurons are innervated by glutamatergic neurons that contribute to excitotoxicity (Turski *et al.* 1991). However, the relative resistance of other DA neurons that reside nearby, such as those in the ventral tegmental area (VTA), is not well understood (German *et al.* 1996). In the case of the neurotoxin MPP⁺, the relative

vulnerability of the SN (pars compacta) has been attributed to their higher density of DA transporters in their terminal fields in the striatum and the relative invulnerability of VTA neurons to the presence of calbindin (Liang *et al.* 1996). But this explanation may not be applicable in understanding the selective vulnerability of SN DA neurons exposed to rotenone (Betarbet *et al.* 2000). Unlike MPP+, this mitochondrial toxin is not selectively accumulated by DA neurons alone. Although it has been suggested that the selective toxicity of rotenone to DA neurons of the SN is related to the high density of microglia in this region of the midbrain (Gao *et al.* 2002; Sherer *et al.* 2003), it is not clear why DA VTA neurons are more resistant to rotenone than nigral DA neurons.

Is it possible that intrinsic differences in the DNA repair response plays a role in vulnerability of DA neurons of the SN? Steady-state levels of oxidative DNA damage, indicated by measures of oxo8dG have been shown to increase in the substantia nigra, basal ganglia and cortex of idiopathic PD cases compared to controls (Alam *et al.* 1997; Sanchez Ramos *et al.* 1994). DA neurons in old C57 mice are much more sensitive to MPTP than young mice (Ricaurte *et al.* 1987) and DNA repair capacity declines in aging mice. C57 mice exhibited an age-dependent accumulation of oxo8dG in brain regions involved in locomotor control, and these increased levels of oxo8dG were associated with a decline in spontaneous locomotor activity and balance in the aged mice (Cardozo-Pelaez *et al.* 1999). In the murine model of PD, MPTP treatment resulted in age-dependent damage to gene-specific nuclear and mitochondrial DNA in the nigro-striatal system. There was an increase in DNA damage to a 10 kb fragment of the mitochondrial genome from the caudate-putamen in “old” mice but there was no significant DNA damage in the nuclear DNA target, γ -polymerase (Mandavilli *et al.* 2000). MPTP treatment led to damage in both the mitochondrial DNA fragment and in nuclear γ -polymerase of the substantia nigra. The increased oxidative DNA damage in the nigrostriatal system is the net result of an increased generation of oxyradical species in DA neurons and/or diminished capacity to scavenge oxyradical species. Repair of the oxidized DNA also plays a critical, though understudied, role in maintaining the integrity of DNA especially in transcriptionally active genes. Recent studies have identified a subpathway of nucleotide-excision repair in which transcriptionally active genes are more rapidly cleared of certain types of DNA lesions than are silent domains of the genome (Hanawalt 1994).

An association between deficient DNA repair and PD, as well as with other neurodegenerative diseases such as Alzheimer's disease, amyotrophic lateral sclerosis (ALS) and Huntington's disease (HD) has been previously reported (Lovell *et al.* 2000; Mazzarello *et al.* 1992). Fibroblast and lymphoblastoid lines from patients with PD and AD were shown to be hypersensitive to X-rays and this was inferred to be a consequence of diminished DNA repair (Robbins *et al.* 1985). It is important to

point out that early studies focused on DNA repair that occurs in replicating cells and relied on measures of survival of cells, ³H-thymidine incorporation, or breaks in chromosomes, following exposure to ionizing radiation or uv light,. The accuracy of overall DNA replication during proliferation is assured by several mechanisms that include nucleotide selection and exonuclease proof-reading activity with DNA polymerases and post-replicative methylation-instructed mismatch repair system (Krokan *et al.* 1997). Post-mitotic cells contain lower levels of DNA repair enzymes and repair DNA slower than proliferating cells (Alexander 1967; Korr and Schultz 1989; Stedeford *et al.* 2001) Repair of oxo⁶-alkylguanine lesions as well as the damage from UV and ionizing radiations is slower in neurons than in other cultured cell types (Mazzarello *et al.* 1992). The decline in DNA repair capacity of post-mitotic cells may be related to the development and achievement of their terminal differentiated state. Post-mitotic cells reduce or "switch-off" activity levels of some enzymes and proteins directly or indirectly involved in DNA replication. Aging brain tissue has been reported to have diminished capacity to upregulate DNA repair enzymes when challenged with an oxidative stress such as hyperoxia (Edwards *et al.* 1998). Not all enzymes involved in neuronal DNA synthesis are switched off and some maintain constant activity levels during the life span of the neuron. For example, DNA polymerase-β is responsible for the whole nuclear DNA polymerase activity in adult neurons.

An important aspect of the DNA repair response involved in the demise of DA neurons has been illustrated by a study using transgenic mice lacking the gene for poly(ADP-ribose) polymerase-1 (PARP-1) (Mandir *et al.* 1999). PARP-1 catalyzes the attachment of ADP ribose units from NAD⁺ to nuclear proteins after DNA damage. Owing to its ability to bind and be activated by DNA strand breaks, PARP-1 and DNA-dependent protein kinase have long been proposed as DNA damage “sensors”. Even though these proteins are not considered to be activators of global DNA damage response, upregulation of PARP-1 is clearly involved in the early response to DNA damage. MPTP injections have been shown to activate PARP-1 exclusively in vulnerable dopamine containing neurons of the substantia nigra (Mandir *et al.* 1999). Animals lacking the gene for PARP-1 were dramatically spared from MPTP neurotoxicity (Mandir *et al.* 1999). Neuroprotection against MPTP toxicity was also achieved by treatment of mice with PARP-1 inhibitors (Cosi and Marien 1999). Since, MPTP caused region- and time-dependent changes in levels of NAD⁺ and ATP in the brain *in vivo*, it has been suggested that the demise of neurons mediated by PARP-1 is a function of energy depletion. However, the DNA damage response is a complex network involving sensors of DNA damage (e.g. PARP-1), transducers of DNA damage (eg ataxia teleangiectasis mutated gene –ATM), and the effectors of DNA repair (e.g., base excision repair “BER”, and nucleotide excision repair “NER”). The simplest type of DNA repair

removes the damaged base directly, e.g. dealkylation, by a one-step mechanism. Most lesions of DNA are repaired by the much more complex recombination repair or excision repair systems. The latter includes nucleotide excision repair (NER), mismatch repair and base excision repair (BER).

In the present study we focused on the initial step in BER, the removal of an oxidized base (oxo8-dG) by the DNA glycosylase, OGG1. Although OGG1 exists in both nuclear and mitochondrial isoforms, the enzymatic method utilized here measured total activity and cannot distinguish between the two isoforms. We have presented evidence that MPTP elicits changes in this enzyme throughout the brain, but only a few regions were unable to maintain repair activity through 72 hours. We postulated that inability to repair oxidative DNA damage is an important factor in the determining neuronal vulnerability to oxidative stressors. Although the evidence partially supports this hypothesis, it is not clear why VTA and hippocampus, regions of brain that do not suffer permanent damage from MPTP, also exhibited an upregulation followed by decline at 72 in OGG1 and SOD activities. One explanation is that these regions will likely undergo degenerative changes at higher doses of MPTP. Another possibility is that the micro-dissection technique employed here cannot assess the behavior of specific neurons in response to the challenge. The “micro-dissected” samples contained heterogeneous mixtures of cells that include various neuronal phenotypes, astrocytes and very likely, reactive microglia. Although the micro-dissected tissue samples were adequate for profiling enzymatic activities across brain tissue, they were inadequate to supply a satisfactory explanation for the selective vulnerability of DA neurons of the SN. Another limitation of the present study is the inability to differentiate mitochondrial OGG1 activity from total OGG1 activity.

Future and ongoing studies will address these limitations and will assess DNA repair gene expression in isolated neurons from SNpc and VTA harvested by laser capture micro-dissection technique. In light of the observations that oxidative DNA damage (oxo8dG) accumulates in mitochondrial DNA in a OGG1 knockout mouse (de Souza-Pinto *et al.* 2001) and that alternative repair pathways function to minimize the effects of an increased load of oxo8dG (Klungland *et al.* 1999), it will be important to study the expression of other DNA repair genes, especially those involved in maintaining mitochondrial DNA integrity. Finally, the role of OGG1 will be further elucidated by studying the extent to which pre-conditioning with a non-cytotoxic agent (that upregulates OGG1 activity) will protect against a subsequent challenge with MPTP and other mitochondrial toxicants.

Acknowledgements:

Supported by a Grant from US Army Med Research and Materiel Command (DAMD #17-03-0501), VA Merit Review Grant and the Helen E. Ellis PD Research fund.

Table 1 Neuroanatomical Regions Sampled with abbreviations

Locus #	ABBREVIATIONS	Neuroanatomical region sampled
1	LC+ LVe + Mve+ MC + PC	lateral vestibular nu + med vestib nu, magnocell & parvicell
2	3Cb	3 rd cerebellar lobule
3	LC+ LVe + Mve+ MC + PC	lateral vestibular nu + med vestib nu, magnocell & parvicell
4	LEnt + MEnt	lateral entorhinal + medial entorhinal cortex
5	ECIC	inferior colliculus
6	MO5 + PnO	motor trigeminal nu + pontine reticulare nu
7	RtTg	reticulotegmental nu pons
8	MO5 + PnO	motor trigeminal nu + pontine reticulare nu
9	ECIC	inferior colliculus
10	LEnt + MEnt	lateral entorhinal + medial entorhinal cortex
11	DG + Mol + LMol	dentate gyrus + molecular layer dentate gyrus + lacunosum moleculare layer
12	CA3	field CA3 of hippocampus
13	SNC + SNR	substantia nigra (compact & reticular parts)
14	VTA + IPC + IPR	ventral tegmental area + interpeduncular nucleus
15	Op + InG + InWh + DpG	areas of superior colliculus
16	SNC + SNR	substantia nigra (compact & reticular parts)
17	CA3	field CA3 of hippocampus
18	DG + Mol + LMol	dentate gyrus + molecular layer dentate gyrus + lacunosum moleculare layer
19	Pir + DEn	piriform cortex + dorsal endopiriform nu
20	GrDG + Mol + LMol	granular layer of dentate gyrus + molecular layer dentate gyrus + lacunosum moleculare layer
21	Po + PC	posterior thalamic nu group + parecentral thalamic nu
22	nc + STh+ PSTh	nigrostriatal bundle + subthalamic nu + parasubthalamic nu
23	DMC + DM	dorsomedial nu, compact + dorsomedial hypothalamic nu
24	nc + STh+ PSTh	nigrostriatal bundle + subthalamic nu + parasubthalamic nu
25	Po + PC	posterior thalamic nu group + parecentral thalamic nu
26	GrDG + Mol + LMol	granular layer of dentate gyrus + molecular layer dentate gyrus + lacunosum moleculare layer
27	Pir + DEn	piriform cortex + dorsal endopiriform nu
28	Pir + DEn	piriform cortex + dorsal endopiriform nu
29	S1BF + S1DZ + S1FL	S1 cx, barrel field + S1 cx, dysgranular region + S1 cx, hindlimb region
30	CPu	caudate putamen (striatum)
31	Cpu + LGP	caudate putamen (striatum) + lateral globus pallidus
32	Pe + MPOL	periventricular hypothalamic nu + medial preoptic nu, lateral
33	Cpu + LGP	caudate putamen (striatum) + lateral globus pallidus
34	CPu	caudate putamen (striatum)
35	S1BF + S1DZ + S1FL	S1 cx, barrel field + S1 cx, dysgranular region + S1 cx, hindlimb region
36	Pir + DEn	piriform cortex + dorsal endopiriform nu
37	M1	primary motor cortex
38	CPu	caudatum putamen (striatum)
39	CPu + AcbC + aca	caudatum putamen + accumbens nu, core + anterior commissure, anterior part
40	Cpu + AcbC + aca	caudatum putamen + accumbens nu, core + anterior commissure, anterior part
41	CPu	caudatum putamen (striatum)
42	M1	primary motor cortex
43	LO + VO + M2	lateral orbital cortex + medial orbital cortex + secondary motor cortex
44	LO + VO + M2	lateral orbital cortex + medial orbital cortex + secondary motor cortex

Table 2 Distribution of OGG1 activity across the mouse brain following a single dose of MPTP (20 mg/kg, ip)

Locus #	Control	12 hours	24 hours	48 hours	72 hours
1	9.91±2.77	19.6±1.37*	18.9±2.06	16.5±2.99	17.8±5.30
2	6.15±1.06	19.3±5.32*	18.2±3.61*	19.8±2.93*	20.0±3.94*
3	7.45±1.63	12.8±3.31	15.6±3.59	16.0±2.10	14.0±2.11
4	6.35±0.86	18.0±2.00*	7.39±1.05	18.2±2.30*	36.4±1.78*
5	5.02±0.82	11.8±0.70	13.6±1.42	17.9±3.53*	18.6±1.26*
6	7.06±1.88	18.9±0.70*	12.0±2.00	19.3±2.32*	16.1±1.99
7	7.55±1.11	17.7±1.79*	11.6±2.36	8.22±0.82	9.86±0.97
8	6.87±1.39	14.7±0.48	14.4±3.88	13.2±2.08	15.1±1.52
9	5.87±0.91	14.5±2.53	18.5±4.05*	15.3±2.72*	19.1±0.45*
10	5.87±1.68	16.0±0.94*	17.1±1.05*	8.38±0.76	11.1±2.63
11	4.61±0.97	14.9±2.37*	12.6±2.13	9.52±1.00	9.53±1.70
12	7.41±1.23	14.4±2.54	14.7±2.46	11.7±1.37	14.3±2.07
13	5.88±1.38	15.1±1.67*	20.6±4.61*	16.4±1.73*	8.32±1.54
14	6.55±1.80	13.3±2.39	19.7±3.18*	27.0±1.75*	11.2±0.91
15	5.16±1.25	8.08±1.46	21.3±3.28*	26.8±3.27*	14.4±4.02
16	5.78±1.33	3.88±0.64	18.8±2.71*	27.3±1.87*	8.15±0.72
17	7.25±1.42	5.85±0.93	19.3±2.60*	15.0±0.39	12.4±0.96
18	5.77±1.77	7.24±0.89	18.8±3.22*	23.7±5.20*	8.68±0.54
19	7.89±0.97	10.1±0.08	19.1±2.60*	9.75±1.36	32.1±6.64*
20	7.97±1.14	10.0±0.38	12.0±1.16	18.2±3.75*	16.2±1.41
21	6.90±0.56	4.56±0.74	14.9±1.90	24.0±5.76*	7.75±0.81
22	7.50±1.13	6.56±1.51	10.0±2.73	9.31±1.33	17.4±2.54*
23	8.85±1.58	10.2±0.19	14.4±1.78	13.5±2.73	14.5±2.27
24	11.7±1.15	9.29±1.56	11.7±2.46	25.8±2.34*	12.8±1.41
25	5.12±1.49	12.1±1.11	15.6±2.38*	24.8±3.68*	14.8±0.27
26	6.54±1.40	12.6±0.42	19.3±3.06*	13.3±1.12	24.3±2.54*
27	5.81±0.47	19.1±0.76*	12.3±0.65	25.8±2.76	16.3±2.24*
28	8.32±0.91	9.02±1.20	8.37±1.31	12.0±1.31	9.45±0.91
29	7.77±1.59	17.5±0.38	14.9±2.72	9.36±1.28	24.1±2.07*
30	4.57±1.21	11.8±2.17	16.9±1.70*	7.98±0.64	16.1±3.95*
31	10.6±0.52	5.22±1.19	12.9±1.74	9.81±1.90	12.9±2.90
32	12.7±2.81	11.2±2.00	15.9±1.43	29.5±2.38*	11.4±0.31
33	7.69±0.94	7.29±1.44	12.9±2.18	13.9±0.46	11.7±2.27
34	8.03±0.78	9.46±3.19	20.6±4.15*	10.9±1.65	20.3±3.94*
35	7.87±1.67	18.6±2.33*	15.0±1.17	19.1±1.83*	10.4±1.17
36	7.61±1.67	12.3±0.37	5.94±0.93	11.2±1.32	37.2±0.83*
37	5.38±0.61	12.0±0.69	11.7±1.45	20.2±2.06*	37.2±2.55*
38	7.09±1.22	18.5±2.27*	18.3±3.99*	25.2±1.64*	19.6±1.97*
39	7.29±1.66	7.42±2.01	9.20±1.08	17.3±1.01*	11.3±2.28
40	8.89±1.28	19.6±4.13	12.0±1.35	17.1±0.43	12.1±0.45
41	5.82±0.77	14.9±3.96	9.07±1.60	18.9±1.87*	13.4±1.35
42	7.34±1.29	11.3±2.39	11.7±1.76	12.6±0.70	15.7±3.08
43	9.81±1.31	15.1±2.44	2.05±0.38	12.4±0.68	17.8±3.35
44	9.00±1.96	17.1±2.73	15.9±1.95	15.7±1.85	21.7±3.34*

The results expressed as fmol of ³²P-labeled duplex oligonucleotide incised by per milligram of protein during 1 h. Values represent mean ± SEM (n=6). Two way ANOVA revealed that both time and neuroanatomical locus contributed significantly (p<0.0001) to total variance; interaction between time and locus was also statistically significant (p<0.0001). Asterisks indicate significance of the differences against control after Bonferroni correction (P<0.05).

Table 3. Distribution of SOD activity across the mouse brain following a single dose of MPTP (mg/kg i.p.)

Locus #	Control	12 hours	24 hours	48 hours	72 hours
1	6.64±0.67	12.93±0.88*	13.36±1.72*	6.81±0.31	9.9±0.25*
2	6.54±0.42	9.41±1.07	11.85±2.22*	6.13±0.34	10.57±0.86*
3	7.08±0.47	11.99±1.21*	12.57±2.45*	9±0.24*	11.26±1.23
4	6.76±0.43	12.36±1.81*	8.94±0.67	6.17±0.20	15.77±0.36*
5	6.85±0.39	12.21±1.75*	14.59±1.75*	6.02±0.37	10.21±0.46
6	6.62±0.45	9.47±1.03	13.83±1.92*	6.57±0.34	9.53±0.56*
7	6.48±0.37	10.5±1.30	9.22±0.73	5.99±0.18	10.56±0.33
8	7.02±0.53	9.79±1.75	15.53±1.06*	6.71±0.40	10.71±0.28
9	6.63±0.39	8.99±1.25	14.94±0.75*	6.81±0.36	12.02±1.01*
10	6.77±0.49	10.94±1.82	8.33±0.63	6.99±0.31	14.77±0.33*
11	6.54±0.46	8.9±0.61*	14.72±1.17*	9.68±0.53	5.56±0.27
12	6.63±0.48	10.78±0.51	14.43±1.54*	10.98±0.27	8.63±0.19
13	6.56±0.44	10.56±1.77	14.62±2.58*	12.98±0.14*	5.93±0.29
14	6.52±0.41	10.36±1.00	13.16±1.89*	23.46±0.34*	5.74±0.27
15	6.14±0.51	11±1.82*	14.02±2.49*	14.25±0.10*	5.31±0.44
16	6.36±0.40	10.3±1.26	14.18±1.84*	13.06±0.30*	6.19±0.29
17	7.06±0.14	9.54±1.51	12.66±0.94*	6.81±0.53	5.73±0.44
18	6.9±0.29	13.3±0.96*	11.94±1.37*	7.83±0.77	5.71±0.32
19	6.61±0.47	8.98±0.24	9.89±1.79	6.24±0.59	15.08±0.41*
20	7.1±0.46	10.84±1.54	10.09±1.97	6.19±0.54	11.76±1.14
21	6.64±0.41	9.2±1.72	13.42±1.68*	17.86±0.31*	5.92±0.47
22	6.88±0.27	9.82±1.30	10.04±1.60	16.81±2.14*	9.8±0.27
23	6.96±0.30	9.46±1.25	12.14±2.40*	6.29±0.19	14.45±0.14*
24	7.23±0.55	8.99±1.11	13.54±1.14*	15.7±0.40*	8.49±0.28
25	6.62±0.28	9.07±1.35	11.88±1.76*	17.72±0.59*	6.24±0.71
26	7.25±0.59	11.03±2.03	9.84±1.47	9.04±0.98	10.8±0.52
27	6.87±0.73	13.31±1.07*	10.06±1.78	13.7±0.43*	15.76±1.19*
28	6.76±0.28	10.65±0.83	11.1±1.36	5.84±0.33	15.04±1.08*
29	7.02±0.56	11.02±1.32	13.08±1.83*	6.49±0.27	5.46±0.67
30	6.67±0.56	9.28±1.67	11.68±1.73*	5.96±0.37	13.69±0.74*
31	6.92±0.41	10.21±1.75	12.45±1.64*	6.27±0.40	5.81±0.10
32	14.56±1.26	7.43±0.41*	11.65±1.01	19.26±3.36*	5.87±0.25*
33	6.76±0.50	11.65±1.44*	14.13±0.24*	6.09±0.40	5.87±0.33
34	5.74±0.38	7.54±0.97	15.46±0.33*	6.01±0.56	15.95±0.28*
35	6.83±0.49	10.21±1.32	12.46±2.49*	8.29±1.25	5.77±0.24
36	6.2±0.56	9.61±1.22	10.18±1.59	5.9±0.32	14.94±1.29*
37	6.64±0.98	9.04±1.10	10.37±0.25	5.72±0.37	17.99±0.50*
38	6.82±0.70	10.44±1.91	10.11±0.77	14.8±1.35*	5.04±0.57
39	6.77±0.48	11.63±1.99*	9.77±0.86	13.77±2.57*	5.95±0.25
40	6±0.44	10.75±0.27*	11.32±1.29*	14.39±2.52*	5.59±0.42
41	6.64±0.55	9.1±1.05	10.74±0.46	14.59±2.86*	5.7±0.39
42	6.86±1.00	9.52±1.05	9.34±0.05	6.15±0.26	17.34±0.76*
43	8.08±0.42	10.58±1.50	11.53±0.79	6.12±0.44	13.29±0.42*
44	6.74±0.64	8.79±1.41	10.94±0.44	5.77±0.19	14.08±0.51*

Values represent mean ± SEM. The SOD activity was calculated per milligram of protein. Two way ANOVA revealed that both time and neuroanatomical locus contributed significantly ($p < 0.0001$) to total variance; interaction between time and locus was also statistically significant ($p < 0.0001$). Asterisks indicate significance of the differences against control after Bonferroni correction ($P < 0.05$).

FIGURE LEGENDS

Fig 1. Representative distribution and numbering system of sampled regions of brain. Coronal sections (1 mm thick) photographed through stereo microscope after sampling of neuroanatomical regions. Each section includes the A-P position relative to Bregma.

Fig. 2. Temporal profile of DA levels of micro-dissected loci of brain following an acute dose of MPTP. Mean of DA concentrations at all time points were significantly different from the control levels for each region ($P < 0.05$). CP= caudate-putamen; Acb= nucleus accumbens; SN= substantia nigra; VTA= ventral tegmental area.

Fig. 3 Temporal profile of SOD activity in midbrain loci (upper panel), caudate-putamen (middle panel) and ventral striatum (lower panel). Neuroanatomical locus # is in parentheses in the key. Asterisks indicate statistically significant difference compared to activity at time 0 ($p < 0.05$).

Fig. 4 Temporal profile of OGG1 activity in in midbrain loci (upper panel), caudate-putamen (middle panel) and ventral striatum (lower panel). Neuroanatomical locus # is in parentheses in the key. Asterisks indicate statistically significant difference compared to activity at time 0 ($p < 0.05$).

Fig 5 Correlation between OGG1 and SOD activity in SN and VTA of mouse brain in response to MPTP administration.

Fig 6 Summary map of temporal profiles of OGG1 activity across 44 brain loci following MPTP administration. Inset is the color key to the OGG1 activity scale. This image is based on summary data from Table 2.

Fig. 7 Temporal profile of OGG1 activity in hippocampal loci (upper panel), cortical loci (middle panel) and ponto-cerebellar loci (lower panel). Neuroanatomical locus # is in parentheses in the key. Asterisks indicate statistically significant difference compared to activity at time 0 ($p < 0.05$).

Fig. 8 Temporal profile of SOD activity in hippocampal loci (upper panel), cortical loci (middle panel) and ponto-cerebellar loci (lower panel). Neuroanatomical locus # is in parentheses in the key . Asterisks indicate statistically significant difference compared to activity at time 0 ($p < 0.05$).

Fig. 9 Correlation factor between OGG1 and SOD activities calculated at each time point across whole brain (calculated for all 44 loci).

Fig 10 Representative fluorescence photo micrographs of TUNEL immunoreactivity in substantia nigra of mouse brain exposed to single dose of MPTP (20 mg.kg, ip). Left panels represent DAPI stained nuclei and right panels depict TUNEL-positive (apoptotic) cells. Upper panels represent control and lower ones were obtained from animals 72 hr after MPTP (magnification x 200).

Graph in lower panel: The Y-axis depicts the percentage of TUNEL-positive cells in the substantia nigra (expressed as percent of total number of DAPI+ nuclei) following a single dose of MPTP (20 mg/kg i.p.). The mean percentage (\blacktriangledown SEM) of apoptotic cells in SN was determined from the average of the ratio of TUNEL+/DAPI+ nuclei in 3 SN sections obtained from 3 animals in each experimental group (control, 24, 48 and 72 hours).

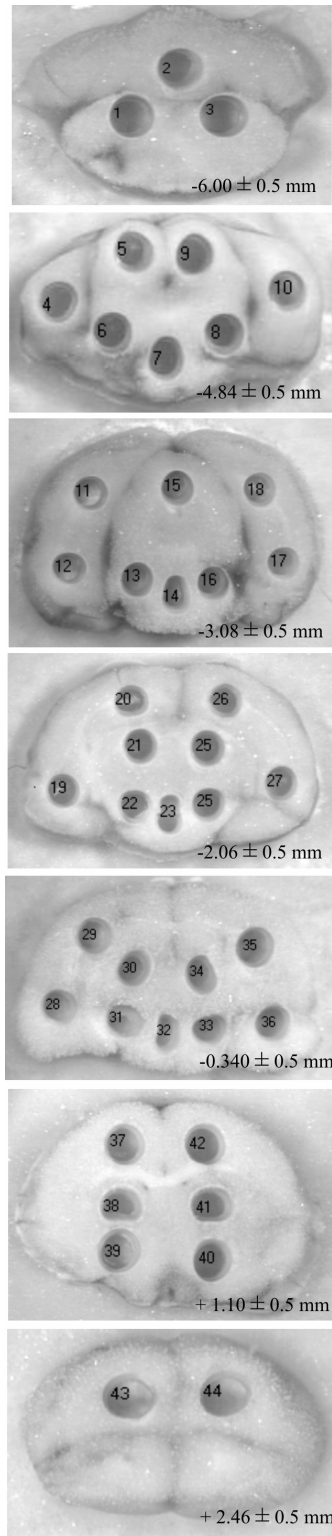


Fig 1. Representative distribution and numbering system of sampled regions of brain. Photomicrographs of coronal sections (1 mm thick) after sampling of neuroanatomical regions. Each section includes the A-P position relative to Bregma (Paxinos and K.B.J. 2001).

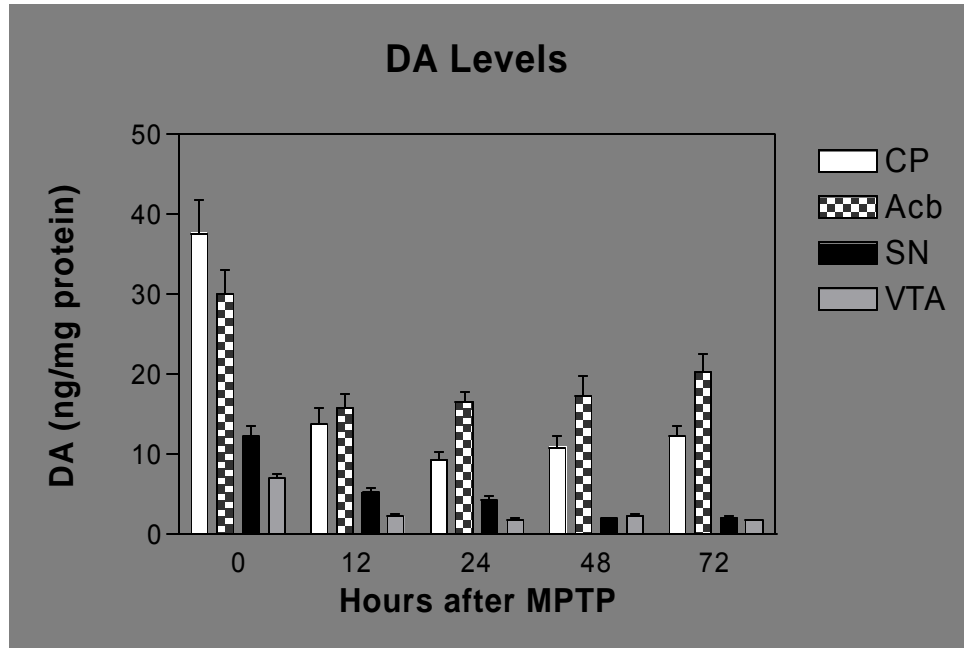


Figure 2 Temporal profile of DA levels of micro-dissected loci of brain following an acute dose of MPTP. Mean of DA concentrations at all time points were significantly different from the control levels for each region ($P < 0.05$). CP= caudate-putamen; Acb= nucleus accumbens; SN= substantia nigra; VTA= ventral tegmental area.

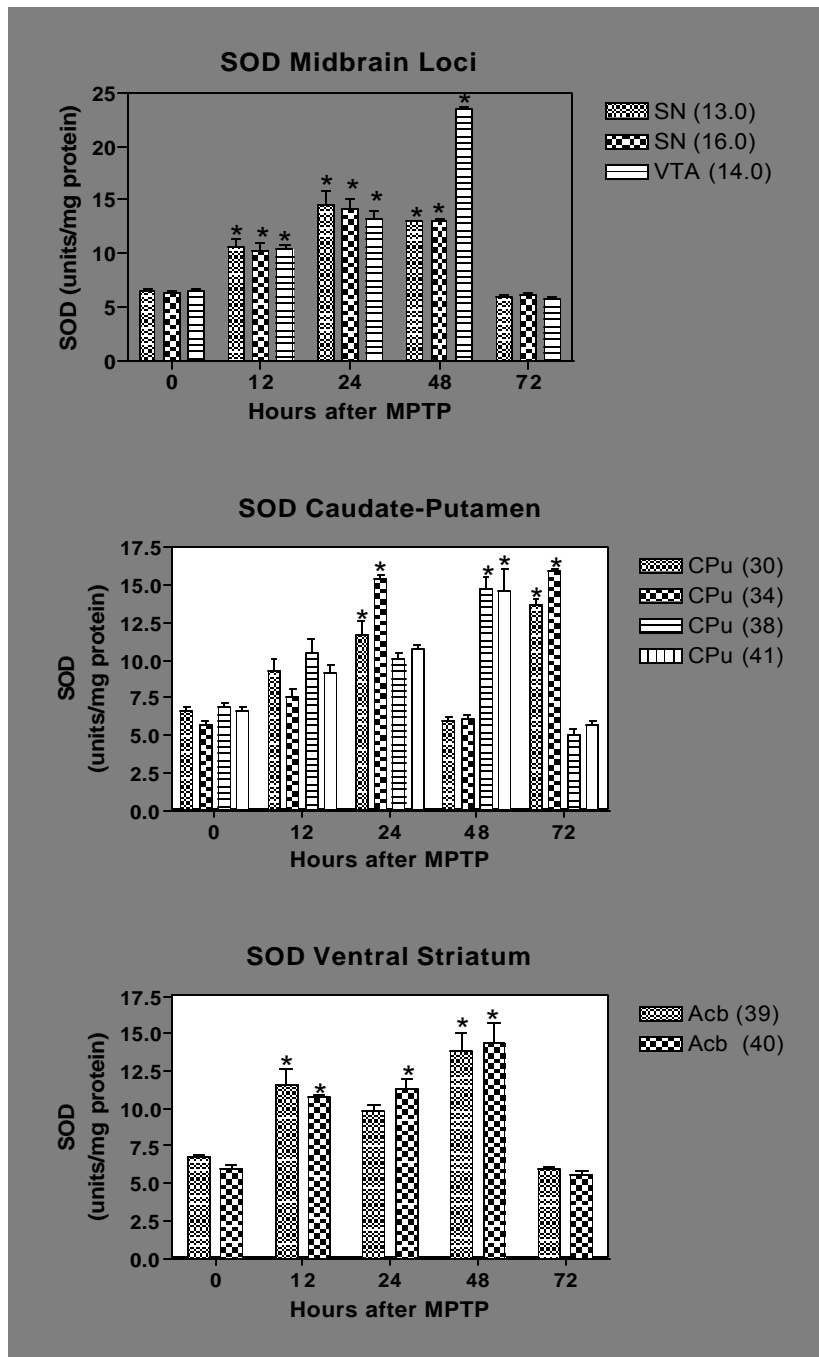


Figure 3. Temporal profile of SOD activity in midbrain loci (upper panel), caudate-putamen (middle panel) and ventral striatum (lower panel). Neuroanatomical locus # is in parentheses in the key. Asterisks indicate statistically significant difference compared to activity at time 0 ($p < 0.05$).

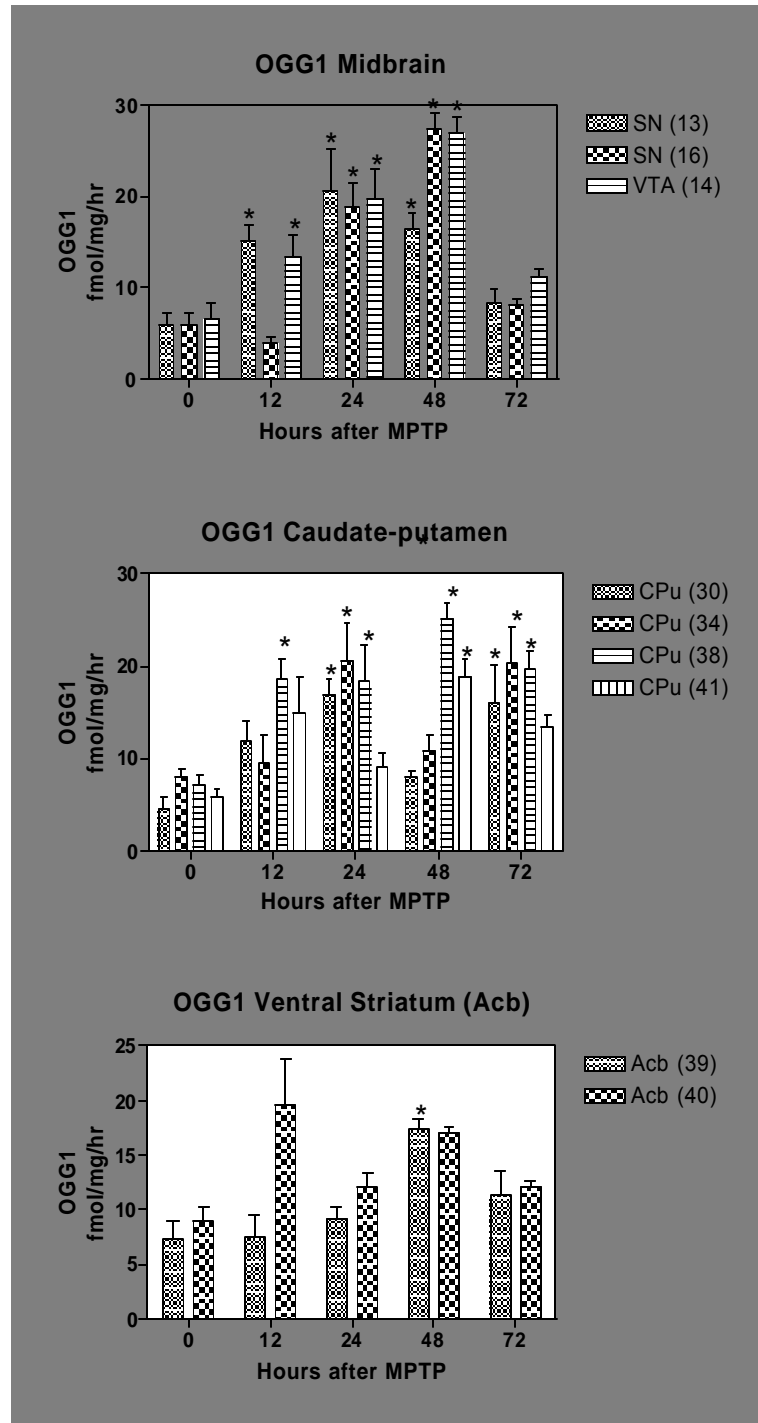


Fig. 4 Temporal profile of OGG1 activity in midbrain loci (upper panel), caudate-putamen (middle panel) and ventral striatum (lower panel). Neuroanatomical locus # is in parentheses in the key. Asterisks indicate statistically significant difference compared to activity at time 0 ($p < 0.05$).

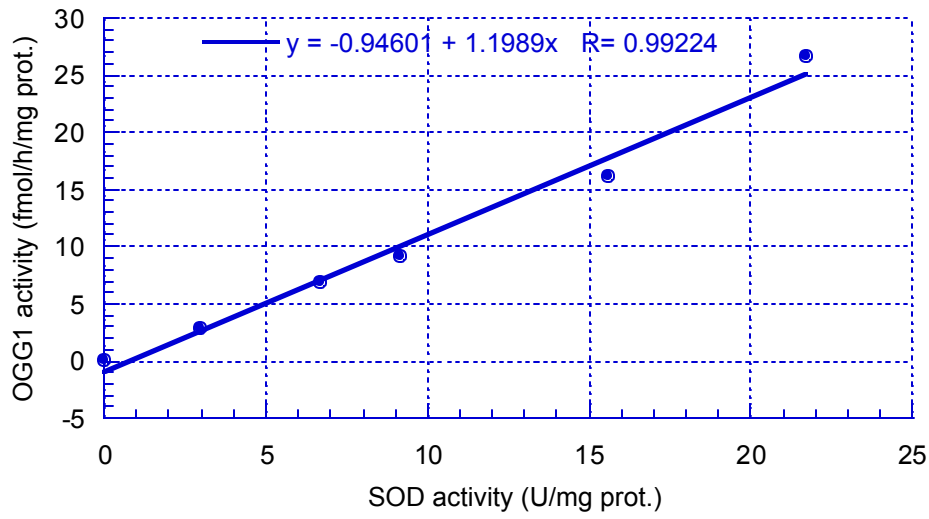


Figure 5 Correlation between OGG1 and SOD activity in SN and VTA of mouse brain in response to MPTP administration.

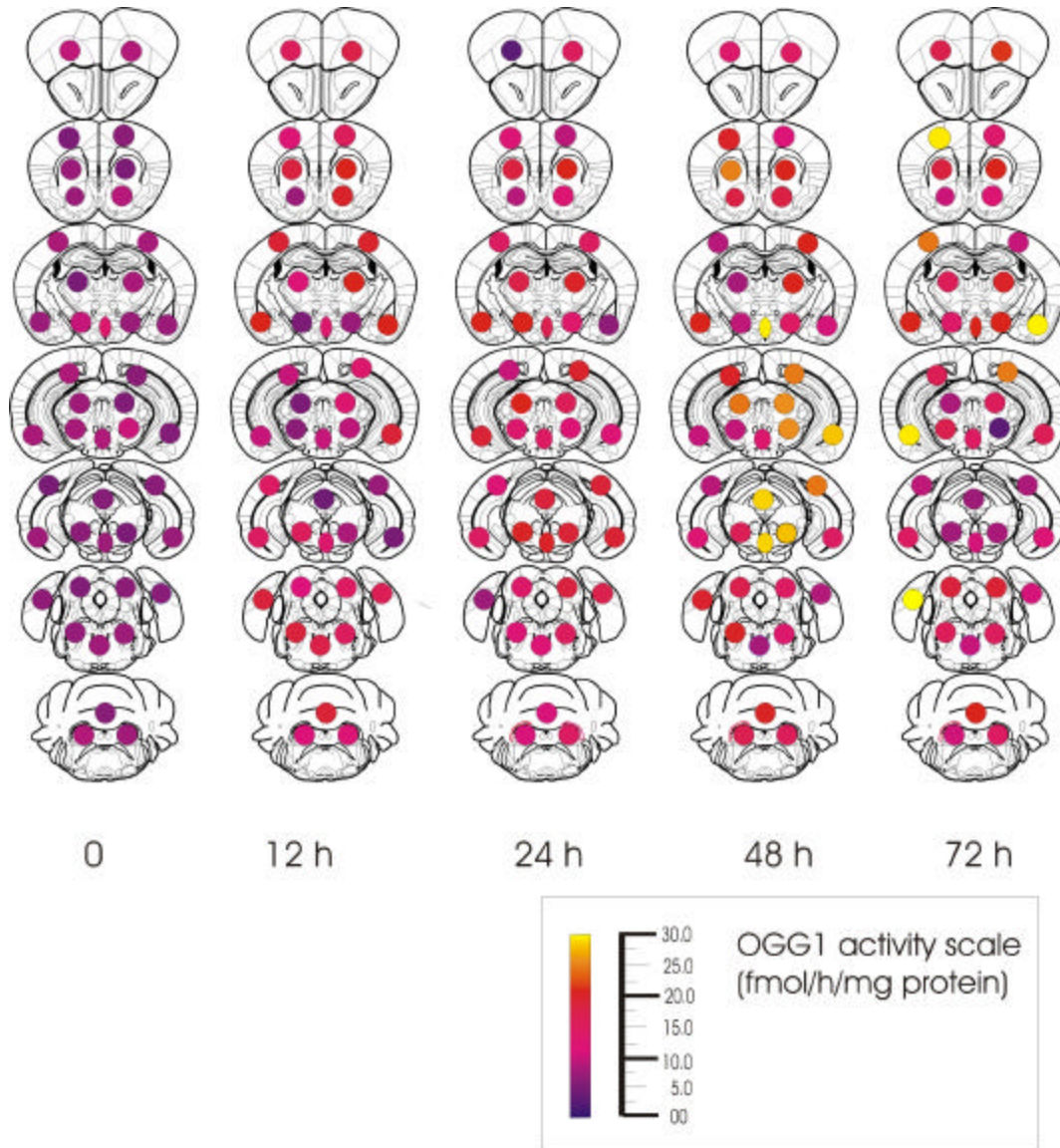


Figure 6 Summary of temporal profiles of OGG1 activity across 44 brain loci following MPTP administration. Inset is the color key to the OGG1 activity scale. This image illustrates the summary data from Table 2.

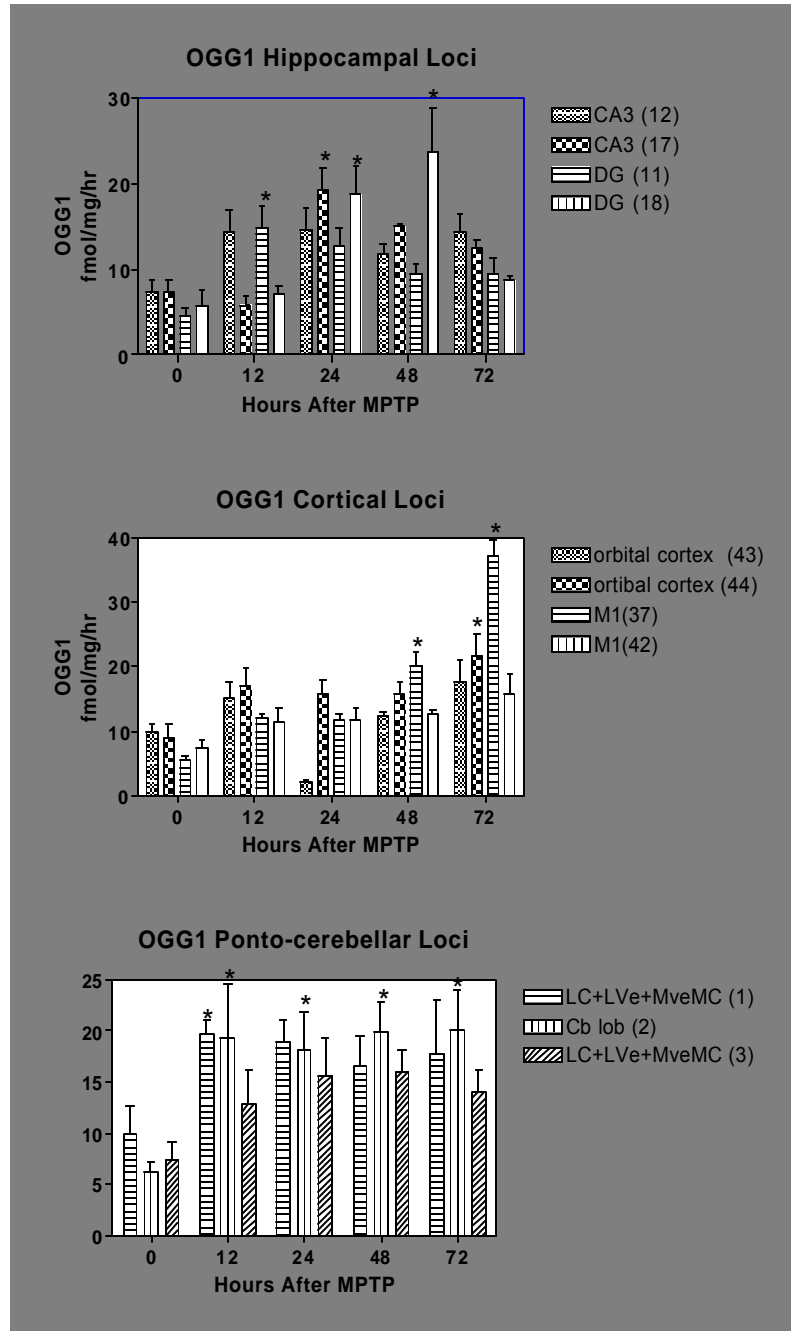


Figure 7 Temporal profile of OGG1 activity in hippocampal loci (upper panel), cortical loci (middle panel) and ponto-cerebellar loci (lower panel). Neuroanatomical locus # is in parentheses in the key. Asterisks indicate statistically significant difference compared to activity at time 0 ($p < 0.05$).

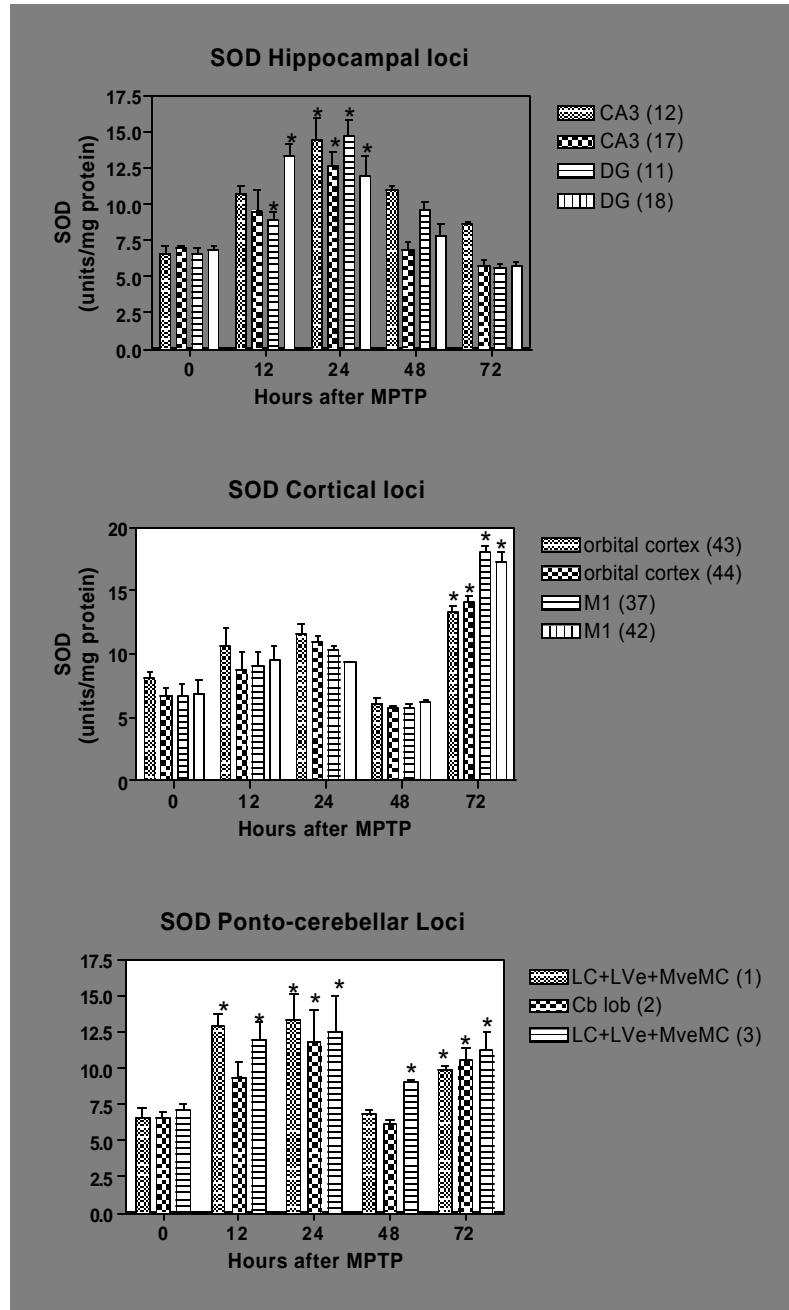


Figure 8 Temporal profile of SOD activity in hippocampal loci (upper panel), cortical loci (middle panel) and ponto-cerebellar loci (lower panel). Neuroanatomical locus # is in parentheses in the key. Asterisks indicate statistically significant difference compared to activity at time 0 ($p < 0.05$).

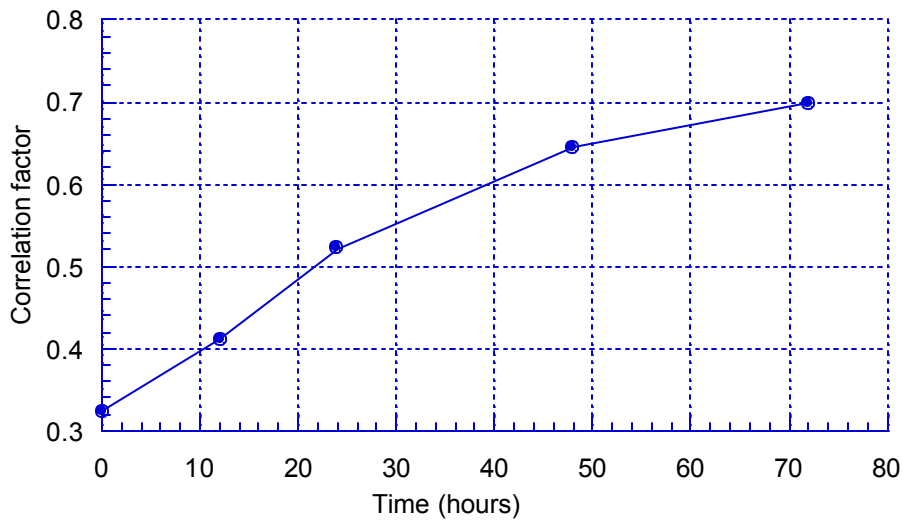


Fig. 9. Correlation factor between OGG1 and SOD activities calculated at each time point across whole brain (calculated for all 44 loci).

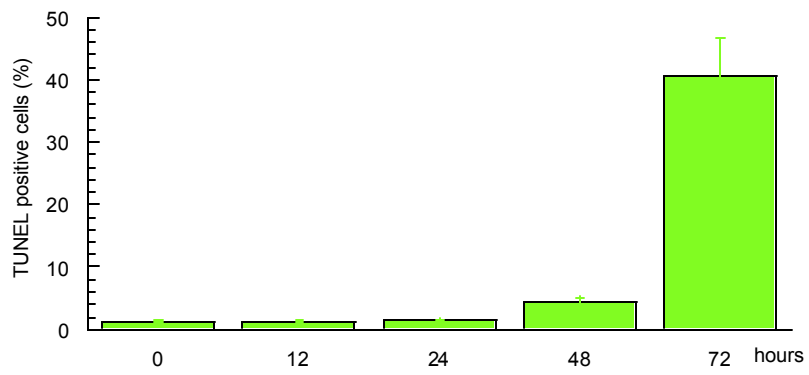
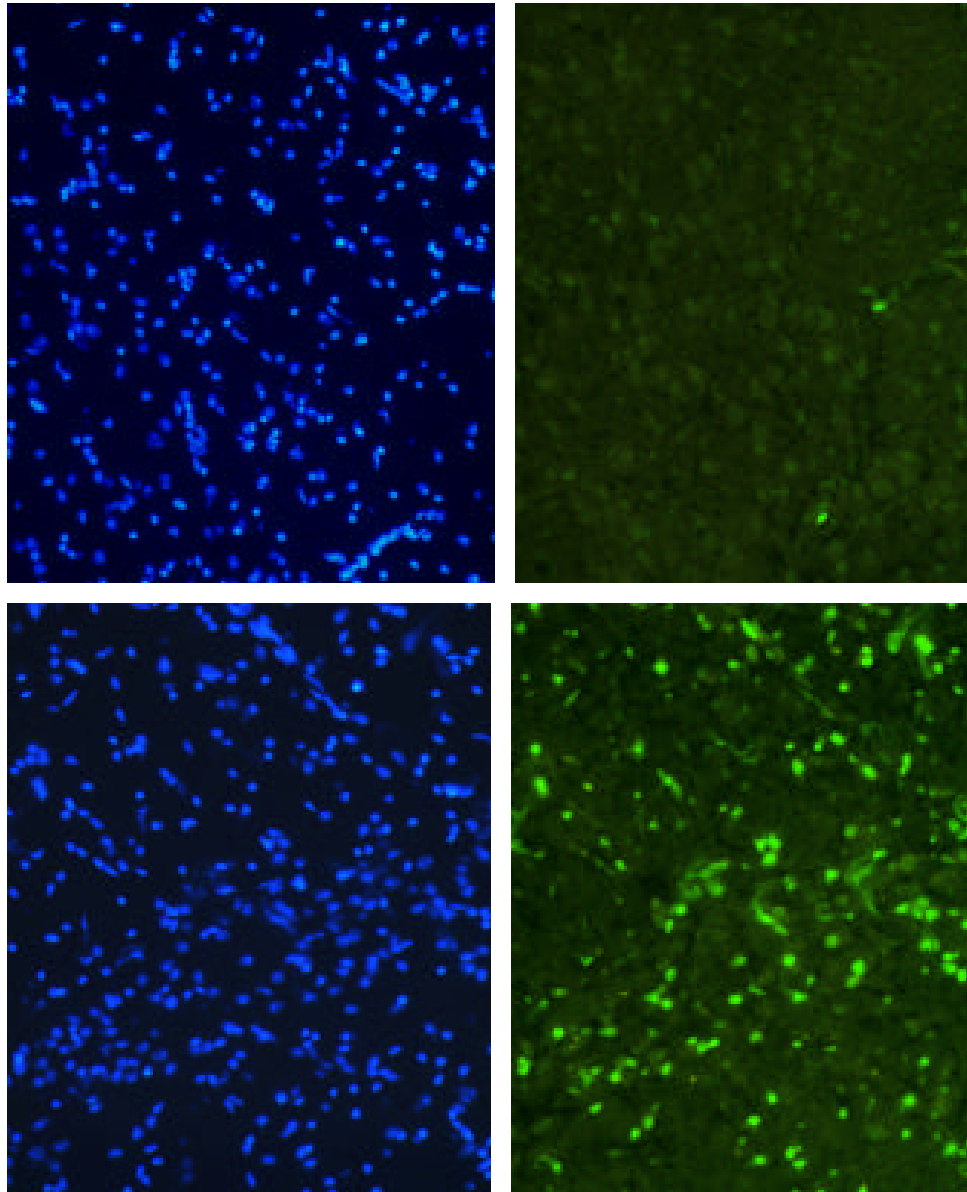


Fig. 10. Representative fluorescence photomicrographs of TUNEL immunoreactivity in substantia nigra of mouse brain exposed to single dose of MPTP (20 mg.kg, ip). Left panels represent DAPI stained nuclei and right panels depict TUNEL-positive (apoptotic) cells. Upper panels represent control and lower ones were obtained from animals 72 hr after MPTP (magnification x 200).

Graph in lower panel: The Y-axis depicts the percentage of TUNEL-positive cells in the substantia nigra (expressed as percent of total number of DAPI+ nuclei) following a single dose of MPTP (20 mg/kg i.p.). The mean percentage (▼ SEM) of apoptotic cells in SN was determined from the average of the ratio of TUNEL+/DAPI+ nuclei in 3 SN sections obtained from 3 animals in each experimental group (control, 24, 48 and 72 hours).

References

- Alam, Z. I., Jenner, A., Daniel, S. E., Lees, A. J., Cairns, N., Marsden, C. D., Jenner, P., and Halliwell, B. (1997). Oxidative DNA damage in the parkinsonian brain: an apparent selective increase in 8-hydroxyguanine levels in substantia nigra. *J Neurochem* 69, 1196-203.
- Alexander, P. (1967). The role of DNA lesions in processes leading to aging in mice. *Symp. Soc. Exp. Biol.* 21, 29-50.
- Betarbet, R., Sherer, T. B., MacKenzie, G., Garcia-Osuna, M., Panov, A. V., and Greenamyre, T. (2000). Chronic systemic pesticide exposure reproduces features of Parkinson's disease. *Nature Neuroscience* 3, 1301-1306.
- Cardozo-Pelaez, F., Brooks, P. J., Stedeford, T., Song, S., and Sanchez-Ramos, J. (2000). DNA damage, repair, and antioxidant systems in brain regions: a correlative study. *Free Radical Biology & Medicine* 28, 779-85.
- Cardozo-Pelaez, F., Song, S., Parthasarathy, A., Hazzi, C., Naidu, K., and Sanchez-Ramos, J. (1999). Oxidative DNA damage in the aging mouse brain. *Movement Disorders* 14, 972-80.
- Cardozo-Pelaez, F., Stedeford, T. J., Brooks, P. J., Song, S., and Sanchez-Ramos, J. R. (2002). Effects of diethylmaleate on DNA damage and repair in the mouse brain. *Free Radical Biology and Medicine* 33, 292-298.
- Cosi, C., and Marien, M. (1999). Implication of poly (ADP-ribose) polymerase (PARP) in neurodegeneration and brain energy metabolism. Decreases in mouse brain NAD⁺ and ATP caused by MPTP are prevented by the PARP inhibitor benzamide. *Annals of the New York Academy of Sciences.* 890, 227-39.
- de Souza-Pinto, N. C., Eide, L., Hogue, B. A., Thybo, T., Stevnsner, T., Seeberg, E., Klungland, A., and Bohr, V. A. (2001). Repair of 8-oxodeoxyguanosine lesions in mitochondrial dna depends on the oxoguanine dna glycosylase (OGG1) gene and 8-oxoguanine accumulates in the mitochondrial dna of OGG1-defective mice. *Cancer Res* 61, 5378-81.
- Edwards, M., Rassin, D. K., Izumi, T., Mitra, S., and Perez-Polo, J. R. (1998). APE/Ref-1 responses to oxidative stress in aged rats. *Journal of Neuroscience Research* 54, 635-638.
- Elstner, E. F., and Heupel, A. (1976). Inhibition of nitrite formation from hydroxyl-ammonium chloride: a simple assay for superoxide dismutase. *Anal Biochem* 70, 616-620.
- Fraga, C., Shigenaga, M., Park, J., Degan, P., and Ames, B. (1990). Oxidative Damage to DNA During Aging: 8-Hydroxy-2'-Deoxyguanosine in Rat Organ DNA and Urine. *PNAS* 87, 4533-4537.
- Gao, H. M., Hong, J. S., Zhang, W., and Liu, B. (2002). Distinct role for microglia in rotenone-induced degeneration of dopaminergic neurons. *J Neurosci* 22, 782-90.
- German, D., Nelson, E., Liang, C., Speciale, S., Sinton, C., and Sonsalla, P. (1996). The Neurotoxin MPTP Causes Degeneration of Specific Nucleus A8, A9 and A10 Dopaminergic Neurons in the Mouse. *Neurodegeneration* 5, 229-312.
- Hanawalt, P. C. (1994). Transcription-coupled repair and human disease: perspective. *Science.* 266, 1957-1958.
- Hornykiewicz, O. (1992). The primary site of dopamine neuron damage in Parkinson's disease: Substantia nigra or Striatum? *Movement Disorders* 7, 288-291.
- Klungland, A., Rosewell, I., Hollenbach, S., Larsen, E., Daly, G., Epe, B., Seeberg, E., Lindahl, T., and Barnes, D. E. (1999). Accumulation of premutagenic DNA lesions in mice defective in removal of oxidative base damage. *Proc Natl Acad Sci U S A* 96, 13300-5.

- Korr, H., and Schultz, B. (1989). Unscheduled DNA synthesis in various types of cells of the mouse brain in vivo. *Experimental Brain Research*, 573-578.
- Krokan, H. E., Standal, R., and Slupphaug, G. (1997). DNA glycosylases in the base excision repair of DNA. *Biochemical Journal* 325, 1-16.
- Langston, J. W., Irwin, I., and Ricuarte, G. A. (1987). Neurotoxins, Parkinsonism and Parkinson's Disease. *Pharmacol Ther* 32, 19-49.
- Liang, C., Sinton, C., Sonsalla, P., and German, D. (1996). Midbrain Dopaminergic Neurons in the Mouse that Contain Calbindin-D 28k Exhibit Reduced Vulnerability to MPTP-induced Neurodegeneration. *Neurodegeneration* 5, 313-318.
- Lovell, M. A., Xie, C., and Markesbery, W. R. (2000). Decreased base excision repair and increased helicase activity in Alzheimer's disease brain. *Brain Research* 855, 116-23.
- Mandavilli, B. S., Ali, S. F., and Van Houten, B. (2000). DNA damage in brain mitochondria caused by aging and MPTP treatment. *Brain Research* 885, 45-52.
- Mandir, A. S., Przedborski, S., Jackson-Lewis, V., Wang, Z.-Q., Simbulan-Rosenthal, C. M., Smulson, M. E., Hoffman, B. E., Guastella, D. B., Dawson, V. L., and Dawson, T. M. (1999). Poly(ADP-ribose) polymerase activation mediates 1-methyl-4-phenyl-1,2,3,6-tetrahydropyridine (MPTP)-induced parkinsonism. *PNAS* 96, 5774-5779.
- Mazzarello, P., Poloni, M., Spadari, S., and Foche, F. (1992). DNA repair mechanisms in neurological diseases: facts and hypotheses. *Journal of the Neurological Sciences* 112, 4-14.
- Mecocci, P., MacGarvey, U., Kaufman, A. E., Koontz, D., Shoffner, J. M., Wallace, D. C., and Beal, M. F. (1993). Oxidative damage to mitochondrial DNA shows marked age-dependent increases in human brain. *Ann Neurology* 34, 609-616.
- Paxinos, G., and K.B.J., F. (2001). *The Mouse Brain in Stereotaxic Coordinates*. Academic Press, San Diego, Calif and London, England.
- Ricuarde, G. A., Irwin, I., Forno, L. S., DeLanney, L. E., Langston, E., and Langston, J. W. (1987). Aging and 1-methyl-4-phenyl-1,2,3,6-tetrahydropyridine-induced degeneration of dopaminergic neurons in the substantia nigra. *Brain Res* 403, 43-51.
- Riederer, P., Sofic, E., Rausch, W. E., and et al. (1989). Transition metals, ferritin, glutathione and ascorbic acid in parkinsonian brain. *J Neurochem* 52, 515-520.
- Robbins, J. H., Otsuka, F., Tarone, R. E., and et al. (1985). Parkinson's disease and Alzheimer's disease: hypersensitivity to X-rays in culture cell lines. *J Neurol Neurosurg Psychiatry* 48, 916-923.
- Sanchez Ramos, J., Overvik, E., and Ames, B. N. (1994). A marker of oxyradical-mediated DNA damage (oxo8dG) is increased in Nigro-Striatum of Parkinson's Disease Brain. *Neurodegeneration (Exp Neurol)* 3, 197-204.
- Sanchez-Ramos, J. R., Hefti, F., Hollinden, G. E., Sick, T., and Rosenthal, M. (1989). *Mechanisms of MPP+ neurotoxicity: oxyradical and mitochondrial inhibition hypotheses*. Plenum Press, New York.
- Sherer, T. B., Betarbet, R., Kim, J. H., and Greenamyre, J. T. (2003). Selective microglial activation in the rat rotenone model of Parkinson's disease. *Neurosci Lett* 341, 87-90.
- Smith, P. K., Krohn, R. I., Hermanson, G. T., Mallia, A. K., Gartner, F. H., Provenzano, M. D., Fujimoto, E. K., Goeke, N. M., Olson, B. J., and Klenk, D. C. (1985). Measurement of protein using bicinchoninic acid. *Anal Biochem* 150, 76-85.
- Stedeford, T., Cardozo-Pelaez, F., Nemeth, N., Song, S., Harbison, R. D., and Sanchez-Ramos, J. R. (2001). Effects of Dieldrin on DNA Repair in PC12 Cells. *Free Radical Biology & Medicine*. 1272-8, 2001 31, 1272-8.
- Turski, L., Bressler, K., Rettig, K. J., Loschmann, P. A., and Wachtel, H. (1991). Protection of substantia nigra from MPP+ neurotoxicity by N-methyl-D-aspartate antagonists. *Nature* 349, 414-8.

**RUBATOXIN-B ELICITS ANTI-OXIDATIVE AND DNA REPAIR
RESPONSES IN MOUSE BRAIN**

V. Sava^{1,2}; D. Mosquera^{1,2}; S. Song^{1,2}; T. Stedeford^{2,4}, K. Calero¹;
F. Cardozo-Pelaez³; R. Harbison⁴, J. Sanchez-Ramos^{1,2*}

¹Neurology, University of South Florida, Tampa, FL

²Research Service, James Haley VA, Tampa, FL

³Department of Pharmaceutical Sciences, University of Montana, Missoula, MT

⁴College of Public Health, University of South Florida, Tampa, FL, USA

* **Corresponding author:** Dr. Juan R. Sanchez-Ramos, The Helen E. Ellis Professor of Neurology, University of South Florida, Department of Neurology (MDC 55), 12901 Bruce B. Downs Blvd., Tampa, FL 33612, USA; Tel: (813) 974-6022; Fax: (813) 974-7200; E-mail: jsramos@hsc.usf.edu

Abstract

Rubratoxin-B (RB) is a mycotoxin with potential neurotoxic effects that have not yet been characterized. Based on existing evidence that RB interferes with mitochondrial electron transport to produce oxidative stress in peripheral tissues, we hypothesized that RB would produce oxidative damage to macromolecules in specific brain regions. Parameters of oxidative DNA damage and repair, lipid peroxidation and superoxide dismutase (SOD) activity were measured across 6 mouse brain regions 24 hrs after administration of a single dose of RB. Lipid peroxidation and oxidative DNA damage was either unchanged or decreased in all brain regions in RB-treated mice compared to vehicle-treated mice. Concomitant with these decreased indices of oxidative macromolecular damage, SOD activity was significantly increased in all brain regions. Oxyguanosine glycosylase activity (OGG1), a key enzyme in the repair of oxidized DNA, was significantly increased in three brain regions cerebellum (CB), caudate/putamen (CP), and cortex (CX) but not hippocampus(H), midbrain(MB), and pons/medulla(PM). The RB-enhanced OGG1 catalytic activity in these brain regions was not due to increased OGG1 protein expression, but was a result of enhanced catalytic activity of the enzyme. In conclusion, specific brain regions responded to an acute dose of RB by significantly altering SOD and OGG1 activities to maintain the degree of oxidative DNA damage equal to, or less than, that of normal steady-state levels.

Running Head: Rubratoxin-B elicits anti-oxidative response

Keywords: Rubratoxin-B, oxidative stress, DNA damage and repair, SOD, mouse brain regions

INTRODUCTION

Mycotoxins are toxic fungal metabolites which are structurally diverse, common contaminants of the ingredients of animal feed and human food. These fungal products exhibit a range of pharmacological activities that have been utilized in development of mycotoxins or mycotoxin derivatives as antibiotics, growth promoters, and other kinds of drugs; still others have been developed as biological and chemical warfare agents [1]. Bombs and ballistic missiles laden with biological agents including aflatoxin were believed to be deployed by Iraq during Operation Desert Storm[2]. In light of the excess incidence of amyotrophic lateral sclerosis in young Gulf War veterans [3], it is important not to forget the potential neurotoxic effects of low doses of mycotoxins. Although much is known about the lethal effects of the aflatoxins, little is known about the acute and long-term effects of less potent mycotoxins, such as Rubratoxin B (RB), on adult nervous system.

Rubratoxin B (RB) is a metabolite of the molds *Penicillium rubrum* and *Penicillium purpurogenum*. These molds commonly contaminate cereals, foodstuffs and grow on damp tents and fabrics. RB is not known to produce a serious health hazard in this naturally occurring form, but pure RB is a bisanhydride lactone with hepatotoxic [4] and teratogenic properties [5, 6, 7]. Investigation of the effects of acute and chronic exposure to RB on the nervous system has been scarce, even though neuronal tissue appears to be very susceptible to the deleterious effect of RB in teratogenic studies [8].

RB has numerous biochemical actions including the inhibition of (Na⁺- K⁺)-ATPase [9], inhibition of the hepatic cytochrome P-450-dependent monooxygenase system[10], reduction of hepatic and renal nonprotein sulfhydryl content [11] and inhibition of gap junctional intercellular communication [12]. It was found that RB caused shifts in the

ultraviolet absorption spectra of DNA and RNA [13]. The observed binding properties of RB can disrupt the integrity of DNA and RNA. RB has been shown to induce apoptosis [14, 15] and internucleosomal fragmentation of DNA [14].

Studies with isolated mouse liver mitochondria revealed that RB disrupted mitochondrial respiration and depressed oxygen consumption[8]. The principal site of action of RB in the mitochondrial electron transport system was found to be between cytochrome C1 and the termination of electron flow [8]. Ochratoxin, a related mycotoxin, has been reported to alter mitochondrial respiration and oxidative phosphorylation through impairment of the mitochondrial membrane and inhibition of the succinate-dependent electron transfer activities of the respiratory chain [16].

The overall objective was to study RB neurotoxicity in the context of oxidative stress induced by inhibition of mitochondrial electron transport in brain tissues. Inhibition of oxidative phosphorylation would be expected to result in increased generation of oxyradicals and decreased production of ATP[17]. We hypothesized that RB-induced alteration of oxidative processes would not be homogeneous across all brain regions but would reflect the capacity of distinct brain regions to upregulate anti-oxidative mechanisms and repair processes. Parameters of oxidative stress measured included lipid peroxidation (thiobarbituric acid-reactive substances or TBARS), SOD activity, oxidative DNA damage and repair in each of six brain regions cerebellum (CB), cortex (CX), hippocampus (HP), midbrain (MB), caudate/putamen (CP) and pons/medulla (PM). Accumulation of 8-oxodG was chosen as an indicator of DNA damage and activity of DNA glycosylase was used as an index of DNA repair.

MATERIALS AND METHODS

Materials

Rubratoxin-B, superoxide dismutase, xantine oxidase, ribonuclease T1, HEPES, dithiotreitol, bovine serum albumin and acrylamide/bisacrylamide (19:1) mixture were purchased from Sigma (St. Louis, MO). TEMED was from Bio-Rad Laboratories (Hercules, CA). Protease inhibitors and 8-oxoguanine DNA glycosylase (mOGG1) were from Boehringer Mannheim (Indianapolis, IN). Synthetic oligonucleotide contained 8-oxodG was from Trevigen (Gaithersburg, MD). ³²P-ATP (7,000 Ci/mmol) was from ICN Biomedical, Inc. (Costa Mesa, CA). Phosphorylation buffer, 3'-phosphate free T4 polynucleotide kinase, RNase, proteinase K, nuclease P1, alkaline phosphatase were from Roche Diagnostic Co. (Indianapolis, IN). G-25 Microcentrifuge Spin Column was from Shelton Scientific (Shelton, CT). mOGG1 antibody was from Alpha Diagnostic (San Antonio, TX). ECL western blotting analysis system was from Amersham Biosciences (Piscataway, NJ). All other reagents were ACS grade and from Sigma Chemical Co.

Animals and Treatment

The animal protocol used in this study was approved by the University of South Florida (USF) IUCAC committee. The protocol was also reviewed and approved by the USF Division of Comparative Medicine which is fully accredited by AAALAC International and managed in accordance with the Animal Welfare Regulations, the PHS Policy, the FDA Good Laboratory Practices, and the IACUC's Policies. Male Swiss ICR mice (22 ± 2 g) were obtained from the Jackson Laboratories (Bar Harbor, ME). They were housed five per cage at the temperature of 21 ± 2 °C with 12 light/dark cycle and free access to food and water. Mice were divided into experimental (n=10) and control (n=5) groups. Animals were injected with

either RB dissolved in DMSO (5 mg/kg ip) or vehicle. Mice were sacrificed with CO₂ twenty four hours after treatment. The brains were removed and immediately dissected in a Petri dish on ice (~ 0 °C).

Isolation of Brain Regions

Brain was separated into 6 regions under a dissecting microscope in following order. The cerebellar peduncles were cut first, and brain stem was removed from the diencephalon. The ventral and dorsal parts of midbrain (MB) were dissected at the level of the caudal end of the cerebral peduncles at the junction with the pons. The pons and medulla (PM) were separated together by cutting the ponto-medullary junction. The cerebral hemispheres were opened with a sagittal cut along the longitudinal tissue and hippocampus (HP) was isolated, followed by caudate and putamen (CP). Finally, cerebellum (CB) and cerebral cortex (CX) were harvested and all the samples were kept frozen at -70 °C until assay.

Measurement of DNA damage

Steady-state level of 8-oxodG was used as a marker of oxidative DNA damage. The procedure for DNA isolation was basically the same as reported before [18]. Approximately 150 mg of brain sample was used for extraction. Briefly, tissue was pulverized in liquid nitrogen, using mortar and pestle, sonicated in 10 mM ethylenediamine tetraacetic acid (EDTA) and centrifuged. The pellet was treated with DNAase-free RNAase followed by digestion with proteinase K. The protein fraction was separated from DNA by three consecutive organic extractions. The DNA was precipitated by ethanol and incubated overnight at -20 °C. The ratio in absorbance at 260/280 nm was employed for qualification of DNA purity.

The purified DNA was digested with nuclease P1 following by treatment with alkaline phosphatase. The mixture of deoxynucleosides was analysed with HPLC using 5% methanol dissolved in 100 mM of sodium acetate (pH 5.2) as a mobile phase, and 8-oxodG was detected with an electrochemical detector (ESA Coulochem Model 5100A) at +0.4 V. 2-dG was detected at 260 nm in the same sample using a Perkin Elmer 785A Programmable Absorbance Detector (Perkin Elmer, Norwalk, CT) connected in series with the electrochemical detector. 8-oxodG level was expressed as ratio of 8-oxodG/2-dG. Data were recorded, stored, and analyzed on a PC Pentium computer using ESA 500 Chromatography Data System Software.

Assessment of 8-oxoguanine-DNA glycosylase activity (OGG1)

The extraction of OGG1 for enzymatic assay was performed as described previously [18]. Briefly, brain tissue was pulverized in liquid nitrogen, using mortar and pestle. Homogenization buffer contained 20 mM Tris-Base (pH 8.0), 1 mM EDTA, 1 mM dithiotrietol (DTT), 0.5 mM spermine, 0.5 mM spermidine, 50% glycerol and protease inhibitors. Homogenates were rocked for 30 min after addition of 1/10 volume 2.5 M KCl and spun at 14,000 rpm for 30 min. The supernatant was aliquoted and specimens were kept frozen at $-70\text{ }^{\circ}\text{C}$ until assay. Protein concentration was measured using the bicinchoninic acid [19].

OGG1 activity was measured by incision assay as previously described [18]. To prepare ^{32}P -labeled duplex oligonucleotide, twenty pmol of synthetic probe contained 8-oxodG (Trevigen, Gaithersburg, MD) was incubated at $37\text{ }^{\circ}\text{C}$ with ^{32}P -ATP and polynucleotide T4 kinase. To separate the unincorporated free ^{32}P -ATP, the reaction mixtures were spun through a G25 spin column. Complementary oligonucleotides were annealed in 10

mM Tris, (pH 7.8), 100 mM KCl, 1 mM EDTA by heating the samples 5 min at 80 °C and gradually cooling at room temperature.

Incision reaction (20 μ L) contained 40 mM HEPES (pH 7.6), 5 mM EDTA, 1 mM DTT, 75 mM KCl, purified bovine serum albumin, 100 fmol of 32 P-labeled duplex oligonucleotide, and protein extract (30 μ g). The reaction mixture was incubated at 37 °C for 2 h and placed on ice to terminate the reaction. A 20 μ L of loading buffer containing 90% formamide, 10mM NaOH and blue-orange dye was added to each sample. After 5 min of heating at 95 °C the samples were resolved in a denaturing 20% polyacrylamide gel containing 7 M urea. The gel was visualized using Biorad-363 Phosphoimager System and OGG1 incision activity was calculated as the amount of radioactivity in the band corresponding to the specific cleavage product over the total radioactivity in the lane.

Kinetic study of OGG1 incision reaction

Reaction mixtures and conditions used for kinetic studies were identical to OGG1 incision activity assay, but amounts of the appropriate 32 P-labeled oligonucleotide duplex were varied. The enzyme concentration and reaction time was adjusted so as to cleave no more than 10% of the substrate. Kinetic parameters were calculated using a Jandel SigmaPlot version 5.00 nonlinear fit routine. Three independent experiments were performed for each analysis.

Western immunoblotting

The 8-oxoguanine DNA glycosylases extracted from different regions of brain were

separated on a 12% SDS-PAGE and transferred onto a nitrocellulose membrane using a Biorad Semi-Dry Transblot technique. The membranes were blocked overnight at 4 °C in a solution containing 5% dry milk and Tris-Buffered Saline (TBS) composed of 200 mM NaCl and 50 mM Tris-HCl (pH7.4), and supplemented with 0.04% Tween-20. The membranes were rinsed in TBS-Tween mixture and incubated overnight at 4 °C with mOGG1 antibody (Alpha Diagnostic, TX) using 1:1000 dilution by 1% dry milk prepared on TBS-Tween. After washing (3 x 10 min) with TBS-Tween at 4 °C, the membranes were incubated with goat anti-mouse antibody (1:2000 dilution) conjugated to horseradish peroxidase (Santa Cruz Biotechnology, CA) for 1 hr at room temperature. The blot was developed by ECL kit (Amersham Biosciences, Piscataway, NJ).

Native PAGE

OGG1 extracted from different regions of brain mixed with native buffer composed of 0.1 M Tris-HCl (pH6.8), 30% glycerol, and 0.01% bromophenol blue and separated on a non-denaturing 10% polyacrylamide gel at 120 V. Gel were sliced by a razor blade along the lanes into section 1 mm thick. A single 1 mm thick section was homogenized with a teflon hand homogenizer in 20 μ L of incision reaction mixture and enzymatic activity of OGG1 was assayed as described above.

Lipid peroxidation

Formation of lipid peroxide derivatives was evaluated by measuring thiobarbituric acid-reactive substances (TBARS) according to [20]. Briefly, the different regions of brain were individually homogenized in ice-cold 1.15% KCl (w/v); then 0.4 mL of the homogenates were mixed with 1mL of 0.375% TBA, 15% TCA (w/v), 0.25 N HCl and 6.8 mM butylated-

hydroxytoluene (BHT), placed in a boiling water bath for 10 min, removed and allowed to cool on ice. Following centrifugation at 3000 r.p.m. for 10 min, the absorbance in the supernatants was measured at 532 nm. The amount of TBARS produced was expressed as nmol TBARS per milligram of protein using malondialdehyde bis(dimethyl acetal) for calibration.

Superoxide dismutase (SOD) assay

Determination of superoxide dismutase activity in mouse brain regions was based on inhibition of nitrite formation in reaction of oxidation of hydroxylammonium with superoxide anion radical [21]. Nitrite formation was generated in a mixture contained 25 μ L xanthine (15 mM), 25 μ L hydroxylammonium chloride (10 mM), 250 μ L phosphate buffer (65 mM, pH 7.8), 90 μ L distilled water and 100 μ L xanthine oxidase (0.1 U/mL) used as a starter of the reaction. Inhibitory effect of inherent SOD was assayed at 25°C during 20 min of incubation with 10 μ L of brain tissue extracts. Determination of the resulted nitrite was performed upon the reaction (20 min at room temperature) with 0.5 mL sulfanilic acid (3.3 mg/mL) and 0.5 mL α -naphthylamine (1 mg/mL). Optical absorbance at 530 nm was measured with Ultrospec III spectrophotometer (Pharmacia, LKB). The results were expressed as units of SOD activity calculated per milligram of protein. The amount of protein in the samples was determined using the bicinchoninic acid [19].

Statistical analysis

The results were reported as mean \pm SE for at least five different preparations, assayed in duplicate. For electrophoresis two different gels were run. The differences between samples were analyzed by the Student's *t*-test, and a $P < 0.05$ was considered as statistically significant.

RESULTS

Administration of a single dose of RB to mice (ip injection, 5 mg/kg body weight) was chosen on the basis of a dose-toxicity curve (data not shown) that resulted in no visible gross damage to brain. This single dose did, however, produce alterations in brain biochemistry. Lipid peroxidation, indicated by TBARS levels, was decreased in all regions of brain of the animals exposed to RB as compared to control mice (Fig. 1). In HP, MB and PM the TBARS levels were significantly ($P < 0.05$) different from the control. In PM region, a 2.2 fold decrease in TBARS was observed.

Oxidative DNA damage, indicated by steady-state levels of 8-oxodG, showed a trend towards decreased levels across all brain regions (Table 1). Statistically significant differences in 8-oxod-dG were found in only the PM region, where levels were reduced to 30% below control. Oxidative damage in MB was also distinctly decreased, but did not reach statistical significance.

The decreased levels of oxidative DNA damage were associated with increased activity of the repair enzyme OGG1 (Table 1). There was a statistically significant increase in OGG1 activity in CB, CP and CX regions as compared to the respective controls. In HP the activity of OGG1 was higher than in control though the difference did not reach statistical significance. The OGG1 activity was reduced in MB and PM. The trend of reduced OGG1

activity within the MB-PM array presented in Table 1 was unexpectedly associated with decreased levels of 8oxodG in those regions. Nevertheless, we observed that relative extent of DNA damage decreased linearly (Fig. 2) with relative activity of OGG1 (correlation factor was - 0.9545). For both specific OGG1 and 8-oxodG relative indices were calculated as follows:

$$\text{Relative indices} = \frac{100 \cdot (V_{RB} - V_C)}{V_C}$$

where V_{RB} are values obtained in RB experiment and V_C – in control

The results in Table 1 demonstrated up-regulation of SOD activity in RB-treated animals as compared to control. The extent of increased SOD activity in different regions of brain revealed a negative correlation with the level of 8-oxodG. Namely, the association between 8-oxodG and SOD activity can be expressed by the linear equation with the correlation factor of - 0.8521:

$$[8\text{-oxodG}] = - 0.19[SOD] + 4.6$$

Western blot analysis was carried out to elucidate the source of OGG1 activity (Fig.3). It was found that protein expression levels of OGG1 were not significantly affected by RB exposure and there were no differences in regional levels of OGG1 when normalized to the total protein variations. One of the bands in the Western blot attributed to OGG1 matched the single band of pure enzyme. However, we found an additional band that was also labeled with OGG1 antibody. This band may be due to non-specific binding with antibody or otherwise caused by existence of various isoforms of OGG1. To clarify this issue, we resolved OGG1

in native PAGE followed by cutting the gel into 1 mm strips and assaying the strips for OGG1 enzymatic (incision) activity. Fig. 4 indicates presence of two distinct bands with incision activity, which likely can be attributed to different isoforms of OGG1. Assaying the pure enzyme with the same procedure showed one single band possessing electrophoretic mobility identical to the major band of the tested sample (not shown).

The data are in agreement with kinetic behavior of OGG1 extracted from mouse brain. As can be seen from Fig. 5 the oligonucleotide incision activity plotted against concentration reveals bi-modal curves. The first part of incision activity reached saturation level in a range between 0 and 120 pM of substrate, but second part needed higher concentrations of substrate (up to 500 pM). Computer modeling generated kinetic curves representing the experimental curve as a superposition of low- and high-saturated enzymatic isoforms. Separated incision activities were analyzed using Michaelis-Menten kinetics with the corresponding calculation of kinetic constants as shown in Table. 2.

DISCUSSION

Until the present report, the toxic effects of RB in adult brain had not been investigated. Administration of a single dose (5mg/kg) did not produce gross pathological changes in brain, but resulted in paradoxically less oxidative damage to both lipids and DNA. In fact the level of lipid peroxidation in hippocampus, midbrain and pons/medulla was significantly less than that found in vehicle-treated controls. Similarly, RB did not increase oxidative DNA damage in any region of brain after the injection rather tended to lower the degree of damage. These results were unexpected in light of the putative pro-oxidant effects of the mycotoxin, but were explained by the robust upregulation of anti-oxidative and repair

systems. RB treatment elicited an increase in activity of SOD, a major oxyradical scavenger, across all brain regions. In addition, measures of oxidative DNA repair were observed to increase in three of six brain regions following RB treatment.

Measurement of oxidative DNA damage revealed a trend towards decreased steady-state levels of 8-oxodG across all brain regions with a statistically significant decreased level in pons/medulla (PM). The DNA repair response assessed from the change in OGG1 activity was significantly increased in three brain regions (CX, CB, CP) but it is noteworthy that maintenance of normal steady state levels of 8-oxodG was facilitated by the greatly enhanced SOD activity in regions of brain where OGG1 did not increase.

The index of DNA damage utilized in this study was 8-oxodG, a major pre-mutagenic DNA lesion generated from the reaction of oxyradicals with guanosine. Repair of this DNA lesion involves DNA N-glycosylases that hydrolyse the N-glycosylic bond between the 8-oxoG and deoxyribose, releasing the free base and leaving an apurinic/apyrimidinic (AP) site in DNA. Such AP sites are cytotoxic and mutagenic, and must be further processed. Some DNA glycosylases also have an associated AP lyase activity that cleaves the phosphodiester bond 3' to the AP site [22]. Formamidopyrimidine glycosylase (fpg, also named fapy-DNA glycosylase) is a prokaryotic protein originally identified in *E. coli* that catalyzes the excision of damaged purine bases such as 8-oxodG and 2,6-diamino-4-hydroxy-5-N-methylformamidopyrimidine from double stranded DNA. Two distinct homologues of fpg were identified in yeast, OGG1 and OGG2 (8-oxo-guanine glycosylase). The counterpart of yeast OGG1 has been identified in eukaryotes, and in particular human brain (hOGG1). hOGG1 has been cloned and shares 50% homology with mouse 8-oxoguanine glycosylase

(mOGG1) [22, 23]. In the present report, the role of the brain's DNA response to RB focused on the activity and regulation of the mammalian base excision repair enzyme OGG1.

In addition to the enzymatic assay, the expression of OGG1 protein was measured by Western immunoblotting. However, the detection of a second band with molecular weight essentially different from mOGG1 required more careful characterization. Separation of DNA glycosylases with native PAGE followed by assays of incision activity in various portions of gel disclosed heterogeneity of enzyme activity. Thus, enzymatic incision activity of tested extracts from mouse brain was comprised of two distinct isoforms of OGG1.

A detailed characterization of the isoforms of DNA glycosylase was performed by enzymatic kinetic analysis. Calculation of kinetic constants showed that RB treatment caused an increase in catalytic efficacy in both isoforms of OGG1. The response to RB-induced oxidative DNA damage was to enhance OGG1 catalytic activity (V_{\max}/K_m) by a factor of 1.74. RB also increased affinity of OGG1 for the substrate that was demonstrated by decrease in magnitudes of the Michaelis-Menten constant, K_m .

The augmentation of SOD activities in all brain regions and the increased affinity and catalytic activity of OGG1 elicited by RB treatment maintained 8-oxodG levels equal to, or below, the levels found in control animals. In the hippocampus, the levels of oxidative DNA damage following RB treatment was 2.7 fold less than that found in control mice. A similar phenomenon in mouse brain has been reported following treatment with the pro-oxidant diethylmaleate [18]. A single treatment with diethylmaleate elicited a significant increase in the activity of OGG1 in three brain regions with low basal levels of activity. There was no change in the activity of OGG1 in those regions with high basal levels of activity (HP, CP,

and MB). This protective response elicited by prooxidants such as DEM and RB demonstrate efficient homeostatic mechanisms that maintain a healthy redox status in brain tissues.

The capacity to regulate OGG1 may be important for maintaining genomic integrity in the face of oxidative stress, but endogenous antioxidant defenses also played a role in the brain's response to RB. In fact, the magnitude of the increases in SOD activity across all regions of brain was greater than the observed increases in OGG1 activity. There was a correlation between OGG1 and SOD activities in different regions of brain, suggesting that both enzymes may be regulated by a common signal triggered by oxidative stress.

The mechanisms underlying the vulnerability of the brain to different neurotoxicants is complex, but we hypothesize that the capacity to regulate and repair oxidative DNA damage, and to modulate endogenous anti-oxidant enzymes, are important determinants of a brain region's susceptibility to RB. In the present study, which focused on a single time point 24 hrs after injection with RB, it was not the intent to determine the earliest signals for triggering and amplifying SOD and OGG1 activities. We imposed the limitation of a single time point for this study in order to focus on the differential response across brain regions. The robust anti-oxidant response and enhanced OGG1 catalytic activity in some regions resulted in much lower levels of oxidized base in those brain regions, providing a clue as to the selective vulnerability of specific neuronal populations located in those regions.

The data presented here clearly raises many questions that drive on-going and future investigations. In order to further characterize the regulation of OGG1 in response to RB and similar neurotoxicants, it will be important to discover whether the earliest changes in SOD and OGG1 activity (3 to 6 hrs after exposure) are due to modification in catalytic activities of the protein and to what extent the response requires upregulation of SOD and OGG1 mRNA

and protein expression. Just as importantly, the effects of RB on viability of specific populations of neurons (e.g., dopaminergic neurons, striatal neurons) in the specific brain regions will need to be investigated and correlated with measures of oxidative DNA damage and repair. Finally, studies with graded doses of RB will determine whether RB can produce a rigid-akinetic parkinsonian syndrome similar to that produced by other mitochondrial toxicants such as rotenone.

ACKNOWLEDGEMENTS

This study was supported by VA Merit Grant and DOD grant USAMRMC 03281031.

REFERENCES

- [1] Bennett, J. W. and Klich, M., Mycotoxins. Clin Microbiol Rev. 16: 497-516; 2003
- [2] Zilinskas, R. A., Iraq's biological weapons. The past as future? Jama. 278: 418-424; 1997
- [3] Haley, R. W., Excess incidence of ALS in young Gulf War veterans. Neurology. 2003; 61: 750-756.
- [4] Natori S, Sakaki S, Kurata H, Udagawa SI and Ichinoe M. Production of rubratoxin B by *Penicillium purpurogenum* Stoll. Appl Microbiol. 19:613-617;1970
- [5] Hood RD, Innes JE and Hayes AW. Effects of rubratoxin B on prenatal development in mice. Bull Environ Contam Toxicol 1973; 10: 200-207;1973
- [6] Hood RD. Effects of concurrent prenatal exposure to rubratoxin B and T-2 toxin in the mouse. Drug Chem Toxicol. 19: 185-190;1986
- [7] Koshakji RP, Wilson BJ and Harbison RD. Effect of rubratoxin B on prenatal growth and development in mice. Res Commun Chem Pathol Pharmacol; 5: 584-592; 1973
- [8] Hayes AW. Action of rubratoxin B on mouse liver mitochondria. Toxicology.6:253-561;1976
- [9] Phillips TD, Hayes AW, Ho IK and Desai D. Effects of rubratoxin B on the kinetics of cationic and substrate activation of (Na⁺-K⁺)-ATPase and p-nitrophenyl phosphatase. J Biol Chem. 253: 3487-3493; 1978
- [10] Siraj MY and Hayes AW. Inhibition of the hepatic cytochrome P-450-dependent monooxygenase system by rubratoxin B in male mice. Toxicol Appl Pharmacol 48: 351-359;1979

- [11] Engelhardt JA, Carlton WW, Carlson GP and Hayes AW. Reduction of hepatic and renal nonprotein sulfhydryl content and increased toxicity of rubratoxin B in the Syrian hamster and Mongolian gerbil. *Toxicol Appl Pharmacol.* 96: 85-92; 1988
- [12] Nagashima H, Nishida M, Ishizaki Y, Morita I, Murota S, Goto T. Cytological effects of rubratoxin B: morphological change and gap Junctional intercellular communication. In: Funatsu K, Shirai Y, Matsushita T (eds.) *Animal Cell Technology: Basis & Applied Aspects* 1997; vol. 8. Kluwer Academic Publishers, Dordrecht, pp. 571-575
- [13] Watson SA and Hayes AW. Evaluation of possible sites of action of rubratoxin B-induced polyribosomal disaggregation in mouse liver. *J Toxicol Environ Health.* 2(3): 639-650;1997
- [14] Nagashima H and Goto T. Rubratoxin B induces apoptosis in HL-60 cells in the presence of internucleosomal fragmentation. *Mycotoxins.* 46: 17-22; 1998
- [15] Nagashima H, Ishizaki Y, Nishida M, Morita I, Murota S, Goto T. Rubratoxin B induces apoptosis in p53-null cells. *Mycotoxins* 46: 35-37;1998
- [16] Wei YH, Lu CY, Lin TN and Wei RD. Effect of ochratoxin A on rat liver mitochondrial respiration and oxidative phosphorylation. *Toxicology* 36: 119-30; 1985
- [17] Hasegawa, E., Takeshige, K., Oishi, T. and et al., MPP⁺ induces NADH-dependent superoxide formation and enhances NADH-dependent lipid peroxidation in bovine heart submitochondrial particles. *Biochem Biophys Res Com.* 170: 1049-1055, 1990
- [18] Cardozo-Pelaez F, Stedeford TJ, Brooks PJ, Song S and Sanchez-Ramos JR. Effects of diethylmaleate on DNA damage and repair in the mouse brain. *Free Radical Biology and Medicine* 33: 292-298;2002

- [19] Smith PK, Krohn RI, Hermanson GT, Mallia AK, Gartner FH, Provenzano MD, Fujimoto EK, Goeke NM, Olson BJ, Klenk DC. Measurement of protein using bicinchoninic acid. *Analytical Biochemistry* 150: 76-85;1985
- [20] Cascio C, Guarneri R, Russo D, De Leo G, Guarneri M, Piccoli F, Guarneri P. Pregnenolone sulfate, a naturally occurring excitotoxin involved in delayed retinal cell death. *J Neurochem.* 74(6): 2380-2391;2000
- [21] Elstner EF and Heupel A. Inhibition of nitrite formation from hydroxylammoniumchloride: a simple assay for superoxide dismutase. *Anal. Biochem.* 70: 616-620; 1976
- [22] Krokan HE, Standal R. and Slupphaug G. DNA glycosylases in the base excision repair of DNA. *Biochem Journal* 325: 1-16;1997
- [23] Dianov G, Bischoff C, Piotrowski J and Bohr VA. Repair pathways for processing of 8-oxoguanine in DNA by mammalian cell extracts. *J Biol Chem* 273: 33811-33816;1998

Table 1. Evaluation of Oxidative DNA damage, Oxidative DNA Repair (OGG1) and Superoxide Dismutase Activities across different regions of mouse brain exposed to RB in comparison with control.

Brain regions	Animal groups	DNA damage* (ppm)	OGG1 incision activity ($\mu\text{M}^{-1}\text{min}^{-1}\text{mg prot}^{-1}$)	Activity of SOD (U/mg prot.)
CB	Control	18.4 \pm 2.2	2.6 \pm 0.2	42.5 \pm 4.6
	RB intoxication	16.7 \pm 2.1	4.06 \pm 0.55**	63.8 \pm 7.5**
CP	Control	20.6 \pm 3.8	3.05 \pm 0.24	42.4 \pm 2.7
	RB intoxication	18.2 \pm 1.8	4.27 \pm 0.45**	72.6 \pm 6.1**
CX	Control	20.7 \pm 0.8	2.52 \pm 0.4	34.8 \pm 1.5
	RB intoxication	20.1 \pm 5.1	3.86 \pm 0.32**	64.5 \pm 11.25**
HP	Control	19.4 \pm 1.2	2.86 \pm 0.31	32.6 \pm 3.2
	RB intoxication	16.1 \pm 1.9	3.42 \pm 0.33	78.14 \pm 12.1**
MB	Control	26.9 \pm 8.3	2.79 \pm 0.22	48.6 \pm 2.1
	RB intoxication	20.2 \pm 6.4	2.43 \pm 0.19	112.5 \pm 16.4**
PM	Control	33.0 \pm 2.4	3.4 \pm 0.26	38.7 \pm 3.8
	RB intoxication	22.7 \pm 0.9**	3.0 \pm 0.27	105.5 \pm 14.8**

*The extent of DNA damage was calculated from the amount of 8-oxodG (fmol) contained in 1 nmol of 2-dG and expressed as parts per million (ppm)

**The values are significantly ($P < 0.05$) different compared to controls. All results represented by mean \pm SE.

Table 2. Kinetic characterization of OGG1 isoforms obtained from CP of control mouse and from CP of mouse subjected to RB

Isoforms of OGG1	Samples tested	Kinetic constants		
		K_m (pM)	V_{max} (pM min ⁻¹ mg ⁻¹)	V_{max}/K_m (min ⁻¹ mg ⁻¹)
High-saturated	CP exposed to RB	147.7?12	20.1?2.1	0.136?0.01
	CP control	312.9?29	24.7?2.6	0.078?0.007
Low-saturated	CP exposed to RB	105.3?9	17.7?2	0.16?0.02
	CP control	140.5?11	16.2?1.5	0.11?0.01

Figure Captions

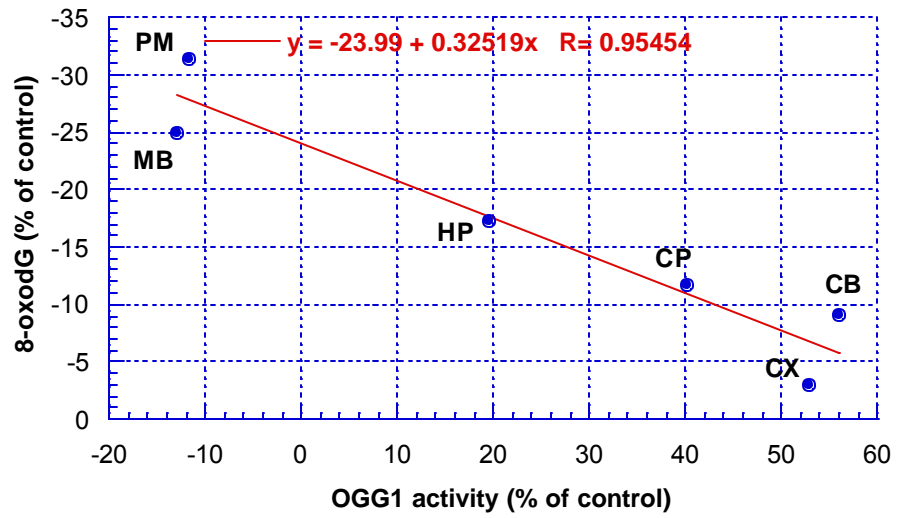
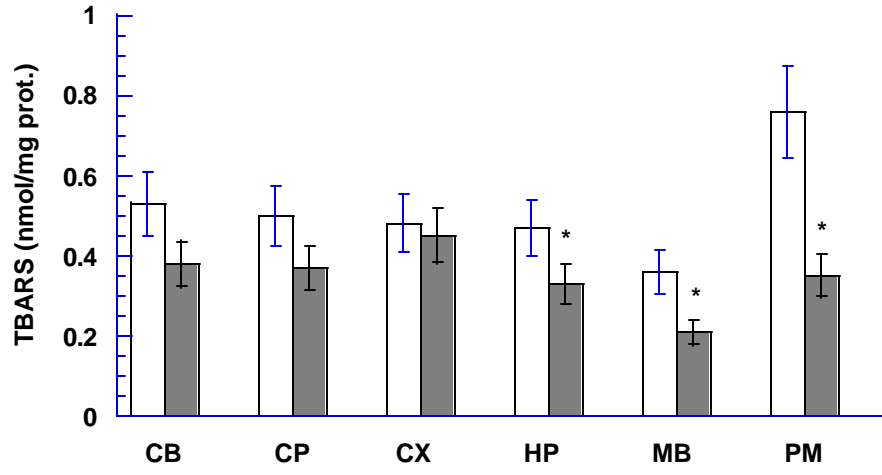
Fig. 1. Content of TBARS in different regions of mouse brain exposed to RB (closed bars) in comparison to control (opened bars). All values represent by mean \pm SE. The significantly ($P < 0.05$) different levels of TBARS in comparison to control indicated by asterisks.

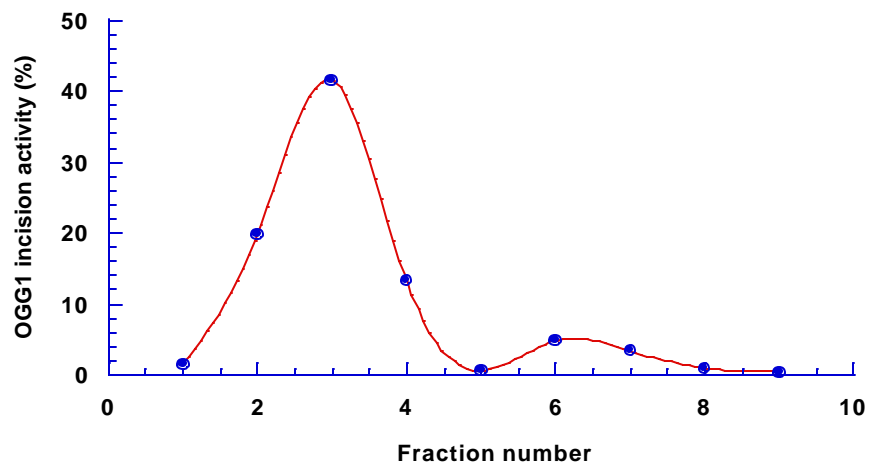
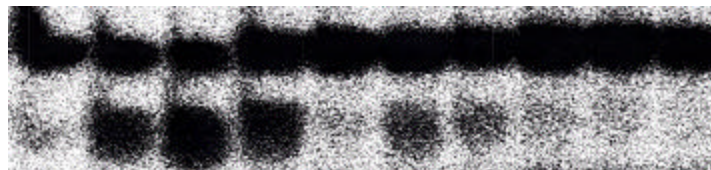
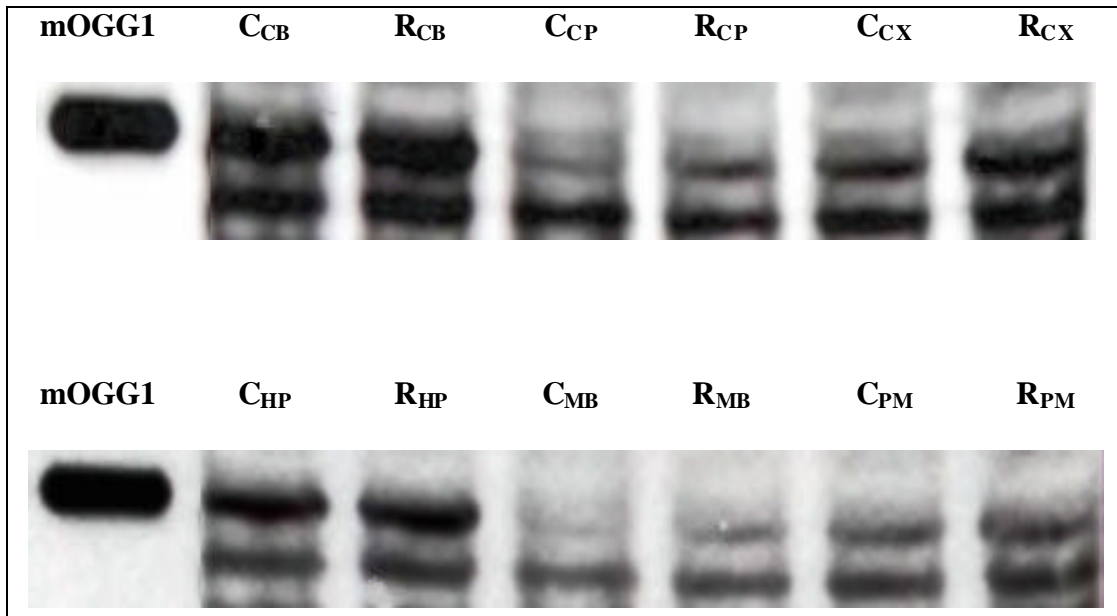
Fig.2. Relationship between relative indices of OGG1 activity and accumulation of 8-oxodG in various regions of mouse brain. Relative indices represent values normalized to the correspondent controls.

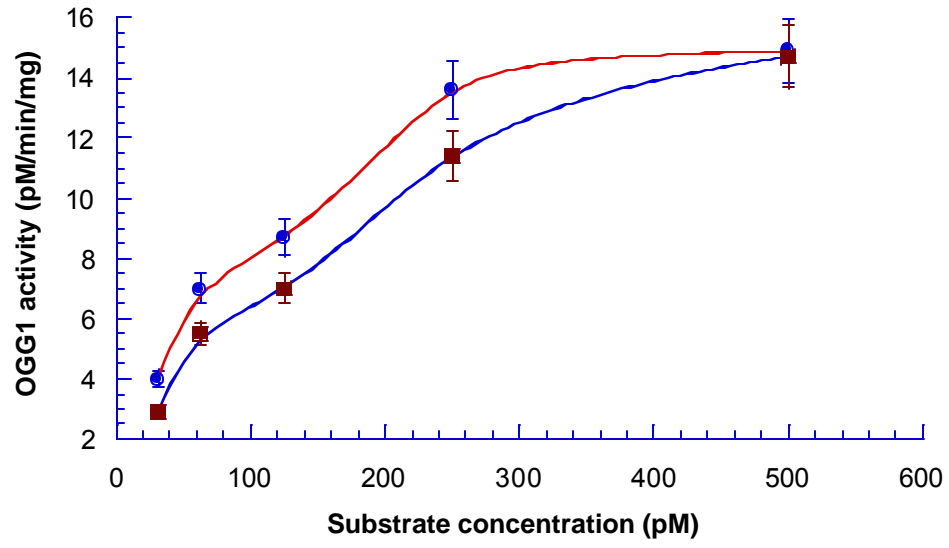
Fig. 3. OGG1 expression in different regions of mouse brain. The Western blot lanes depicted by $C_{CB} - C_{PM}$ array show the level of OGG1 in control mouse, and lanes from R_{CB} to R_{PM} represent OGG1 expression in the brain of RB-intoxicated animal. Pure enzyme presented as a positional marker for OGG1 identification.

Fig. 4. Determination of OGG1 on native PAGE. Enzymatic activity of OGG1 was assayed in every single fraction by using ^{32}P -duplex oligonucleotide. Upper panel represent ^{32}P -duplex oligonucleotide products visualized with Biorad-363 Phosphoimager System. Lower panel represent the averaged data of three experiments with OGG1 extracted from HP of control mouse. OGG1 activity was calculated as the % of radioactivity in the band of specifically cleaved product over the total radioactivity in the lane.

Fig. 5. Kinetic behavior of OGG1 extracted from different regions of brain. Circles represent OGG1 obtained from CP of mouse exposed to RB. Squares represent OGG1 obtained from CP of control mouse. Data expressed by means of 3 replications.







In press, J. Neurosci (2006)

Can Low Level, Non-lethal Exposure to Ochratoxin-A Cause Parkinsonism?

Sava, V^{1,2}, Reunova, O^{1,2}, Velasquez^{1,2}, A and Sanchez-Ramos, J^{1,2}

¹ *University of South Florida, Tampa FL, USA*

² *James Haley VA Hospital, Tampa, FL, USA*

Correspondant:

Juan Sanchez-Ramos, PhD, MD
Dept of Neurology (MDC 55)
University of South Florida
12901 Bruce B. Downs Blvd
Tampa, FL 33612

email: jsramos@hsc.usf.edu
FAX: 813-974-720

Can Low Level, Non-lethal Exposure to Ochratoxin-A Cause Parkinsonism?

Abstract Mycotoxins are fungal metabolites with pharmacological activities that have been utilized in production of antibiotics, growth promoters, and other classes of drugs. Some mycotoxins have been developed as biological and chemical warfare agents. Bombs and ballistic missiles loaded with aflatoxin were stockpiled and may have been deployed by Iraq during the first Gulf War. In light of the excess incidence of amyotrophic lateral sclerosis (ALS) in veterans from Operation Desert Storm, the potential for delayed neurotoxic effects of low doses of mycotoxins should not be overlooked. Ochratoxin-A (OTA) is a common mycotoxin with complex mechanisms of action, similar to that of the aflatoxins. Acute administration of OTA at non-lethal doses (10% of the LD₅₀) have been shown to increase oxidative DNA damage in brain up to 72 hrs, with peak effects noted at 24 hrs in midbrain (MB), caudate/putamen (CP) and hippocampus (HP). Levels of dopamine (DA) and its metabolites in the striatum (e.g., CP) were shown to be decreased in a dose-dependent manner. The present study focused on the effects of chronic low dose OTA exposure on regional brain oxidative stress and striatal DA metabolism. Continuous administration of low doses of OTA with implanted subcutaneous Alzet minipumps caused a small but significant decrease in striatal DA levels and an upregulation of anti-oxidative systems and DNA repair. It is possible that low dose exposure to OTA will result in an earlier onset of parkinsonism when normal age-dependent decline in striatal DA levels are superimposed on the mycotoxin-induced lesion.

Key words: mycotoxins, ochratoxin-A, DNA damage and repair, Parkinson's Disease, oxyguanosine glycosylase, superoxide dismutase, glutathione, dopamine

Acknowledgements: Supported by Dept of Defense Grant # DAMD17-03-1-0501 and VA Merit Review Grant to J.S-R.

INTRODUCTION

Mycotoxins are toxic fungal metabolites known to be common contaminants of animal feed and human food. Some of the fungal products exhibit pharmacological activities that have been utilized in production of antibiotics, growth promoters, anti-neoplastic agents and many other drugs with therapeutic potential. Some mycotoxins have been developed as bio-terrorist weapons (Zilinskas, 1997). The most studied are the aflatoxins, a family of difuranocoumarin derivatives produced by many strains of *Aspergillus parasiticus* and *Aspergillus flavus* (Bennett and Klich, 2003). Acute aflatoxicosis (disease caused by aflatoxin exposure) results in death. Chronic aflatoxicosis results in cancer, immune suppression, and may be responsible for other delayed onset pathological conditions (Bennett and Klich, 2003).

Aflatoxin has achieved some notoriety in the popular literature and public media as a poison, although experts consider its use to be a “toxicologically improbable way to kill someone” (Bennett and Klich, 2003). Nevertheless, aflatoxin’s reputation as a potent poison may explain why it has been adapted for use in bioterrorism. Iraqi scientists developed aflatoxins as part of their bioweapons program during the 1980s (Zilinskas, 1997; Stone, 2002). Toxigenic strains of *Aspergillus flavus* and *Aspergillus parasiticus* were cultured, and aflatoxins were extracted to produce over 2,300 liters of concentrated toxin. The majority of this aflatoxin was used to fill warheads; the remainder was stockpiled (Zilinskas, 1997). Aflatoxins seem an unlikely choice for chemical warfare because the induction of liver cancer is “hardly a knockout punch on the battlefield” (Bennett and Klich, 2003). There are certainly more potent mycotoxins, such as those from the trichothecene family (e.g. T-2). These can act immediately upon

contact, and exposure to a few milligrams of T-2 is potentially lethal (Bennett and Klich, 2003). Even so, the fear and anxiety caused by the use of any chemical and biological weapon is the kind of psychological response that terrorists seek to inflict on their enemies. Furthermore, if used against rival ethnic groups, such as the Kurds in Iraq, the long-term physical and psychological results would be devastating. Finally, some experts think aflatoxin might have been selected simply because it was the favorite toxin of an influential Iraqi scientist (Stone, 2002).

The extent to which military personnel and civilian populations were exposed to aflatoxin during the first Gulf War is not known, but the incidence of motor neuron disease --amyotrophic lateral sclerosis (ALS)—was increased in returning veterans, suggesting a war-related environmental trigger (Haley, 2003a, b). This observation has provided the impetus to the present project. If low-dose exposure to mycotoxins results in progressive neurodegenerative disorders in humans, it may be possible to replicate this in the laboratory using mice exposed to another *Aspergillus* derived mycotoxin with mechanisms of action similar to the aflatoxins (Haley, 2003a, b)

Ochratoxin-A (OTA) is a metabolite produced by *Aspergillus ochraceus* and *Penicillium verrucosum* that accumulates in the food chain because of its long half-life (Kuiper-Goodman and Scott, 1989; Galtier, 1991). The possible contribution of OTA to the development of human and animal systemic diseases has been investigated by many authors (See review, (Marquardt and Frohlich, 1992)). Embryonic development of nervous tissue appears to be very susceptible to the deleterious effects of OTA (Hayes et al., 1974; Wangikar et al., 2004). OTA induces teratogenic effects in neonates (rats and mice) exposed *in utero*, characterized by microcephaly and

modification of the brain levels of free amino acids (Belmadani et al., 1998). OTA was also reported to be neurotoxic to adult male rats fed OTA in the diet. Neurotoxicity, indicated by concentration of lactic dehydrogenase released from the dissected brain tissue, was more pronounced in the ventral mesencephalon, hippocampus, and striatum than in the cerebellum (Belmadani et al., 1998).

Acute administration of OTA has recently been reported to cause oxidative stress and DNA damage in all brain regions (Sava et al., 2005). OTA also caused depletion of striatal dopamine (DA) and its metabolites, as well as decreased tyrosine hydroxylase immunoreactivity in the corpus striatum (caudate/putamen). No evidence for apoptosis was found in the substantia nigra (SN), striatum or hippocampus, suggesting an effect on striatal DA innervation rather than on the neuronal cell bodies in the SN (Sava et al., 2005).

The primary objectives of the present study were 1) to evaluate the pharmacokinetics of OTA, 2) to assess the effects of chronic low dose OTA administration on parameters of oxidative stress and DNA repair in mouse brain and 3) to determine whether continuous low dose exposure caused DA depletion and parkinsonism in mice. The focus on DNA repair was based on recently published findings on the acute effects of OTA in mouse brain regions (Sava et al., 2005) and on older reports that deficits in DNA repair underlie a number of neurodegenerative diseases, including Alzheimer's Disease, Amyotrophic Lateral Sclerosis and Parkinson's Disease (Robbins et al., 1985). The overall goal was to determine the extent to which regional differences in distribution of the toxin and anti-oxidative and DNA repair capacity result in striatal DA depletion and the development of parkinsonism in mice.

2. MATERIALS AND METHODS

Materials

Ochratoxin-A, SOD and dihydrobenzylamine were purchased from Sigma (St. Louis, MO). Protease inhibitors and DNA glycosylase were from Boehringer Mannheim (Indianapolis, IN, USA). ^{32}P -ATP was from NEN Life Science Products (Wilmington, DE).

Animals and Treatment

The animal protocol was approved by the Division of Comparative Medicine of the University of South Florida, which is fully accredited by AAALAC International and managed in accordance with the Animal Welfare Regulations, the PHS Policy, the FDA Good Laboratory Practices, and the IACUC's Policies.

Male Swiss ICR mice (22 ± 2 g) were obtained from the Jackson Laboratories (Bar Harbor, ME). They were housed five per cage at the temperature of 21 ± 2 °C with 12 hr light/dark cycle and free access to food and water. Mice were divided into experimental (total $n=70$) and control (total $n=20$) groups. Animals were injected with either OTA dissolved in 0.1M NaHCO_3 mg/kg i.p) or vehicle (0.1M NaHCO_3). After injection with OTA or vehicle, mice were observed for changes in spontaneous behavior three times each day until euthanasia. The response to handling was also noted. In particular, evidence for toxic effects such as clasping of limbs in response to being held by the tail was to be recorded. Groups of mice were euthanatized with CO_2 at 6, 24, and 72 hrs after injection with OTA or vehicle. The brains were removed and immediately dissected on ice.

For *chronic administration of OTA*, four groups of male Swiss ICR mice (n=7 in each group) were implanted with Alzet osotic minipumps. Each group received different cumulative doses of OTA; vehicle alone, 4 mg/kg, 8 mg/kg, or 16 mg/kg over a 2 week infusion period. Animals were then euthanatized and parameters of oxidative stress were measured in 8 regions of brain.

Isolation of Brain Regions

Brains were separated into 8 regions under a dissecting stereo-microscope in the following order. The cerebellar peduncles were cut first and cerebellum (CB) was removed. The pons (PN) and medulla (MD) were separated by cutting the ponto-medullary junction. The ventral and dorsal parts of midbrain (MB) were dissected at the level of the caudal end of the cerebral peduncles. Cerebral hemispheres were opened with a sagittal cut. Then caudate/putamen (CP) was isolated, followed by thalamus/hypothalamus (T/H) and hippocampus (HP). Finally, cerebral cortex (CX) was harvested and all the samples were kept frozen at $-70\text{ }^{\circ}\text{C}$ until assayed.

Measurement of dopamine and metabolites

HPLC with electrochemical detection was employed to measure levels of dopamine (DA) as previously reported (Cardozo-Pelaez et al., 1999). In short, tissue samples were sonicated in 50 volumes of 0.1 M perchloric acid containing 50 ng/mL of dihydrobenzylamine (Sigma Chemical, MA) as internal standard. After centrifugation (15,000 x g, 10 min, 4 °C), 20 μL of supernatant was injected onto a C18-reversed phase Microsorb-MV 300-5 column (Varian,CA) operated through Series 200

Autosampler (PerkinElmer, CT). The mobile phase consisted of 90% of a solution of 50 mM sodium phosphate, 0.2 mM EDTA, and 1.2 mM heptanesulfonic acid (pH 4) and 10% methanol. Flow rate was 1 mL/min. Peaks were detected by a Coulchem 5100A detector (ESA). Data were collected and processed with TotalChrom software (Perkin Elmer Instruments).

Assessment OGG1 activity

The procedure for extraction of DNA glycosylase was similar to that described previously (Cardozo-Pelaez et al., 2000). Pure OGG1 served as positive control. The incision activity of OGG1 was calculated as the amount of radioactivity in the band representing specific cleavage of the ^{32}P labeled oligonucleotide over the total radioactivity. Results were normalized to equal concentration of protein measured using the bicinchoninic acid assay (Smith et al., 1985).

Measurement of ochratoxin concentrations in brain

The method utilized HPLC with fluorescence detection. Brain samples of about 100 mg were sonicated in 2 volumes of absolute ethyl alcohol containing 50 ng/ml of ochratoxin-A (Sigma Chemical, MA) as internal standard. Supernatants obtained after centrifugation (14,000 x g, 5 min, 4°C) passed through Acrodisc LC 13 mm syringe filter and 20 μL of supernatant samples were injected onto C18 reverse phase Microsorb-MV 300-5 column (Varian, inc., CA). The mobile phase consisted of 57% of water, 42% of acetonitrile and 1% of acetic acid. Flow rate was 0.9 mL/min. Peaks were detected with

Series 200 fluorescent detector and data were collected and processed with TotalChrom software (PerkinElmer Instruments, CT).

Statistical analysis

The results were reported as mean \pm SEM for at least five individual samples of specific brain regions, assayed in duplicate. Two ways ANOVA was performed to assess the contribution of brain region, time of analysis and their interaction on variance. The differences between samples were analyzed by the Student's *t*-test, and a $P < 0.05$ was considered as statistically significant. The Pearson correlation coefficients between DNA repair (OGG1) and basal DNA damage (comet assay) was calculated using GraphPad Software, Inc. (San Diego, CA).

Results

Administration of OTA at doses less than 6 mg/kg i.p (below the reported LD₅₀ of 39.5 mg/kg i.p in mice (Moroi et al., 1985)) did not elicit obvious alterations in mouse behavior and locomotor activity at any time up to 3 days after treatment. Behavior was not measured instrumentally, but was based on visual inspections over the course of 3 days and the response to handling. In particular, there was no abnormal posturing or clasping of limbs when mice were picked up by the tail.

Regional Distribution of OTA in brain

A single dose of OTA (3.5 mg/kg i.p., the ED₅₀ for depletion of striatal DA) was administered to mice. Animals were euthanatized in groups of six after 3, 6, 12, 24 and

72 hrs. Brains were collected, dissected and assayed for levels of OTA. At three hrs, the highest concentrations of OTA were measured in the cerebellum (CB), followed by pons (PN), cerebral cortex (CX), and medulla (MD) (**Figure 1**). Pharmacokinetic parameters were calculated and are summarized in **Table 1**. The rank order of concentrations of OTA based on area under the curve (AUC) is as follows: CB > PN > CX > MD > MB > CP > HP > TI/H. Comparing the half-life of elimination ($T_{1/2}$) for each region shows that the pons and midbrain eliminated OTA very slowly ($T_{1/2} = 224$ and 75 hr, respectively) in contrast to the rapid elimination of the toxin from cerebellum ($T_{1/2} = 20$ hr).

INSERT TABLE 1

Relationship between brain regional concentration of OTA and parameters of oxidative stress

Correlation analysis of the present pharmacokinetic data with previously published data on the effects of OTA on parameters of oxidative stress (Sava et al., 2005) revealed that the distribution of oxidative stress and the DNA repair response across brain regions did not correlate with concentrations of the toxin (AUC) in each region (**Figure 2**). Therefore the regional vulnerability to the toxin does not bear a linear relationship to the concentration of the toxin in each region. This observation is consistent with the hypothesis that vulnerability to injury induced by this toxin is determined by regional differences in capacity to scavenge oxyradicals and/or to repair oxidative DNA damage caused by the toxin, rather than the actual level of the toxin.

Effects of chronic OTA on behavior and levels of DA and its metabolites:

Continuous sub-cutaneous infusion of OTA with Alzet minipumps resulted in a dose-dependent decrease of DA in caudate/putamen. After 2 weeks of continuous OTA administration (cumulative dose of 8 mg/kg), DA declined by 24% (76% of control level) **(Figure 3)**. At that dose of OTA, DOPAC concentration was elevated 1.9-fold (as compared to control). A similar profile was recorded for HVA. The turnover of DA calculated as ratio of (HVA+DOPAC)/DA was significantly increased at a cumulative dose of 8 mg/kg OTA. However, DA turnover was reduced at both the higher and lower cumulative doses, i.e. 4 and 16 mg/kg.

Notably, the chronic exposure did not alter behavior or spontaneous locomotor activity, nor did it result in abnormal claspings or posturing of the limbs when handled by the tail. This is similar to the absence of motor deficits following acute doses of OTA that depleted striatal DA to 50% of control levels (Sava et al., 2005).

Effects of Chronic OTA infusion on DNA Repair (OGG1 activity): Chronic OTA infusion resulted in a dose-dependent increase in OGG1 activities in all brain regions **(Figure 4)**. No region of brain showed an inhibition or decrease in OGG1 activity at any dose, unlike the early responses to acute doses of OTA, when all regions showed initial and transient inhibition of OGG1 activity (Sava et al., 2005). Even though all brain regions were capable of marked increases in OGG1 activity, not all regions were equally sensitive to the toxin. Using the dose-response curve functions generated from each brain region to estimate an ED₅₀ (the dose of OTA that resulted in half the maximal rate of OGG1 activity), it was clear that the caudate/putamen was most sensitive to the

toxin; a cumulative dose of 0.65 mg/kg produced half maximal OGG1 activity. The cerebellum was the least sensitive, with respect to dose of OGG1 required to attain half-maximal OGG1 activity ($ED_{50}=2.65$ mg/kg). **See Figure 4.**

Discussion

The impetus to this project was provided by reports that veterans of the first Gulf War were developing ALS at a higher frequency than the normal population, suggesting a war-related environmental trigger (Haley, 2003a, b). Since there was no clear evidence of high dose (lethal) exposure to aflatoxin in these veterans, it was possible they were exposed to sub-lethal low doses of the mycotoxin during routine operations in the field or while destroying enemy munition storage facilities. The present project attempted to replicate low-dose exposure to a mycotoxin, OTA, with some similarities to aflatoxin in laboratory mice.

Acute administration of OTA has previously been reported to cause widespread oxidative stress in mouse brain, evidenced by significant increases in lipid peroxidation and oxidative DNA damage across 6 brain regions (Sava et al., 2005). Furthermore, OTA treatment elicited an early and sustained surge in activity of SOD, a major oxyradical scavenger, across all brain regions (Sava et al., 2005). Unlike the monophasic SOD activation, the oxidative DNA repair response exhibited a biphasic response, with an initial inhibition of OGG1 activity followed by a trend towards recovery to normal levels after 3 days. It was hypothesized that variation in DNA repair was a potential factor in determining neuronal vulnerability. Deficient DNA repair processes have been associated with Parkinson's Disease (PD) as well as with other

neurodegenerative diseases such as Alzheimer's disease, amyotrophic lateral sclerosis (ALS) and Huntington's disease (HD) (Robbins et al., 1985; Mazzarello et al., 1992; Lovell et al., 2000). In addition, it was previously shown that the uneven distribution of oxidative DNA damage across brain regions caused by endogenous or exogenous factors was determined, in part, by the intrinsic capacity to repair oxidative DNA damage (Cardozo-Pelaez et al., 1999; Cardozo-Pelaez et al., 2000).

Those earlier studies, and the present report on the effects of OTA, were focused on oxyguanosine glycosylase (OGG1), a key enzyme involved in the repair of the oxidized base, 8-hydroxy-2'deoxoguanosine (oxo8dG). Un-repaired DNA damage in post-mitotic cells, such as neurons, can result in disruption of transcriptionally active genes, cellular dysfunction and apoptosis (Hanawalt, 1994). Hence it was reasonable to hypothesize that diminished DNA repair capacity in populations of neurons would be associated with increased vulnerability to potentially genotoxic agents. Since the CP and MB showed a relatively diminished OGG1 activity and increased oxidative DNA damage, it was postulated that the DA terminals of the striatum would suffer damage. This concept was supported by an earlier report of increased oxidative DNA damage in substantia nigra and striatum in post-mortem brain from PD cases (Sanchez-Ramos et al., 1994), and by the observation that MB and CP were less able to upregulate OGG1 repair activity in response to the pro-oxidant, diethylmaleate (Cardozo-Pelaez et al., 2002). This hypothesis was further supported by the report that acute doses of OTA caused a dose-dependent decrease of striatal DA and a decrease in DA turnover (Sava et al., 2005). The nearly 50% reduction in striatal DA caused by a single dose (3.5 mg/kg i.p) did not produce observable changes in daytime mouse behavior or locomotor

activity, though it is likely that more sensitive, quantitative measures of behavior may reveal alterations. This dose of OTA also resulted in diminished tyrosine hydroxylase immunoreactivity in the CP and MB as well as in the locus ceruleus (which contains noradrenergic neurons). The effects of OTA on catecholaminergic systems appeared to reflect a potentially reversible action rather than a cytotoxic effect since no evidence of cell death was found by 72 hrs. There were no apoptotic profiles found in SN and CP or any other region of the brain. In addition, there did not appear to be cytotoxic effects on striatal neurons identified by DARPP32 immunostaining (Sava et al., 2005).

To determine whether uneven distribution of the toxin across brain regions was responsible for the vulnerability of DA terminals in striatum, pharmacokinetic studies were performed. Surprisingly, the distribution of oxidative stress and the DNA repair response across brain regions did not correlate with regional concentrations of the mycotoxin (AUC). The CB had the highest concentrations and the slowest clearance of OTA and yet was least affected by the toxin. Therefore, the regional vulnerability to the toxin was not directly related to the concentration of the toxin in each region.

Continuous, low-dose infusion of OTA resulted in a dose-dependent decrease of striatal DA. After 2 weeks of continuous OTA exposure, DA had declined by 24% (e.g. to 75% of control levels) and DA turnover was significantly increased following delivery of a cumulative dose of 8 mg/kg OTA. The decline of striatal DA following chronic infusion was much less than that caused by a single acute dose of 3.2 mg/kg i.p. This may simply be a result of lower steady-state brain levels of the toxin when infused continuously through the minipump. In addition, chronic, low-dose exposure

may have permitted a more robust upregulation of the anti-oxidative and DNA repair systems in the striatum.

Chronic OTA infusion also resulted in a dose-dependent increase in DNA repair (e.g., OGG1 activities) in all brain regions. No region of brain showed an inhibition or decrease in OGG1 activity at any dose, unlike the early responses to acute doses of OTA, when all regions showed initial and transient inhibition of OGG1 activity (Sava et al., 2005). Even though all brain regions were capable of marked increases in OGG1 activity, not all regions were equally sensitive to the toxin. Using the dose-response curve functions generated from each brain region to estimate an ED₅₀ (the dose of OTA that resulted in half the maximal rate of OGG1 activity), it was clear that the caudate/putamen (CP) was most sensitive to the toxin; a cumulative dose of 0.65 mg/kg produced half maximal OGG1 activity. The cerebellum was the least sensitive, with respect to dose of OGG1 required to attain half-maximal OGG1 activity (ED₅₀=2.65 mg/kg).

What is the most likely mechanism to explain the vulnerability of the caudate/putamen to OTA? These experiments showed that the susceptibility to oxidative stress, oxidative DNA damage and depletion of striatal DA is not directly related to the pharmacokinetics of the mycotoxin. A potential explanation for the observations reported here relates to bioenergetic compromise evoked by OTA. This mycotoxin has been reported to inhibit succinate-dependent electron transfer activities of the respiratory chain, but at higher concentrations will also inhibit electron transport at Complex I. (Wei et al., 1985; Aleo et al., 1991). The nigro-striatal dopaminergic system is well known to be especially vulnerable to the mitochondrial toxicants, MPTP and

rotenone, especially when the latter toxicant is administered chronically at low doses (Vyas et al., 1986; Hasegawa et al., 1990; Betarbet et al., 2000). Other mitochondrial poisons like nitropropionic acid and malonate interfere with succinate dehydrogenase/Complex II. These Complex II inhibitors result in lesions primarily localized to striatum (Schulz et al., 1996; Calabresi et al., 2001). Bioenergetic compromise may lead to persistent activation of NMDA receptors which results in excitotoxicity mediated by the neurotransmitter glutamate in regions of brain richly innervated by glutamatergic fibers, accounting for the vulnerability of the striatum and pallidum, and possibly the SN (Turski and Turski, 1993; Greenamyre et al., 1999). In addition, Ca^{2+} entering neurons through NMDA receptors has 'privileged' access to mitochondria, where it causes free-radical production and mitochondrial depolarization (Greenamyre et al., 1999). Hence the bioenergetic compromise induced by OTA may be responsible for the generation of free radicals and reactive oxygen species that resulted in global oxidative damage to DNA and lipids, as reported here and damage to proteins through generation of oxygen free radicals and nitric oxide, as reported elsewhere (Thomas and Mallis, 2001; Bryan et al., 2004).

Of course OTA may also be toxic through other mechanisms. Due to its chemical structure, (chlorodihydroisocoumarin linked through an amide bond to phenylalanine), OTA inhibits protein synthesis by competition with phenylalanine in the aminoacylation reaction of phenylalanine-tRNA (Bunge et al., 1978; Creppy et al., 1983) and phenylalanine hydroxylase activity (Creppy et al., 1990). These actions could lead to impairment of the synthesis of DOPA, dopamine and catecholamines or enzymes involved in metabolism of DA.

Conclusions: The continuous subcutaneous administration of OTA at low doses over a period of two weeks caused small, but significant depletion of striatal DA. OTA also caused pronounced global oxidative stress, evoking a strong anti-oxidative and DNA repair response across the entire brain. Even though the depletion of striatal DA did not cause overt parkinsonism in these mice, it is important to consider that the superimposition of normal age-related decline in striatal DA will ultimately result in signs of parkinsonism such as slowness of movement and rigidity in the mice. Without completing understanding why DA terminals in striatum are especially vulnerable to OTA, it is likely that a toxic insult to the nigro-striatal system will increase the risk of developing Parkinson's Disease at an earlier age than normal. This hypothesis can be tested by studying the long term consequences of episodes of OTA exposure in mice during the aging process. In the real world, it will be important to monitor the neurological status of Gulf War veterans as they age.

Acknowledgements: Supported by Dept of Defense Grant # DAMD17-03-1-0501 and VA Merit Review Grant to J.S-R.

Table 1: Pharmacokinetic data for OTA across brain regions

Brain Regions	k_{el} (1/h)	$T_{1/2}$ (h)	AUC (ng*h/uL)	CL (uL/mg*h)
CB	0.034	20.175	32.107	0.125
PN	0.003	224.699	31.026	0.129
MD	0.020	33.859	6.175	0.648
MB	0.009	75.107	5.578	0.717
HP	0.016	42.582	5.266	0.760
T/H	0.022	31.104	3.426	1.167
CP	0.015	47.222	5.202	0.769
CX	0.021	32.578	10.087	0.397

The **elimination rate constant** (k_{el}) was calculated from the slope of semi-logarithmical plot of OTA concentration versus time using the least square regression analysis.

The **half-life of OTA** elimination ($T_{1/2}$) was calculated from the equation:

$$T_{1/2} = \ln 2 / k_{el}$$

The **area under curve** (AUC) was calculated by integration of OTA concentration from time zero to infinity according to the formula:

$$AUC_{0-\infty} = AUC_{0-t} + C_f / k_{el}$$

where C_f represents the final measured OTA concentration made at time t .

The **clearance** (CL) of OTA was determined using the following formula:

$$CL = D / AUC_{0-\infty}$$

where **D** represents OTA dose, namely, 3.5 mg/kg.

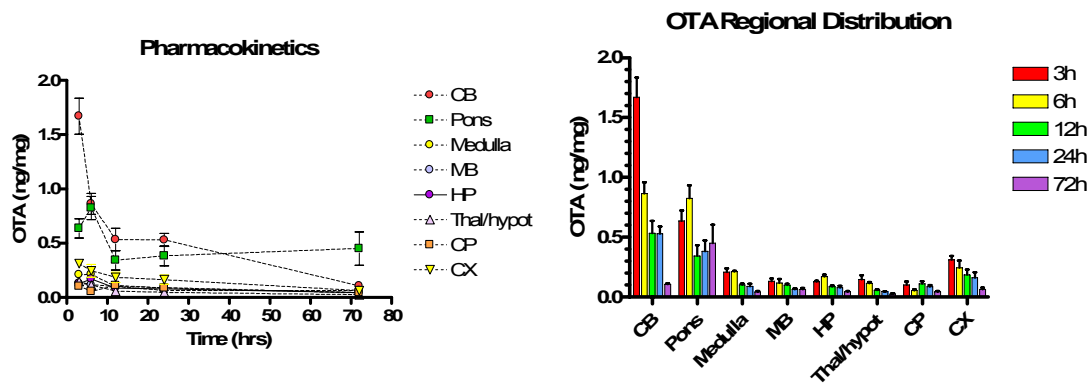


Figure 1. Left panel summarizes the changes over time in regional brain concentrations of OTA following an acute dose of 3.5 mg/kg (i.p.) The right panel depicts the same data organized according to brain region. CB=cerebellum; MB=midbrain; HP=hippocampus; Thal/hypot=thalamus/hypothalamus; CP=caudate/putamen; CX=cerebral cortex

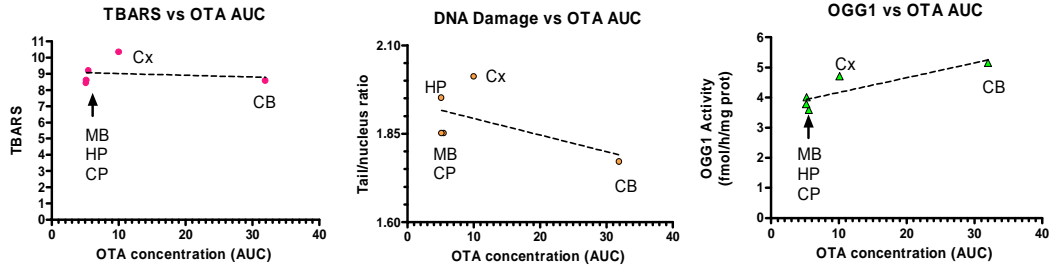


Figure 2. Parameters of oxidative stress plotted as a function of OTA concentration. The pharmacokinetic parameter that reflects the average concentration of OTA over time in each brain region (“area under the curve” or AUC) is plotted on the X-axis. The upper panel plots the relationship between TBARS (index of lipid peroxidation) in each brain region as a function of AUC for OTA. The middle and lower panels show the plots of DNA damage vs AUC and DNA repair activity (OGG1) vs AUC, respectively. The dashed regression line does not differ significantly from zero in all three panels, indicating that there is no linear relationship between the selected parameter of oxidative stress and the AUC in specific brain regions

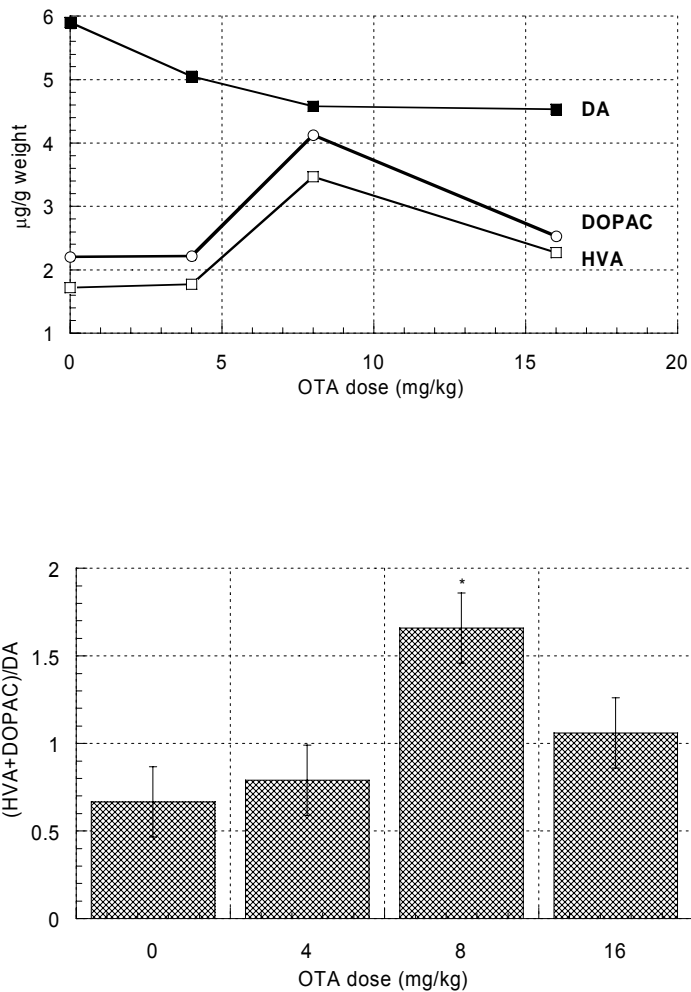


Figure 3. Effects of chronic infusion of OTA via osmotic minipump on levels of DA and its metabolites across brain regions.

Upper panel: Levels of DA and its metabolites in caudate/putamen of ICR mice exposed to different doses of OTA during 2 weeks. OTA was administered using Alzet osmotic mini pumps implanted under the skin of animals.

Lower panel: Turnover of DA in caudate/putamen of ICR mice subjected to chronic exposure of different doses of OTA during 2 weeks. Asterisk depicted a significantly different value as compared to the control ($P < 0.05$).

Effects of Chronic OTA on OGG1 Activity

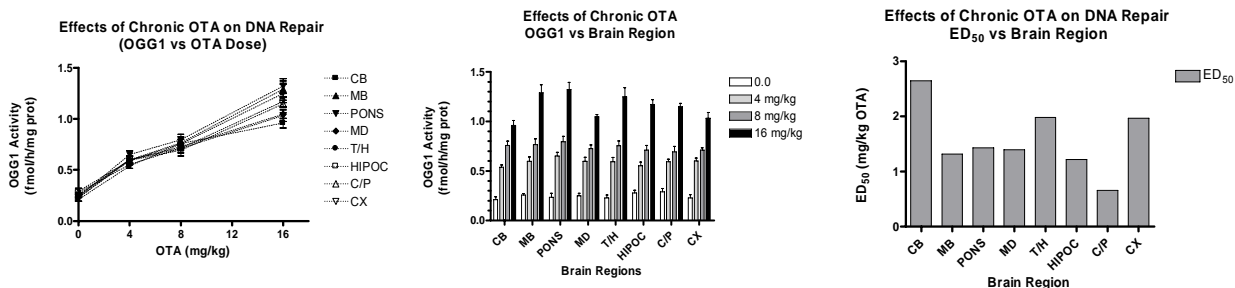


Fig 4. Effects of chronic infusion of OTA via osmotic minipump on OGG1 activities across brain regions.

Left panel: OGG1 activity plotted against cumulative OTA dose delivered over 2 weeks. All brain regions exhibited a dose-dependent increase in OGG1.

Middle panel: OGG1 activity plotted against brain region on the X-axis. Shading of the bars depicts cumulative dose administered over 2 weeks as indicated in the legend.

Right panel: The ED₅₀ (dose of OTA that increased OGG1 to 50% of the maximum response) was determined from the dose-response curves of each brain region. The X-axis depicts brain region and the Y-axis depicts the ED₅₀ of OTA (in mg/kg) for each region. The CB, CX and Thalamus/hypothalamus exhibited the highest ED₅₀s (i.e. higher doses were required to produce half maximal response), while the CP had the lowest ED₅₀ (lowest dose required to reach half maximal OGG1 response).

References

- Aleo MD, Wyatt RD, Schnellmann RG (1991) Mitochondrial dysfunction is an early event in ochratoxin A but not oosporein toxicity to rat renal proximal tubules. *Toxicol Appl Pharmacol* 107:73-80.
- Belmadani A, Tramu G, Betbeder AM, Steyn PS, Creppy EE (1998) Regional selectivity to ochratoxin A, distribution and cytotoxicity in rat brain. *Arch Toxicol* 72:656-662.
- Bennett JW, Klich M (2003) Mycotoxins. *Clin Microbiol Rev* 16:497-516.
- Betarbet R, Sherer TB, MacKenzie G, Garcia-Osuna M, Panov AV, Greenamyre T (2000) Chronic systemic pesticide exposure reproduces features of Parkinson's disease. *Nature Neuroscience* 3:1301-1306.
- Bryan NS, Rassaf T, Maloney RE, Rodriguez CM, Saijo F, Rodriguez JR, Feelisch M (2004) Cellular targets and mechanisms of nitros(yl)ation: an insight into their nature and kinetics in vivo. *Proc Natl Acad Sci U S A* 101:4308-4313.
- Bunge I, Dirheimer G, Roschenthaler R (1978) In vivo and in vitro inhibition of protein synthesis in *Bacillus stearothermophilus* by ochratoxin A. *Biochem Biophys Res Commun* 83:398-405.
- Calabresi P, Gubellini P, Picconi B, Centonze D, Pisani A, Bonsi P, Greengard P, Hipskind RA, Borrelli E, Bernardi G (2001) Inhibition of mitochondrial complex II induces a long-term potentiation of NMDA-mediated synaptic excitation in the striatum requiring endogenous dopamine. *J Neurosci* 21:5110-5120.
- Cardozo-Pelaez F, Brooks PJ, Stedeford T, Song S, Sanchez-Ramos J (2000) DNA damage, repair, and antioxidant systems in brain regions: a correlative study. *Free Radical Biology & Medicine* 28:779-785.
- Cardozo-Pelaez F, Stedeford TJ, Brooks PJ, Song S, Sanchez-Ramos JR (2002) Effects of diethylmaleate on DNA damage and repair in the mouse brain. *Free Radic Biol Med* 33:292-298.
- Cardozo-Pelaez F, Song S, Parthasarathy A, Hazzi C, Naidu K, Sanchez-Ramos J (1999) Oxidative DNA damage in the aging mouse brain. *Movement Disorders* 14:972-980.
- Creppy EE, Chakor K, Fisher MJ, Dirheimer G (1990) The mycotoxin ochratoxin A is a substrate for phenylalanine hydroxylase in isolated rat hepatocytes and in vivo. *Arch Toxicol* 64:279-284.
- Creppy EE, Kern D, Steyn PS, Vleggaar R, Roschenthaler R, Dirheimer G (1983) Comparative study of the effect of ochratoxin A analogues on yeast aminoacyl-tRNA synthetases and on the growth and protein synthesis of hepatoma cells. *Toxicol Lett* 19:217-224.
- Galtier P (1991) Pharmacokinetics of ochratoxin A in animals. *IARC Sci Publ*:187-200.

- Greenamyre JT, MacKenzie G, Peng TI, Stephans SE (1999) Mitochondrial dysfunction in Parkinson's disease. *Biochem Soc Symp* 66:85-97.
- Haley RW (2003a) Excess incidence of ALS in young Gulf War veterans. *Neurology* 61:750-756.
- Haley RW (2003b) Gulf war syndrome: narrowing the possibilities. *Lancet Neurol* 2:272-273.
- Hanawalt PC (1994) Transcription-coupled repair and human disease: perspective. *Science* 266:1957-1958.
- Hasegawa E, Takeshige K, Oishi T, et al. (1990) MPP+ induces NADH-dependent superoxide formation and enhances NADH-dependent lipid peroxidation in bovine heart submitochondrial particles. *Biochem Biophys Res Com* 170:1049-1055.
- Hayes AW, Hood RD, Lee HL (1974) Teratogenic effects of ochratoxin A in mice. *Teratology* 9:93-97.
- Kuiper-Goodman T, Scott PM (1989) Risk assessment of the mycotoxin ochratoxin A. *Biomed Environ Sci* 2:179-248.
- Lovell MA, Xie C, Markesbery WR (2000) Decreased base excision repair and increased helicase activity in Alzheimer's disease brain. *Brain Research* 855:116-123.
- Marquardt RR, Frohlich AA (1992) A review of recent advances in understanding ochratoxicosis. *J Anim Sci* 70:3968-3988.
- Mazzarello P, Poloni M, Spadari S, Focher F (1992) DNA repair mechanisms in neurological diseases: facts and hypotheses. *Journal of the Neurological Sciences* 112:4-14.
- Moroi K, Suzuki S, Kuga T, Yamazaki M, Kanisawa M (1985) Reduction of ochratoxin A toxicity in mice treated with phenylalanine and phenobarbital. *Toxicol Lett* 25:1-5.
- Robbins JH, Otsuka F, Tarone RE, et al. (1985) Parkinson's disease and Alzheimer's disease: hypersensitivity to X-rays in culture cell lines. *J Neurol Neurosurg Psychiatry* 48:916-923.
- Sanchez-Ramos J, Overvik E, Ames BN (1994) A marker of oxyradical-mediated DNA damage (oxo8dG) is increased in Nigro-Striatum of Parkinson's Disease Brain. *Neurodegeneration (incorporated into Exp Neurology)* 3:197-204.
- Sava V, Reunova O, Velasquez A, Harbison R, Sanchez-Ramos J (2005) Acute neurotoxic effects of the fungal metabolite ochratoxin-A. *Neurotoxicology*.
- Schulz JB, Henshaw DR, MacGarvey U, Beal MF (1996) Involvement of oxidative stress in 3-nitropropionic acid neurotoxicity. *Neurochem Int* 29:167-171.
- Smith PK, Krohn RI, Hermanson GT, Mallia AK, Gartner FH, Provenzano MD, Fujimoto EK, Goeke NM, Olson BJ, Klenk DC (1985) Measurement of protein using bicinchoninic acid. *Anal Biochem* 150:76-85.
- Stone R (2002) Biodefense. Peering into the shadows: Iraq's bioweapons program. *Science* 297:1110-1112.
- Thomas JA, Mallis RJ (2001) Aging and oxidation of reactive protein sulfhydryls. *Exp Gerontol* 36:1519-1526.

- Turski L, Turski WA (1993) Towards an understanding of the role of glutamate in neurodegenerative disorders: energy metabolism and neuropathology. *Experientia* 49:1064-1072.**
- Vyas I, Heikkila RE, Nicklas WJ (1986) Studies on the neurotoxicity of MPTP; inhibition of NAD-linked substrate oxidation by its metabolite, MPP+. *J Neurochem* 46:1501-1507.**
- Wangikar PB, Dwivedi P, Sharma AK, Sinha N (2004) Effect in rats of simultaneous prenatal exposure to ochratoxin A and aflatoxin B(1). II. Histopathological features of teratological anomalies induced in fetuses. *Birth Defects Res B Dev Reprod Toxicol* 71:352-358.**
- Wei YH, Lu CY, Lin TN, Wei RD (1985) Effect of ochratoxin A on rat liver mitochondrial respiration and oxidative phosphorylation. *Toxicology* 36:119-130.**
- Zilinskas RA (1997) Iraq's biological weapons. The past as future? *Jama* 278:418-424.**

**ACUTE OCHRATOXIN-A NEUROTOXICITY: KINETICS OF DISTRIBUTION
OF THE TOXIN, INDICES OF OXIDATIVE STRESS AND DNA REPAIR
ACTIVITIES IN MOUSE BRAIN**

V. Sava^{1,2}; A. Velasquez^{1,2}; O. Reunova^{1,2}, J. Sanchez-Ramos^{1,2*}

1. Neurology, University of South Florida, Tampa, FL, USA 2. Research Service, James Haley VA, Tampa, FL, USA

Ochratoxin A (OTA) is a mycotoxin with a chemical structure consisting of the amino acid phenylalanine linked through an amide bond to chlorodihydro-isocoumarin. OTA is a contaminant of many foodstuffs and is responsible for multiple adverse effects that involve kidney and brain. Hypothesizing that neurotoxicity of OTA is mediated through oxidative stress mechanisms, we investigated the temporal relationships between distribution of OTA and the appropriate bio- and histochemical indices of oxidative stress throughout the brain. Male ICR mice were given OTA (4 mg/kg, i.p.) and 6 brain regions were analyzed for OTA content and quantitative parameters of oxidative stress at various intervals up to 72 h after exposure. Three hrs administration of OTA, the concentrations of the toxin (ng/mg tissue) were as follows: cerebellum (CB: 1.67 ± 0.02), pons (0.63 ± 0.01), cortex (CX: 0.3 ± 0.006), midbrain (MB: 0.13 ± 0.003), hippocampus (HP: 0.12 ± 0.003) and caudate putamen (CP: 0.1 ± 0.005). The total amount of OTA distributed across the brain represented 0.1% to 0.002% of the administered dose. The half-life of OTA elimination was from 20 to 36 h. OTA induced lipid peroxidation and elicited significant changes in reduced glutathione: the levels of reduced glutathione were increased (1.2 - 2 fold) in CB, pons, and MB but were decreased (0.7 - 0.9 fold) in CX, HP and CP. OTA also elicited a transient increase in SOD activity that declined below normal after 24 h of intoxication. There were no correlation found between biochemical indices and OTA concentration. The oxidative DNA repair activity was inhibited in all regions of brain at the beginning of OTA exposure. Most of the regions that were highly affected by the mycotoxin recovered by 72 h. However DNA repair remained inhibited in striatum and midbrain. OTA was found to be toxic for dopaminergic neurons of the nigro-striatal tract. Namely, mycotoxin decreased striatal DA levels and reduced immunoreactivity in TH+ fibers of striatum and TH+ cells of S. nigra. Altogether, results demonstrated that neurotoxicity of OTA involves the entire brain, but regions unable to repair oxidative DNA damage appear to be more vulnerable.

Supported by: Dept of Defense Grant #DAMD17-03-1-0501 and VA Merit Review Grant

**ABSTRACT OF INVITED LECTURE PRESENTED AT WORLD FEDERATION OF
NEUROLOGY, SYMPOSIUM ON NEUROTOXICOLOGY, SYDNEY, AUSTRALIA (11/2005)**

Mycotoxins: Can Low Level, Non-lethal Exposure Result in Parkinsonism?

Sanchez-Ramos, J^{1,2}, Sava, V^{1,2}

¹ *University of South Florida, Tampa FL, USA*

² *James Haley VA Hospital, Tampa, FL, USA*

Mycotoxins are fungal metabolites with pharmacological activities that have been utilized in production of antibiotics, growth promoters, and other kinds of drugs; still others have been developed as biological and chemical warfare agents. Bombs and ballistic missiles loaded with mycotoxins were believed to be deployed by Iraq during Operation Desert Storm. In light of the excess incidence of amyotrophic lateral sclerosis in young Gulf War veterans, it is important not to forget the potential neurotoxic effects of low doses of mycotoxins. Ochratoxin A (OTA) is a common mycotoxin with a long biological half-life and mitochondrial toxicity. It is found in damp environments and moldy foods (contaminated with *Aspergillus* and *Penicillium*). As part of a program to study the brain's DNA repair response to a range of neurotoxicants, we measured the effects of acute and chronic administration of OTA on the activity of the DNA repair enzyme, oxyguanosine glycosylase (OGG1), in cerebellum (CB), cortex (CX), hippocampus (HP), midbrain (MB), caudate/putamen (CP) and pons/medulla (PM) of Swiss ICR mice. Based on the observation of pronounced alterations of OGG1 in the CP, we then measured DA and its metabolites, homovanillic acid and (HVA) dihydroxyphenylacetic (DOPAC) by HPLC in the same regions. Acute administration of OTA (0.37 to 6 mg/kg ip) resulted in a dose-dependent depletion of DA with the greatest effects in CP and frontal cortex. The highest dose caused a 6 fold decrease of DA concentration in CP. The ED50 for DA depletion ranged between 3 and 4 mg/kg. OGG1 activities, which served as an index of repair of oxidative DNA damage, were associated with changes in DA, HVA and DOPAC concentration. Ongoing studies of chronic exposure to OTA and its effects on DA content may provide new insights into the pathogenesis of Parkinson's disease.

Supported by: Dept of Defense Grant #DAMD17-03-1-0501 and VA Merit Review Grant

CALL FOR ABSTRACTS

Symposia on Etiology, Pathogenesis, and Treatment of Parkinson's Disease and Other Movement Disorders

Deadline for Receipt of Regular Abstracts: June 1, 2005

Deadline for Receipt of Late Breaking Research Abstracts: July 5, 2005

Electronic submission for Regular Abstracts and Late Breaking Research Abstracts is required

Electronic submission is required. An electronic version of this form is available by sending an e-mail request to abstract@ctcc.rochester.edu. If there are problems contact Tracy Morgan, University of Rochester (585-275-0555).

ALL INFORMATION MUST BE FILLED IN BELOW • PLEASE TYPE

Please check type of abstract:

Regular Abstract

Late Breaking Research Abstract

Please check appropriate symposium; and if OMD, then indicate topic most relevant to your abstract:

Parkinson's Disease Symposium: Rajesh Pahwa, MD, Chair, University of Kansas Medical Center, Kansas City, KS

Other Movement Disorders Symposium: Tetsuo Ashizawa, MD, Chair, University of Texas Medical Branch, Galveston, TX

Ataxia

Restless Leg Syndrome

Dystonia

Tourette's Syndrome

Huntington Disease

Tremor

Myoclonus

Other (specify) _____

Title: Regulation of DNA Repair in the MPTP Mouse Model of Parkinson's Disease

Authors (list in order using following format: M.A. Rudolph, T. Morgan): V. Sava, A. Velazquez, S. Song, J. Sanchez-Ramos

Institution name, city, state/province, country of each author: University of South Florida and James Haley VA Hospital, Tampa, FL

Name, address, telephone, fax and e-mail of presenting author: J. Sanchez-Ramos, PhD, MD; Dept Neurolog (MDC 55); USF, 12901 B. B. Downs Blvd, Tampa FL 33612; phone: 813-974-5841; FAX 813-974-7200 email: jsramos@hsc.usf.edu

ABSTRACT FORM

Platform Preferred

Poster Preferred

(Abstract Not To Exceed 250 Word – Electronic Submission Required - Do Not Use Illustrations)

Oxidative DNA damage, and its repair by enzymes such as 8-oxoguanosine DNA glycosylase (OGG1), has been implicated in the pathogenesis of PD. Steady-state levels of oxidative DNA damage, indicated by measures of 8-hydroxy-2'-deoxyguanosine (8-oxodG) are increased in the substantia nigra (SN), basal ganglia and cortex of PD cases³. Recently, the expression of mitochondrial isoforms of OGG1 enzymes were found to be increased in SN in cases with short duration of PD and decreased in those cases with long duration of disease². Study of the regulation of OGG1 in mouse brain might shed light on vulnerability of nigral neurons. Mice exhibit an age-dependent accumulation of 8-oxodG in midbrain, striatum and cerebellum; levels of 8-oxodG were associated with a decline in spontaneous locomotor activity and balance. OGG1 activity can be up-regulated *in vitro* and *in vivo* in mouse brain by agents that increase oxidative stress; the extent of DNA repair activity is proportional to cellular survival^{1,4}. In the present report, we will describe results from study of the temporal course of the DNA repair response across 44 brain regions of mouse treated with a single dose of MPTP. All regions across the brain upregulated OGG1 activity immediately, but SN and striatum were unable to maintain OGG1 repair beyond 72. In summary, regulation of DNA repair in post-mitotic cells is a critical determinant of cellular vulnerability to oxidative stress.

1. Cardozo-Pelaez et al., *Free Radical Biology and Medicine* 33:292-298, 2002
2. Fukae et al., *Acta Neuropathol (Berl)* 109:256-262, 2005
3. Sanchez-Ramos, *Neurodegeneration (Exp Neurol)* 3:197-204, 1994
4. Sava et al., *Free Radic Biol Med* 36:1144-1154, 2004

Deadline for Receipt of Regular Abstracts: June 1, 2005

Deadline for Receipt of Late Breaking Research Abstracts: July 5, 2005